SYNTHESIS AND CHARACTERIZATION OF Fe_3O_4 /Al_2O_3 /MnO_2 TERNARY MIXED OXIDE NANOCOMPOSITE FOR PHOSPHORUS DESORPTION FROM ACID SOILS USING DIALYSIS MEMBRANE TUBE

MSc THESIS

HIRPO HINSENE DUBE

JUNE 2018

HARAMAYA UNIVERSITY, HARAMAYA

Synthesis and Characterization of Fe_3O_4 /Al_2O_3 /MnO_2 Ternary Mixed Oxide Nanocomposite for Phosphorus Desorption from Acid Soils Using Dialysis Membrane Tube

A Thesis Submitted to the Department of Chemistry,

Postgraduate Program Directorate

HARAMAYA UNIVERSITY

In Partial Fulfillment of the Requirements for the Degree of MASTER OF SCIENCE IN CHEMISTRY (ANALYTICAL CHEMISTRY)

Hirpo Hinsene Dube

June 2018

Haramaya University, Haramaya

HARAMAYA UNIVERSITY

POSTGRADUATE PROGRAM DIRECTORATE

I hereby certify that I have read and evaluated this Thesis titled '**Synthesis and Characterization of $Fe_3O_4/Al_2O_3/MnO_2$ Ternary Mixed Oxide Nanocomposite for Phosphorus Desorption from Acid Soils Using Dialysis Membrane Tube**' prepared under our guidance by Hirpo Hinsene. I recommend that it be submitted as fulfilling the thesis requirement.

Abi Taddesse (PhD)	_____	_____
Major Advisor	Signature	Date
Endale Teju (PhD)	_____	_____
Co-Advisor	Signature	Date
Isabel Diaz (Prof.)	_____	_____
Co-Advisor	Signature	Date

As member of the Board of Examiners of the MSc Thesis Open Defense Examination, I certify that I have read and evaluated the thesis prepared by Hirpo Hinsene and examined the candidate. I recommend that the thesis be accepted as fulfilling the Thesis requirement for the degree of Master of Science in Chemistry (Analytical Chemistry).

_____	_____	_____
Chairperson	Signature	Date
_____	_____	_____
Internal Examiner	Signature	Date
_____	_____	_____
External Examiner	Signature	Date

DEDICATION

This thesis manuscript is dedicated to my mother Ermole Kesamo and to all my families who encouraged and strengthened me in all my life.

STATEMENT OF THE AUTHOR

By my signature below, I declare and affirm that this Thesis is my own work and I have followed all ethical and technical principles of scholarship in the preparation, data collection, data analysis and complication of this thesis. Any scholarly matter that is included in the Thesis has been given recognition through citation.

This Thesis is submitted in partial fulfillment of the requirements for MSc Degree in the Haramaya University. The Thesis is deposited in the Haramaya University Library and is made available to borrowers under the rules of the Library. I solemnly declare that this Thesis has not been submitted to any other institution anywhere for the award of any academic degree, diploma or certificate.

Brief quotations from this Thesis may be made without special permission provided that accurate and complete acknowledgment of source is made. Requests for extended quotations from or reproduction of this Thesis in whole or in part may be granted by Head of the Department or Director of Postgraduate Program Directorate when in his or her judgment the proposed use of the material is in the interests of scholarship. In all other instances, however, permission must be obtained from the author of the Thesis.

Name: Hirpo Hinsene Signature: _____

Date: _____

Department: Chemistry

BIOGRAPHICAL SKETCH

The author was born in Western Arsi Zone, Arsi Negelle Woreda Oromia Region on May 10, 1987. He attended his elementary and junior education from 1993-2000 at Sokido Primary School and secondary education at Arsi Negelle Secondary and Preparatory School from 2001-2004. After completing preparatory school, he joined Ambo University in 2005 and graduated in 2008 from Department of Chemistry with Bachelor of Science Degree in Applied Chemistry. Soon after graduation, the author was employed at Dera Preparatory School as a teacher and served for three years and five months and later he joined Debre Berhan University on 2012 and he served for three years as graduate assistant in the Department of Chemistry. In 2015, he joined the Postgraduate Program Directorate of the Haramaya University as a candidate for Master of Science Degree in Chemistry (Analytical Chemistry) in October 2015.

ACKNOWLEDGMENTS

I consider it a profound pleasure to express my deep sense of indebtedness, gratitude and thanks to my Advisors, Dr. Abi Taddesse, Dr. Endale Teju and Isabel Diaz (Prof.) for their critical comments and helpful guidance which provided me a chance to explore further.

I want to thank the Ministry of Education and Debre Berhan University for providing me financial support to accomplish this work. I would like to give great respect and thank to Dr. Yonas Chebude (from AAU) for running FTIR of as-synthesized sample in his research laboratory.

I would like to give great respect and heartfelt thanks to Prof. Isabel Diaz for her support in characterizing the as-synthesized samples using XRD, BET, SEM and EDX at the Instituto de Catálisis Y. Petroleoquímica, CSIC, C/Marie Curie 2, Madrid, Spain.

I gratefully acknowledge the Department of Chemistry, Haramaya University, for providing me access to the research laboratory with instrumentation and other facilities required for this work. My special thanks are to Mr. Zewdu Bezu, Wakshuma Yadesa, Fituma Diriba, Kemal Habib, Wubshet Legasse, Fekadu Tsegaye, Dilnesa Bayle, Yibrehu Bogale and Dewit Alemu for assisting me with some techniques during lab work. I am very grateful to the farmers who allowed us to take soil samples from their farms.

Last, but not least, I wish to thank my family and friends for all their help, support and guidance throughout my studies.

ACRONYMS AND ABBREVIATIONS

ANOVA	Analysis of Variance
AAS	Atomic Absorption Spectrometry
BET	Brunauer–Emmett–Teller
CV	Coefficient of Variation
CD28P	Cumulative Desorbed P
DMT	Dialysis Membrane Tube
DMT-HFO	Dialysis Membrane Tube Filled with Hydrous Fe(hydr)oxide
DMT-HFAMO	Dialysis Membrane Tube Filled with Hydrous Iron-Alumina-Manganese Ternary Mixed Oxide
EDX	Energy Dispersive Analysis of X-ray
FAAS	Flame Atomic Absorption Spectrometry
FAO	Food and Agricultural Organization
FTIR	Fourier Transform Infrared Spectrometry
HFAMO	Hydrous Iron-Alumina-Manganese Ternary Mixed Oxide Nanocomposite
Fe-Al-Mn	Iron-Alumina-Manganese Ternary Mixed Oxide Nanocomposite
Masl	Meter Above Sea Level
MWCO	Molecular Weight Cutoff
NMnOs	Nano Sized Manganese Oxides
NMOs	Nano Sized Metal Oxides
SOM	Soil Organic Matter
P	Phosphorus
SEM	Scanning Electron Microscope
SPSS	Statistical Package for the Social Sciences
Uv-Vis	Ultraviolet-Visible Spectrophotometer
XRD	X-ray Diffraction

TABLE OF CONTENTS

TABLE OF CONTENTS (Continued)

TABLE OF CONTENTS (Continued)

LIST OF TABLES

Table **Page**

LIST OF FIGURES

Figure **Page**

LIST OF TABLES IN THE APPENDIX

Appendix Table **Page**

LIST OF FIGURES IN THE APPENDIX

Appendix Figure **Page**

SYNTHESIS AND CHARACTERIZATION OF $Fe_3O_4/Al_2O_3/MnO_2$ TERNARY MIXED OXIDE NANOCOMPOSITE FOR PHOSPHORUS DESORPTION FROM ACID SOILS USING DIALYSIS MEMBRANE TUBE

ABSTRACT

In this study, ternary mixed oxide, $Fe_3O_4/Al_2O_3/MnO_2$ adsorbents where synthesized for desorption of phosphorus with ratios of NC_1 (90:5:5), NC_2 (80:15:5) and NC_3 (70:15:15) interms of percentage composition of Fe, Al, and Mn, respectively from its precursor, ferric chloride hexahydrate and ferrous chloride tetra hydrate, aluminum nitrate nonahydrate and manganese oxide by co-precipetation method under nitrogen atmosphere in basic condition and investigated for their phosphorus (P) desorption capacity. Among these NC_2, which was found to have high surface area and small size was selected and used for long-term P desorption and kinetic studies. The as-sythesized adsorbents were characterized with XRD, FTIR, FAAS, BET, SEM and EDX. Crystal structure of selected nanocomposite was slightly amorphous with a particular of size 22.75 nm and 203.69$\pm$1.34 m^2/g surface area. The study of phosphorus desorption were carried out on four different acidic soil samples, which were incubated for three months and twenty two days with four different concentration of (0,50,100 and 150 mg/kg) P. The simulation of P desorption from soil to plant was predicted by dialysis membrane tube filled with hydrous iron-aluminum-manganese oxide. DMT-HFAMO was found to be a promising adsorbent to simulate the plant–P relation in acidic soil or to estimate the properties of soil for P desorption to the soil solution. The observed desorbed P was significant in the order of Boji Dirmaji < Kiltu Kara < Mene Sibu < Nedjo and order of treatments P0 (0) < P1 (50) < P2 (100) < P3 (150) mg/kg for all soil samples. The releasing rate of P from soil to solution followed first order kinetics having rate constant (0.021-0.028 h^{-1}) and rapid release of P with in the first two weeks followed by a slower release and it was still continuing after 28 days of desorption. The physicochemical properties like available P, total P, organic carbon, bulk density, iron extracted by dithionite, iron extracted by oxalate, and manganese extracted by dithionite were correlated with cumulative desorbed P positively or negatively.

Keywords: Acid soil, Desorption, Dialysis membrane tube, Incubation, Kinetics, Magnetic Oxides, Phosphorus

1. INTRODUCTION

Phosphorus is an important nutrient that occurs widely in the environment. It is a second key vital element for every plant and animal next to nitrogen and commonly a limiting nutrient for plant growth in many soil arround the world (McDowell and Stewart, 2006). Phosphorus is mainly used in agriculture as a fertilizer or as food additive in the animal feed. The other applications of phosphorus include ingredients for human food, pharmaceuticals, detergents and some especial chemicals (DEFRA, 2008), plays an important role in RNA/DNA or cellular metabolism (Gilbert, 2009). The amount of phosphorus removed from a field by crops in general varies from 3-33% of applied phosphate fertilizer (Kamper and Claassens, 2005). In acidic soils, P is fixed into slightly soluble forms of precipitation and sorption reaction with Fe and Al compounds as well as crystalline and amorphous colloids (Sanchez and Uehera, 1980). Lack of phosphorus in soil can result in limited crop production (Zhou *et al*., 2018).

The main challenge facing agriculture in developing countries is to increase crop production in ways that are (1) sustainable, (2) have no detrimental effect on the environment and (3) minimally increase in input costs. One way of meeting this challenge is to use soil P more effectively and to manage P fertilizer more efficiently. A better understanding of the longterm desorption and longterm desorption kinetics of soils under cultivation could be valuable to help optimize fertilizer P programs (De Jager and Claassens, 2005). Management of phosphate fertilization is essential for maintaining the concentration of biologically available soil-P at a value adequate for plant growth, while minimizing the movement of dissolved-P and particulate-P to surface water and shallow groundwater. Soils also have a defined capacity to adsorb phosphorus and there will be a great possibility to release excess P into the surface or ground water when a critical phosphorus sorption saturation level is attained (Paulter and Sims, 2000). In the soil, phosphorus is existing in the forms of phosphate ($H_2PO_4^-$, HPO_4^{2-}, and PO_4^{3-}), organic phosphate and polyphosphate (Zhu *et al*., 2013).

The phosphorus availability for plants is usually done using single chemical extraction methods. However, it is accepted that the plant acquires its P from the soil solution that has to be replenished over the growth period. The availability of P to plants therefore depends, among other things, on the rate at which it is released to replenish the soil solution (Raven and Hossner, 1994). Due to P build up a significant residual effect could be expected and this can lead to an underestimation of the available P if not taken into account.

So that soil tests for plant available phosphorus was used worldwide to determine the current phosphorus status of soils so as to estimate fertilizer phosphorus requirements for specific yield goals. The current P status is due to indigenous (native) P present in the soil and P from previous fertilizer P application (residual P). Plant P availability of residual P in soils can be reliably estimated by successive cropping experiments carried out in field or green house conditions, where P is taken up until P deficiency occurs or a response to added P is measured (Indiati, 2000). This approach, however, takes many years to realize which makes it very expensive and time consuming and soil extractions with P sink methods have been proposed to estimate residual P. Contrary to the conventional soil P test methods, these P sink methods may be considered non-destructive methods as they do not react with soil and have minimal effect on the soil physicochemical properties that influence the release of P.

Furthermore, extraction with these sink methods prevents solution P from increasing to levels where further P release is prohbited and hence one can make a series of extractions from a soil sample (Indiati, 1998). Consecutive extraction of soils by these methods may therefore be a convenient laboratory method to characterize the capacity of soil to supply P and to investigate the kinetics of residual P release. Such methods use anion exchange resins (Abrams and Jarrel, 1992), iron oxide impregnated paper strips (Indiati, 2000) or dialysis membrane filled with hydrous ferric oxide solution DMT-HFO (Freese *et al*., 1995; Lookman *et al*., 1995; Koopmans *et al*., 2001; Taddesse *et al*., 2008a,b). Characterizing the residual phosphorus by employing these methods could solve the time frame by which these residual phosphorus become available for plant use in a reasonably short time and have minimal effect on the soil physicochemical properties that influence the release of P but lacks to indicate which P pools involve in replenishing the labile P pool.

Therefore, instead of attempting to tap the residual P by continually cropping till the plant responds, more rapid soil test methods that can approximate this biological measure have been required. In this regard, use of dialysis membrane tube filled with hydrous ferric oxide (DMT-HFO) in place of resin/iron oxide paper strips for studying long-term P dynamics has been proposed (Ochwoh *et al*., 2005; Taddesse *et al*., 2008a,b). This system is mechanically stable and capable of maintaining low P activity in solution for longer period of time and therefore, P release over long periods of time can be measured in a more natural environment than the routine soil tests (Freese *et al*., 1995; Lookman *et al*., 1995).

Multicomponent sorbents comprising mixtures of metal oxides, clay, quartz and organic compounds are ubiquitous in soils and aquatic environments and have been shown to be significant in determining the environmental distribution of various contaminants and nutrients like phosphates (Tofik *et al.*, 2016).

In view of the above facts, we hypothesized the use of Fe-Al-Mn ternary mixed oxide nanocomposite filled in the dialysis membrane tube could simulate better the plant mode of action as the surface property of the mixed metal oxides mimic the natural systems like soils more closely than their individual component (Sujana and Anand, 2010). In the recent years, there is limited information on the phosphorus desorption study using ternary mixed oxides nanocomposite filled in dialysis membrane tube for determination of phosphorus in the soil. In addition to this, effect of solubility, availability and extractability of P in the soil is influenced by the prevailing pH, soil texture, mineralogical composition, total organic matter content, organic carbon and by the presence of Fe and Al (hydr-) oxides (Abdu, 2006). The aim of this work is to evaluate the desorption of phosphorous from acid soil using dialysis membrane tube filled with iron-aluminum-manganese ternary mixed oxide nanocomposite. This study attempted to develop nano sized multi-component $Fe_3O_4/Al_2O_3/MnO_2$ sorbent system filled in the dialysis membrane tube (DMT) to investigate the desorption of phosphorus from acid soil.

Objectives of Study

General Objective

- To Synthesize and characterize nano sized multicomponent $Fe_3O_4/Al_2O_3/MnO_2$ mixed oxide nanocomposite adsorbent system to investigate the desorption of phosphorus from acid soils using dialysis membrane tube.

Specific Objectives

- To synthesize $Fe_3O_4/Al_2O_3/MnO_2$ ternary mixed oxides nanocomposite by using co-precipitation method.
- To characterize the as-synthesized nanocomposite using modern spectroscopic techniques such as FAAS, FTIR, XRD, BET, SEM and EDX.
- To investigate the long-term desorption of phosphorus from acid soils by filling the as-synthesized adsorbent in the dialysis membrane tube.

2. LITERATURE REVIEW

2.1. Nanotechnology

Nanotechnology is a field of applied science, focused on the design, synthesis, characterization and application of materials and devices on nanoscales. It is an emerging field that covers a wide range of technologies which are presently under development. It plays a major role in the development of innovative methods to produce new products, to substitute existing production equipment and to reformulate new materials and chemicals with improved performance resulting in less consumption of energy and materials and reduced harm to the environment as well as environmental remediation (Mansoori *et al*., 2008). As the exciting field of nanotechnology develops, the broader environmental impacts of nanotechnology will also need to be considered. Such considerations might include: the environmental implications of the cost, size and availability of advanced technological devices; models to determine potential benefits of reduction or prevention of pollutants from environmental sources (Nair and Pradeep, 2004).

Nanotechnology has been used for, detection of pesticides, chemical and biological substances including metals (e.g. cadmium, copper, lead, mercury, nickel, zinc), nutrients (e.g., phosphate, ammonia, nitrate, nitrite), cyanide organics, algae (e.g., cyanobacterial toxins) viruses, bacteria, parasites, antibiotics and biological agents (Diallo *et al.,* 2005). Pollution prevention by nanotechnology refers to the one hand to a reduction in the use of raw materials, water or other resources and the elimination or reduction of waste and on the other hand to more efficient use of energy or involvement in energy production (USEPAR, 2007). The implementation of green chemistry principles for the production of nanoparticles and for nanotechnological applications in standard chemical engineering will lead to a great reduction in waste generation, less hazardous chemical syntheses, improved catalysis and finally an inherently safer chemistry (Alamos, 2006).

2.2. Nanomaterials

A nanomaterial are particles with a small size, between 1-100 nm in one or more dimensions (He and Toh, 2006; Tretyakov and Goodilin, 2009) and they are core of an emerging technological revolution. Nanomaterials have been attracting great attention owing to their excellent electrical, optical, magnetic, catalytic properties and etc. With the development of science and technology, the requirements for the material quality are increasingly demanding.

It is currently applied in a wide variety of fields, including environmental and wastewater treatment. The use of nanomaterial has enormously increased during the recent years leading to the development of new generation of technologies for environmental and public health protection (Klabunde, 2001). Nanoparticles, due to their high reactivity, as a result of their small size and smallest pores, can accelerate the removal and degradation rate of contaminants in the source zone, via sorption or complexation, with a consequent decrease of the cost and time of remediation with respect to traditional treatment technologies.

Nanomaterials can be grouped into four type (USEPA, 2005); (1) carbon-based materials, such as fullerene, single walled carbon nanotubes (SWCNTs) and multi walled carbon nanotubes (MWCNTs); (2) metal-based materials such as quantum dots, nanogold, nanozinc, nonaluminum and nanoscale metal oxides like TiO_2, ZnO and Al_2O_3 (3) dendrimers and (4) nanocomposites (Wang, 2005). Other notable advantage of the nanomaterials is they are widely used as separation media in water purification to remove inorganic and organic pollutants from contaminated water. Nanoparticles also have wide application in the medicine, textiles, cosmetics, agriculture, optics, food packaging, optoelectronic devices, semi-conductor devices, aerospace, construction and catalysis and polymeric application (Khayat and Khayat, 2012). Several research groups are exploiting the unique properties of nanoparticles like size, shape, chemical composition, stability, etc to develop high capacity and selective sorbents for metal ions and anions (Li *et al*., 2003).

2.3. Nano Sized Metal Oxides

Metal oxides play a very important role in many areas of chemistry, physics and materials science. In technological applications, oxides are used in the fabrication of microelectronic circuits, sensors, piezoelectric devices, fuel cells, coatings for the passivation of surfaces against corrosion and as catalysts. Metals and their oxides act as a heterogeneous catalyst in many industrial chemical processes. Since the reaction rate on a catalyst surface depends upon the total surface area and the number of active sites present, a good catalyst is required to possess smaller particle and high surface area. Metal oxides generally exhibit both electron and proton transfer abilities and can be used as catalysts in redox as well as acid-base reactions. The redox properties of oxides are exploited in catalytic purification systems for complete oxidation of toxic materials (Hu *et al.*, 2010).

Metal oxides are used for both their redox and acid/base properties in the context of adsorption and catalysis. The three key features essential for their application as adsorbents or catalysts are (i) the coordination environment of surface atoms, (ii) the redox properties, and (iii) the oxidation state at surface layers. In a simple classification, oxides having only s or p electrons in their valence orbital's tend to be more effective for acid/base catalysis, while those having d or f outer electrons find a wider range of uses for example as adsorbent (Yang *et al*., 2008). In the emerging field of nanotechnology, a goal is to make nanostructures or nanoarrays with special properties with respect to those of bulk or single particle species. Oxide nanoparticles can exhibit unique physical and chemical properties due to their limited size and a high density of corner or edge surface sites (Karn *et al*., 2009; Bhattacharje *et al*., 2011).

Among the available adsorbents, nano sized metal oxides (NMOs), including nano sized ferric oxides, manganese oxides, aluminum oxides, titanium oxides, magnesium oxides and cerium oxides are classified as the promising for inorganic anions such as arsenic (Cumbal and SenGupta, 2005), fluoride (Zhang *et al*., 2007) and phosphate (Zhang *et al.,* 2009; Mäkiea *et al*., 2013) removal from environmental solution systems. This is partly because of their large surface areas, high capacity and selectivity and high activities caused by the size-quantization effect. The size and shape of NMOs are both important factors to affect their adsorption performance (Agrawal and Sahu, 2006).

Multicomponent sorbents comprising mixtures of metal oxides, clay, quartz and organic compounds are now a days ubiquitous in soils and aquatic environments and have been shown to be significant in determining the environmental distribution of various contaminants and nutrients like phosphates (Tofik *et al.*, 2016).These sorbents form via dissolution, adsorption, desorption, co-precipitation or colloidal interactions and often exhibit different P sorption behaviors compared to single component sorbents. For example, Manganese dioxide (δ-MnO_2) 1.4 mg/g (pH 8.0) (Masue *et al*., 2007), Zhang *et al*. (2009) reported that a Fe–Mn binary oxide had a high phosphate sorption capacity of 36 mg/g at pH 5.6 and Maeng *et al*. (2013) clearly showed that the phosphate removal efficiencies of Fe-Mn-Si oxide (ternary nanocomposite), which contributed to different maximum adsorption capacities of adsorbents is 47.8 mg/g PO_4^{3-}. The studies of surface property of the mixed metal oxides are important because they mimic (stimulate) the natural systems like soils more closely than their individual component (Sujana and Anand, 2010).

2.3.1. Aluminum Oxide Nanoparticles

Alumina has many appealing properties which makes the material interesting for applications in many different areas. Alumina especially has a high melting point, high strength, corrosion resistance, chemical stability, low thermal conductivity and good electrical insulation properties. As a type of important structural ceramic material, alumina has applications in absorbent, catalyst, carrier and reinforcement of ceramic composites. Alumina occurs in nature as the minerals, corundum (Al_2O_3), diaspora ($Al_2O_3.H_2O$) and gibbsite ($Al_2O_3.3H_2O$) and most commonly as bauxite, which is an impure form of gibbsite. Alumina exists in a number of crystalline phases (polymorphs), three of the most important being γ, θ, and α. The α-alumina structure is thermodynamically stable at all temperatures up to its melting point at 2051 ^oC, but the metastable phases (e.g., γ and θ) still appear frequently in alumina growth studies. Transition aluminium is high surface area oxides formed by controlled calcination of aluminium oxyhydroxide.

The structures of aluminum oxide are of two types, hexagonal and octahedral in which it holds the atoms. Hexagonal sites are the corner atoms in the cell while the octahedral sites are present between two layers of vertical stacking. The oxygen present in octahedral sites permits strong bonding and therefore, gives rise to the characteristics properties of alumina. The basic unit cell structure of corundum i.e., α-alumina has a hexagonal structure but the γ- alumina has a spinel structure. The γ -alumina phase is an unstable phase and it is transformed to the θ-alumina phase at a temperature of 700-800 ^oC. This phase of alumina is used as catalyst and catalyst support because of it shows high surface area.

The lattice structure of gamma alumina has two different lattices, the first lattice is comprised of aluminum ions and it is formed from octahedral and tetrahedral interstitial locations and the oxygen lattice is formed with the face Centre cubic structure. Boehmite (γ-AlOOH) is an aluminum oxyhydroxide, which is used as a precursor for many aluminum oxide materials, especially for the preparation of catalysts, membrane, coating, adsorbents etc. Upon heating at temperatures between 400 and 700 ^oC, boehmite undergoes an amorphous transformation to nano crystalline γ-Al_2O_3 without altering the morphology of the parent material (Cai *et al*., 2010). Among one-dimensional nanostructures, nano fibers show broad application and properties. So, alumina nano fiber has a large number of applications including high temperature insulation, catalyst support in high temperature reactions, fire protection and as reinforcement

for resins, metal and ceramic. Its importance is due to its high strength and modulus, resistance to attack by molten metal's and non-oxide materials, chemical inertness in both oxidizing and reducing atmospheres up to 1000 ^{o}C, low thermal conductivity and good electrical insulation (Yu *et al*., 2012).

2.3.2. Iron Oxide Nanoparticles

Iron oxides are the most important transition metal oxides of technological importance. Sixteen pure phases of iron oxides, i.e., oxides, hydroxides or oxy-hydroxides are known to date. These are $Fe(OH)_3$, $Fe(OH)_2$, $Fe_5HO_8{\cdot}4H_2O$, Fe_3O_4, FeO, five polymorphs of FeOOH and four of Fe_2O_3. Characteristics of these oxide compounds include mostly the trivalent state of the iron, low solubility and brilliant colors. These oxides find applications as catalysts, sorbents, pigments, flocculants, coatings, gas sensors, ion exchangers and for lubrication (Choo and Kang, 2003). The facileness of resource and ease in synthesis render nano sized ferric oxides (NFeOs) to be low-cost adsorbents for toxic metal sorption. The intensively studied NFeOs for heavy metals removal from water/wastewater include goethite (α-FeOOH) and hematite (α-Fe_2O_3) used for removal of Cu(II) (Chen and Li, 2010). Hematite presents a very similar structure to goethite based on a hexagonal close packing of the anion (O^{2-}) (Laurent *et al*., 2008).

The magnetic nanoparticles have many uses such as magnetic drug target, magnetic resonance imaging for clinical diagnosis, catalyst and environment (Bolto, 1990). Iron oxides nanoparticles play a major role in many areas of chemistry, physics and materials science. Magnetite (Fe_3O_4) is one of the magnetic nanoparticles. There are many various ways to prepare Fe_3O_4 nanoparticles, which have been reported in other papers, such as energy milling (Bolto, 1990), reducing (Fuertes and Tartaj, 2008), ultrasonic assisted impregnation (Yang *et al*., 2008), using Tridax procumbens leaf extract (Senthil and Ramesh, 2012) and co-precipitation method which is easy to do with the success rate from 96 to 99.9% (Liong, 2005).

In chemical co-precipitation , ferrous and ferric salt at the ratio of 1 to 2 in alkaline medium react to give magnetite and produced fine, stoichiometry particles of single and multi-component metal oxides (Kentish and Stevens, 2001). The application of magnetic technology to solve environmental problems has received considerable attention in recent years. Many of papers have been published demonstrating that magnetic (Fe_3O_4) can be used for wastewater purification, such as to adsorb arsenite, arsenate, chromium, cadmium, nickel (Mayo, *et al*., 2008). Magnetite also can be used for alkalinity and hardness removal, desalination,

decolourisation of pulp mill effluent and removal of natural organic compounds (Bolto, 1990). After adsorption, Fe_3O_4 can be separated from the medium by a simple magnetic process. Thus, can be an efficient, economic, scalable, and non-toxic.

2.3.3. Manganese Oxide Nanoparticles

Manganese oxides are of considerable interest since these materials can be used in adsorption, catalysis, and other applications. Nano-MnO_2 has a great potential application in environment protection field as a new generation of environmentally friendly catalyst. Nano sized manganese oxides (NMnOs) exhibit an adsorptive performance superior to their bulk counterpart because of their polymorphic structures and higher specific surface area (Wang *et al*., 2012). Manganese oxides, including MnO, MnO_2 and Mn_3O_4 are intriguing composites and have been used in wastewater treatment, catalysis, sensors, super capacitors, and alkaline and rechargeable batteries. Particularly, MnO and MnO_2 nanomaterials have attracted attention for their high theoretical capacity, low cost, environmental benignity and special properties (Cheng *et al*., 2006). Manganese dioxide appears in a number of different polymorphic forms, such as α-MnO_2, β-MnO_2, γ-Mn_2O_4, δ-MnO_2 and MnO.

Moreover, lots of successes on the properties and applications of manganese oxides nanomaterials have been reported in the last few years, for example, a hydrothermal method has been used to synthesize sea urchin shaped α-MnO_2 (Yu *et al*., 2009). Different rearrangements of octahedral MnO give rise to manganese oxides with tunnel and layered structures, which exhibit cation exchange and molecule adsorptive properties, like zeolites and clay minerals. As an important functional metal oxide, manganese oxide nanoparticles are one of the most attractive inorganic materials because of their physical and chemical properties and wide applications in catalysis, ion exchange, molecular adsorption, biosensor and particularly energy storage (Harish *et al*., 2013). In addition, MnO_2 has been shown to adsorb metals and organic compounds, further enhancing its possible use as a removal substrate for noxious environmental agents in water. The MnO_2 reactor, however, removed significantly more 17a ethynylestradiol (EE2) due to its catalytic properties. These catalytic properties could make it a cost-efficient technique for the removal of 17a-ethynylestradiol (EE2) (De Ruddera *et al*., 2004).

2.4. Dialysis Membrane Tube

Dialysis occurs throughout nature and humans have exploited the principles of dialysis for thousands of years using natural animal or plant based membranes. The term dialysis was

first routinely used for scientific or medical purposes in the late 1800s and early 1900s, pioneered by the work of Thomas Graham. The first mass-produced man-made membranes suitable for dialysis were not available until the 1930s based on materials used in the food packaging industry such as Cellophane. In the 1940s, Willem kolff constructed the first dialyzer (artificial kidney) and successfully treated patients with renal failure using dialysis across semi-permeable membranes. Today, dialysis tubing for laboratory applications comes in a variety of dimensions and molecular-weight cutoffs (MWCO). In addition to tubing, dialysis membranes are also found in a wide range of different preformatted devices, significantly improving the performance and ease of use of dialysis.

Different dialysis tubing or flat membranes are produced and characterized as differing molecular weight cutoffs (MWCO) ranging from 11,000,000 kDa. The MWCO determination is the result of the number and average size of the pores created during the production of the dialysis membrane. The MWCO typically refers to the smallest average molecular mass of a standard molecule that will not effectively diffuse across the membrane upon extended dialysis.

Dialysis tubing for laboratory use is typically made of a film of regenerated cellulose or cellulose ester. However, dialysis membranes made of polyethersulfone (PES), etched polycarbonate, or collagen are also extensively used for specific medical, food, or environ-mental application such as water treatment and soil. Dialysis tubing is a cellulose material used in the removal of salts and low molecular weight compounds during the purification of biomolecules. It is a thin polymeric membrane exhibiting maximum wet strength, compatibility with a wide variety of solvents, minimal polarity and uniform pore size. Researchers (Freese *et al.*, 1995; Taddesse *et al*., 2008a,b) have studied that, it also used for the identification of phosphorus-rich and phosphorus leaky soils to estimate the risk of phosphorus (P) using HFO-DMT and DMT-HFAMO (Gemechu *et al*., 2015). As described by these researchers this methods is best methods for estimating plant available phosphate and recommends external phosphate fertilizer requirements.

2.5. Synthesis Techniques of Nano Sorbent

There are different synthesis methods for preparation of nanoparticles, including: sol-gel, hydrothermal, co-precipitation, impregnation, electrochemical adsorption (SEA) and micro emulsion (Salabata *et al*., 2012). Generally, the synthesis methods can be classified into two categories: (1) physical approaches, including inert gas condensation, severe plastic

deformation, high-energy ball milling, ultrasound shot peening and (2) chemical approaches, including reverse micelle (or micro emulsion), controlled chemical co-precipitation, chemical vapor condensation, pulse electrode position, liquid flame spray, liquid phase reduction, gas phase reduction (Li *et al*., 2009). Among these synthesis protocols, co-precipitation (Cushing *et al*., 2004), thermal decomposition or reduction, sol gel method (Park *et al*., 2004) and hydrothermal synthesis (Wang *et al*., 2005) techniques are used widely and are easily scalable with high yields and some of them are presented below.

2.5.1. Hydrothermal Synthesis Method

Hydrothermal synthesis is typically carried out in a pressurized vessel called an autoclave with the reaction in aqueous solution. The temperature in the autoclave can be raised above the boiling point of water, reaching the pressure of vapor saturation. Hydrothermal synthesis is widely used for the preparation of metal oxide nanoparticles which can easily be obtained through hydrothermal treatment of peptized precipitates of a metal precursor with water (Chen and Mao, 2007). Hydrothermal method can be useful to control grain size, particle morphology, crystalline phase and surface chemistry through regulation of the solution composition, reaction temperature, pressure, solvent properties, additives and aging time (Carp *et al*., 2004).

2.5.2. Sol-gel Method

Sol-gel processing is a common chemical approach to produce high purity materials shaped as powders, thin film coatings, fibers, monoliths and self-supported bulk structures (Keshmiri *et al*., 2006). The sol-gel process involves hydrolysis and condensation of the metal alkoxide followed by heat treatment at elevated temperatures which induce polymerization, producing a metal oxide network (Verma *et al*., 2005). The sol-gel method has several advantages over other synthesis techniques such as purity, homogeneity, ease of preparation and ease of introducing dopants, composition and the ability to produce thin film coatings or porous powders. There are two possible routes for carrying out sol-gel synthesis, the non-alkoxide route and the alkoxide route. The non-alkoxide route uses inorganic salts as the starting material (Carp *et al.,* 2004). This requires the removal of the inorganic anion to produce the required oxide. However, halides often remain in the final oxide material and are difficult to remove. The alkoxide route involves hydrolysis of a metal alkoxide, followed by condensation. The

hydrolysis/condensation reactions typically form a three dimensional polymeric structure, that, upon calcination will result metal oxide crystals depending on the calcination temperature.

2.5.3. Co-precipitation Method

The co-precipetation method involves the separation of solid containing target metal ions from solution phase. In this process the metal component of the superconducting materials are first dissolved in solution. Solution combines with precipitants in supersaturated condition to form ion associate or clusters. Co-precipitation method is commonly used for preparation of iron catalysts nanocomposites. Co-precipitation of various salts (nitrates, sulphates, chlorides, perchlorates etc) under a fine control of pH by using NaOH or NH_4OH solutions yields corresponding spinel oxide nanoparticles. For example to prepare $ZnFe_2O_4$, zinc nitrate and ferric nitrate are used as starting precursors. The pH of the medium should be above 8 to get the better end product. Particle size of the co-precipitated material is strongly dependent on pH of the precipitation medium and molarity of the starting precursors. Consequently particle size control can be easily achieved (Fahmida *et al*., 2009). A crystalline phase is achieved even with a pH around 8 if we use a salt that contain Fe^{2+} ions (in the case of inverse spinel ferrite).

The electron mobility between Fe^{2+} and Fe^{3+} acts as the driving force for the spinel phase formation. But when we have to deal with normal spinel ferrites that have only Fe^{3+} ions we have to increase the pH of the medium to achieve crystalline, pH of 12 is desired in this case. If we increase molarity of the solution, particle size gets reduced. But this size reduction is achieved at the expense of large amount of chemicals. Hence a compromise between this leads us to prefer a moderate morality for the starting solutions (Gayathri, 2007). The most important advantage of this technique is its feasibility for large-scale production as well as its simplicity and low cost. Co-precipitation method also offers some other advantages:

- Simple and rapid preparation
- Various possibilities to modify the particle surface state and overall homogeneity
- Homogeneity in mixed precipitates
- High specific surface of the products (Pradhan *et al*., 2001).

2.5.4. Impregnation Method

Impregnation is the most effective process for eliminating the inherent problems of porosity in cast and powdered metal. Properly processed castings are clean and have no change in

appearance or dimensions. Metal-impregnated materials are typically prepared in a multi-step process: (1) oxide formation of precursor, (2) physical or chemical activation of the oxide product, (3) catalyst impregnation (using excess solution, incipient wetness, ion exchange, or chemical vapor deposition techniques) and (4) reduction or pyrolysis to form metal nanoparticles. The process is usually non-continuous and can require substantial time and energy. Each step requires heat, and at the activation and stage requires supplemental reagents to develop porosity.It is advantageous to simplify this process to allow continuous production of metal-impregnated, porous materials. Impregnation method for the synthesis of mixed metal oxide nano sorbent has the following advantages: good homogeneity, low reaction temperature, fine and uniform particle size, easy scale-up, low cost and time saving processing (Haber *et al*., 1995).

2.6. Global Cycling and Phosphate Chemistry

Weathering of geologic materials is the ultimate source of phosphate to the biosphere; however, the amount of phosphate released is a small fraction of that required for the current levels of biological production. This deficiency results in phosphate being highly conserved and very rapidly cycled within the biosphere (Berner and Berner, 1996; Filippelli and Souch, 1999). Vegetation, periphyton, plankton and microbes all acts as biotic phosphorus sinks. However, biotic cycling is not without P loss to abiotic mechanisms, including adsorption by soils and sediments, mineral precipitation and sedimentation. Phosphate lost from the biomass is quickly complexed by iron and aluminum oxides or sorbed by clay minerals (Berner and Berner, 1996).

Dissolution of phosphate minerals and complexes may be expedited by plant root exudates or mycorrhizae, but the major environmental transformations of phosphate are not biologically or chemically driven. The largest flux of phosphate in terms of geochemical cycling is fluvial transport to the oceans. Phosphate cycling within the water column is quite rapid, but constant losses of small amounts from the biomass to the sediments and soils have resulted in oceanic sediments being the largest phosphate reservoir on earth. Phosphorus adsorption by soils and lake sediments has often been correlated to amorphous iron, aluminum, and manganese oxides and hydroxides, as well as calcium and magnesium (Alvarez *et al*., 2004). Once sequestered within soils or sediments, phosphate falls into one of four categories: phosphate minerals, labile or non-labile sorbed phases, or organic phosphate. Non-labile and labile soil phosphate pools fall into calcium bound phosphate and iron or aluminium bound phosphate. Non-labile phosphorus is usually incorporated within the matrices of Fe and Al minerals are usually quite

insoluble. Labile, or more bioavailable, phosphate is sorbed to the surface of silica, calcium carbonate, or other soil minerals. In acidic soils, iron and aluminum phosphate minerals and complexes are dominant, while calcium phosphates are the main controlling phases in alkaline environments.

Several common soil phosphate minerals are; apatite [$Ca_5(PO_4)_3(OH,F,Cl)$], hydroxyapatite [$Ca_5(PO_4)_3OH$], fluorapatite [$Ca_5(PO_4)_3F$], octocalcium phosphate [$Ca_8H_2(PO_4)_2.5H_2O$], strengite [$FePO_4.2H_2O$], vivianite [$Fe_3(PO_4)_2.8H_2O$], variscite [$AlPO_4.2H_2O$] and wavellite [$Al_3(PO_4)_2(OH)_3.5H_2O$] (Brady and Weil, 1999; Alvarez *et al*., 2004).

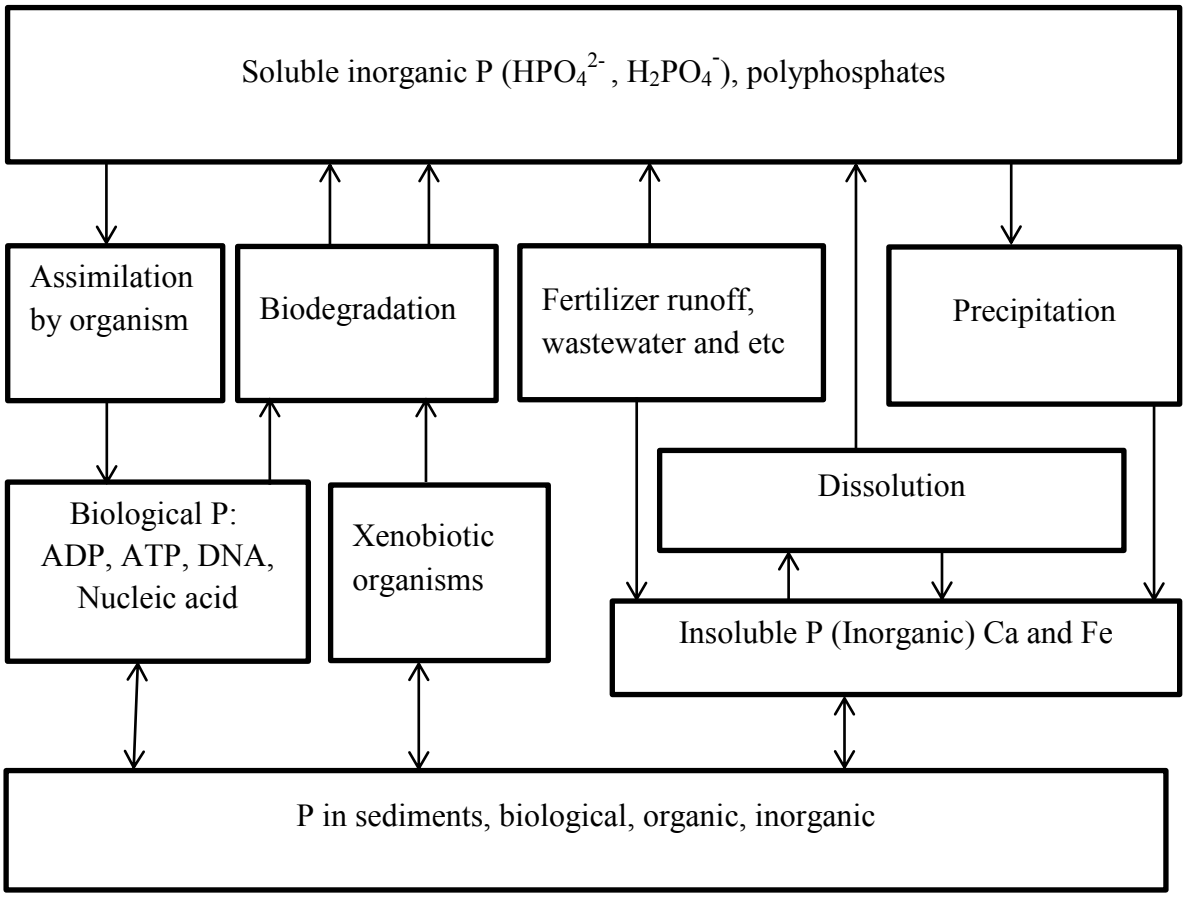

Figure 1. Depiction of the Phosphorus Cycle (Manahan, 1994)

Organic phosphate is typically categorized into three groups. Inositol phosphates make up 10 to 50 percent of the total organic phosphate pool in soils. These compounds are phosphate esters of sugar like molecules and are usually very stable in alkaline conditions and are likely to react with higher molecular weight compounds.The second group consists of phosphate contained within nucleic acids, which may be sorbed by silicate clays and humic acids. Organic phosphate must be converted back to an inorganic form via mineralization in order to be usable by higher

plants. Humus and organic matter will decompose to release HPO_4^{2-} or $H_2PO_4^-$, depending on pH. From this, $H_2PO_4^-$ and HPO_4^{2-} species are present in the pH region between 3 and 11. The concentration of $H_2PO_4^-$ species is high between 3 and 6 while HPO_4^{2-} species prevail at pH between 8 and 11, which means the $H_2PO_4^-$ ions are predominating at pH 3-6 and in the high pH range, the HPO_4^{2-} ions are dominating. Around pH 4 to 5, the highest fraction of $H_2PO_4^-$ exists (Karageorgiou *et al.,* 2007) (Figure 2). The $H_2PO_4^-$ species are more easily adsorbed on metal hydroxide surfaces than HPO_4^{2-} species when pH is below 6, but HPO_4^{2-} species are more likely precipitated with Mg or Ca in the alkaline solution than $H_2PO_4^-$ species (Xiaofang *et al*., 2007).

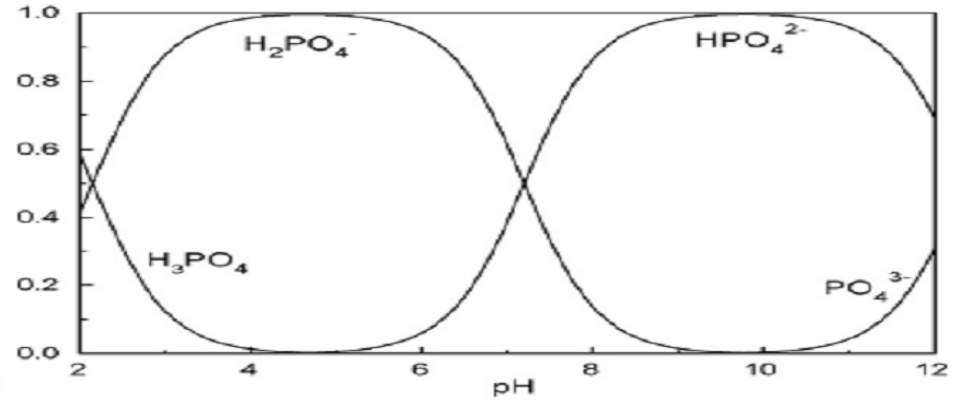

Figure 2. Distribution of major species of inorganic phosphorus

Soil conditions and the presence or absence of carbon will dictate whether the released phosphate is rapidly reincorporated into the biomass, precipitates as a mineral, or retained as a sorbed phase.

2.6.1. Adsorption

In the adsorption process, species from a gas or a liquid bind to the surface of a solid or a liquid. The molecules which are extracted from a phase and concentrated at the surface of a solid or liquid are called adsorbate. When the adsorbate adsorbs on a solid surface, the solid material is called adsorbent.The reverse process, in which the molecules detach from the surface of a solid or liquid to a gas or a liquid is called desorption (Masel, 1996).

Two main kinds of adsorption processes occur: chemical adsorption and physical adsorption. Chemical adsorption implies a (covalent) chemical bond between a specific adsorption site of the adsorbent and the adsorbate. On the other hand, in physical adsorption, weak chemical interactions, such as van der Waals and hydrogen bonding occur between adsorbent and

adsorbate. Therefore, in physical adsorption, the chemical structure of the adsorbate and adsorbent do not undergo any major chemical changes as a result of the adsorption. Chemical adsorption is normally associated with a higher enthalpy of adsorption and slower kinetics of adsorption than physical adsorption (Masel, 1996; Crittenden and Thomas, 1998). Since chemical adsorption implies that the adsorbent reacts with a specific adsorption site of the adsorbent, there is an upper limit to the quantity which may adsorb on the surface i.e. when the adsorbate has covered all the sites available resulting in a monolayer covering the surface. On the other hand, in physical adsorption, multilayers are frequently formed (Crittenden and Thomas, 1998). This is because the adsorbate molecules can adsorb on each other via van der Waals-or hydrogen bonding forces.

2.6.2. Phosphate Adsorption Mechanisms

Adsorption occurs when phosphate ions are removed from solution and become attached to the surface of adsorbent. Adsorption is originally thought to be a simple exchange reaction which took place on the surface of iron, aluminum and manganese hydroxides when it is considered as adsorbent. It seems more likely that chemisorptions reactions are involved. Binuclear or bridging complexes are formed between $H_2PO_4^{2-}$ ions and metal oxide surfaces and OH_2 and OH^- are displaced. The precise nature of these reactions depends on pH , which influences the proportions of OH_2 and OH^- groups on the solid surface and hence on its surface charge. Adsorption also dependent on pH, which seemed to be the major influence on adsorption. In a mechanistic way introduced by Saha *et al*. (2009), the chemical reaction of the phosphate adsorption can be given as in equation.

$$PO_4\text{-}P_{initial} + \text{adsorbent} \leftrightarrow \text{Adsorbent-}P_{initial} + PO_4\text{-Pfree}$$

2.6.3. Sorption Process

Sorption describes two processes (Haygarth and Sharpley, 2000): (a) adsorption, which occur when phosphate ions are adsorbed to the surface of particles and (b) absorption when adsorbed ions diffuse into the solid; and “sorption” is the general term used for these processes. Phosphate may become trapped on the surface of soil minerals under coating of iron oxide precipitates (Moazed *et al*., 2012). The trapped phosphate is termed as occluded. Phosphate ions are more strongly sorbed by iron oxide surfaces due to their large surface area. Soluble P added to soil, initially undergoes a very rapid exothermic reaction (adsorption)

followed by a slow reaction (absorption) resulting in occluded P. Occlusion takes place in the iron oxide structures. A rapid reaction is a ligand-exchange reaction (Samadi, 2006).

Phosphate sorption capacity increases with clay content, because clay particles have a large surface area on which phosphate can be sorbed (phosphate is an anion, therefore soil particles that have an anion exchange capacity will from strong bonds with phosphate). Clayey materials with more than 20% iron or aluminum oxides in their clay-size particles sorb large quantities of added phosphorus, transforming them into slowly soluble iron and aluminum phosphates that are not immediately available to plants. High P retaining soils are often clayey with red or yellowish colours indicative of high contents of iron and aluminum oxides; usually, such soils have a strong granular structure (e.g., Ferralsols). High phosphorus retention is related to high clay content, therefore, most sandy red soils do not fall in this category (Sanchez *et al*., 2003).

Phosphate is chemisorbed on the reactive iron oxide surface groups through a binuclear bridging mechanism. An OH^- or H_2O molecule is released from the surface and phosphate bridging complexes are formed between HPO_4^{2-} ions and iron oxide surface. This sorption reaction is strongly non-reversible and the sorbed P is mostly unavailable for plant uptake (Gichangi *et al*., 2008). At hydroxylated surfaces, a positive or negative charge is created by the adsorption or desorption of H^+ or OH^- ions, which is balanced by an equivalent amount of anion through specific adsorption. Sorption of P is occurs through ligand exchange on variable charge surfaces by the exchange of OH^- on the surface for phosphate ion. There is covalent bond between the metal ion and the phosphate ion. Phosphate is considered to sorb mainly as an inner-sphere complex, which means that the sorption takes place at specific coordination sites on the oxides or hydroxides (Figure 3). These reactions are termed as “ligand exchange reactions” because the anion displaces OH^- or H_2O from coordination positions of iron and/or aluminum ion at the surface that are the sites of chemisorptions. The surface complexes have been directly confirmed by X-ray photoelectron spectroscopy.

The sorption reaction is strongly non-reversible and the sorbed phosphate is mostly unavailable for plant uptake (Gichangi *et al.*, 2008). The precise nature of these reactions depends on pH, which influences the proportions of H_2O and OH^- groups on the solid surface, and hence its surface charge. Unlike metal cations, sorption of oxyanions decreases with increasing pH. Phosphorus is more strongly surface-associated through covalent bonds formed by ligand exchange with oxide surfaces’ OH^- groups compared to SO_4^{2-}, which is a

non-specifically bound oxyanion and is weakly surface-associated due to electrostatic interaction. Phosphate adsorption continually decreased with increasing pH. Phosphorus interacts more strongly with goethite, probably following an adsorption process and was observed more evenly distributed at its surface.

The bounded Al, Fe and Mn to phosphorus in soil determined by dithionite–citrate and acid ammonium oxalate methods (Mehra and Jackson, 1960) that dithionite–citrate removes organically complexed Al, Fe, and Mn, amorphous inorganic Al, Fe, and Mn compounds and noncrystalline aluminosilicates where as acid ammonium oxalate removes organically complexed and amorphous inorganic forms of Al, Fe and to a lesser extent, Mn and noncrystalline aluminosilicates from soils (McKeague, 1967).

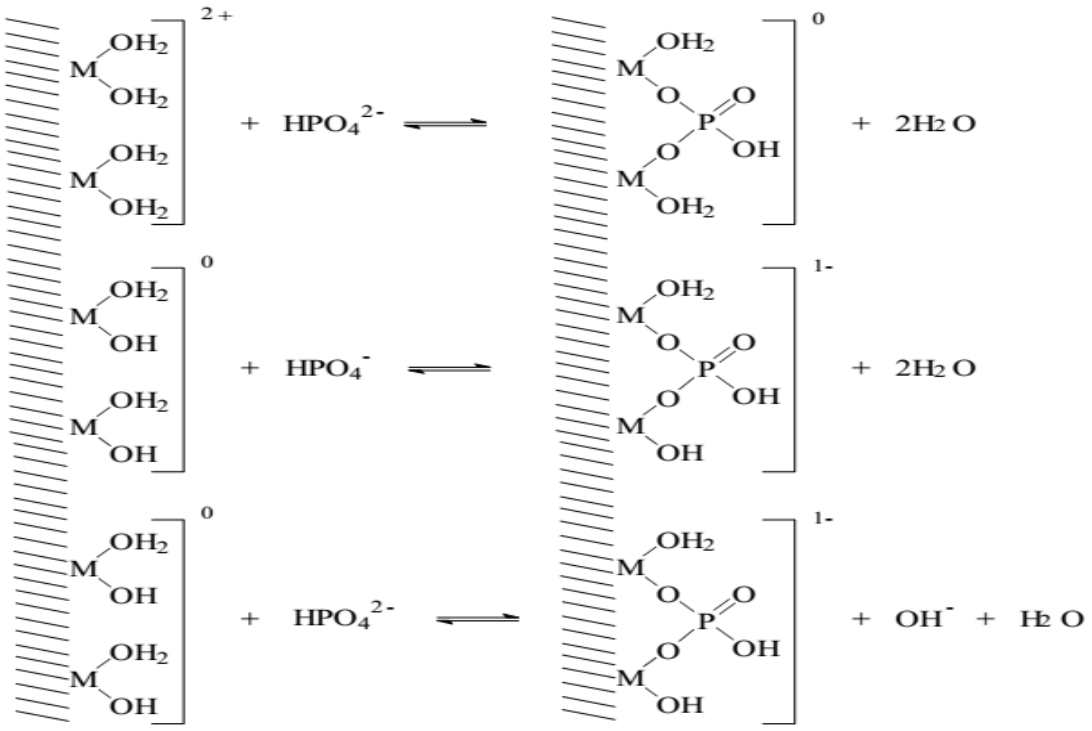

M = Al or Fe

Figure 3. Phosphate adsorption mechanisms due to absorption or penetration

As studied by (Gichangi *et al*., 2008) on seven soil of different samples widely in their capacities to sorb P with four of the soil samples classified as low P fixing and the remaining three (43%) as moderate P fixers and concluded that latter category may need management

interventions to ensure that P availability to crops is not compromised. The contrasting differences in the P fixing capacities of the soils suggested that the use of blanket phosphate fertilizer recommendations may not be a good strategy for the region as it may lead to under-application or over-application of P in some areas with the attendant consequences of compromised crop yields or freshwater quality. The differences in P sorption observed between the different soils were largely explained by variations in their citrate dithionite bicarbonate-extractable aluminum contents indicating that this parameter could be used for indicating the potential soil P sorption in the area.

Soils differed markedly in their ability to hold P, though P adsorption was high in all observed soil when Fe oxides and Al oxides contents dissolved, reactive P could be found in percolating water in consequence of Fe solubility enhanced by reducing condition held P. A relationship between the iron content in high reactivity form and the adsorption of P resulting from a decreased P in solution was found. Therefore, after flooding- drained condition, P availability to plants decreased due to adsorption of P with recently precipitated high reactivity forms of irons oxides (Hernandez and Meurer, 2000).

2.7. Desorption

Desorption is the release of one substance from another, either from the surface or through the surface. For example release of P from the solid phase in to the solution phase. Desorption can occur when an equilibrium situation is altered. The rate of P desorption from the soil solid phase is obviously dependent on the particular desorption conditions, which include the soil/ solution ratio, the vigor of shaking, the gradient of phosphate concentration near the solid phase, concentrations of various cations in solution, and temperature. Although long-term P desorption can be described in terms of two discrete P pools (fast and slowly desorbable P) (Lookman *et al*., 1995). One should bear in mind that most soils appear to exhibit a continuum of desorbable P forms as illustrated, for instance, by the complex chemistry of P-rich soil particles (Horta and Torrent, 2007).

2.7.1. Phosphorus Desorption Kinetics

The kinetics of P desorption is a subject of importance in soil and environmental sciences primarily because P uptake by plants occurs over a period of time. The kinetics of soil P sorption and desorption are characterized by two phases: a first rapid, followed by a second

slower phase (Harvey and Rhue, 2008; Fekri *et al*., 2011; Wang *et al*., 2013). The sorption and desorption kinetics in soil are mainly controlled by the content of soil organic matter (OM), clay content, pH and Fe and Al oxyhydroxides (Nafiu, 2009). With regard to clay, the number of P sorption sites is greater, when the clay content is higher, reducing P availability.

Thus, kinetic information is required to properly characterize the P supplying capacity of soils, to design P-fertilizer management to optimize efficiency, to reduce environmental pollution and to develop guidelines for the disposal of P-rich wastes onto the land. Another reason for kinetic studies is to obtain information on reaction mechanisms. In order to assess long-term P desorption kinetics, it is necessary to sufficiently suppress the backward resorption reaction. This can be done by introducing effective P sink into the system. Van der Zee *et al*. (1987) proposed the use of Fe oxide impregnated filter paper strips (Fe-oxide strips) as a promising method to study the P release kinetics of soils. Acting as a sink for P, the Fe-oxide strips have a sounder theoretical basis than the chemical extractants in estimating available soil P (Sharpley, 1996). However, this method was not found to be suitable for long-term desorption studies as it may lead to errors due to adhesion of fine P rich particles to the paper strips and due to the mechanical instability of the paper when used for long desorption studies (Freese *et al*., 1995; Lookman *et al*., 1995).

Recently, use of dialysis membrane tubes filled with hydrous ferric oxide (DMT-HFO) in place of resin/Fe-oxide paper strips for studying long-term P dynamics has been proposed (De Jager and Claassens, 2005; Ochwoh *et al*., 2005; Ochwoh *et al*., 2016). Nonetheless, relatively little information is available in the literature in relation to the use of this method. Lookman *et al.* (1995) studied the kinetics of P desorption using this procedure. They concluded that P desorption could be well described by a two component first order model. They also reported that no desorption maximum was reached in the entire period of desorption (1600 h). Research was also done which linked short-term soil P tests to longterm soil P kinetics (Koopmans *et al*., 2001; Maguire *et al*., 2001). Recently, studies were also made on some South African soils using the DMT-HFO method as a phosphate sink (De Jager and Claassens, 2005; Ochwoh *et al*., 2016) investigated the desorption kinetics of residual and applied P to acid sandy clay soils.

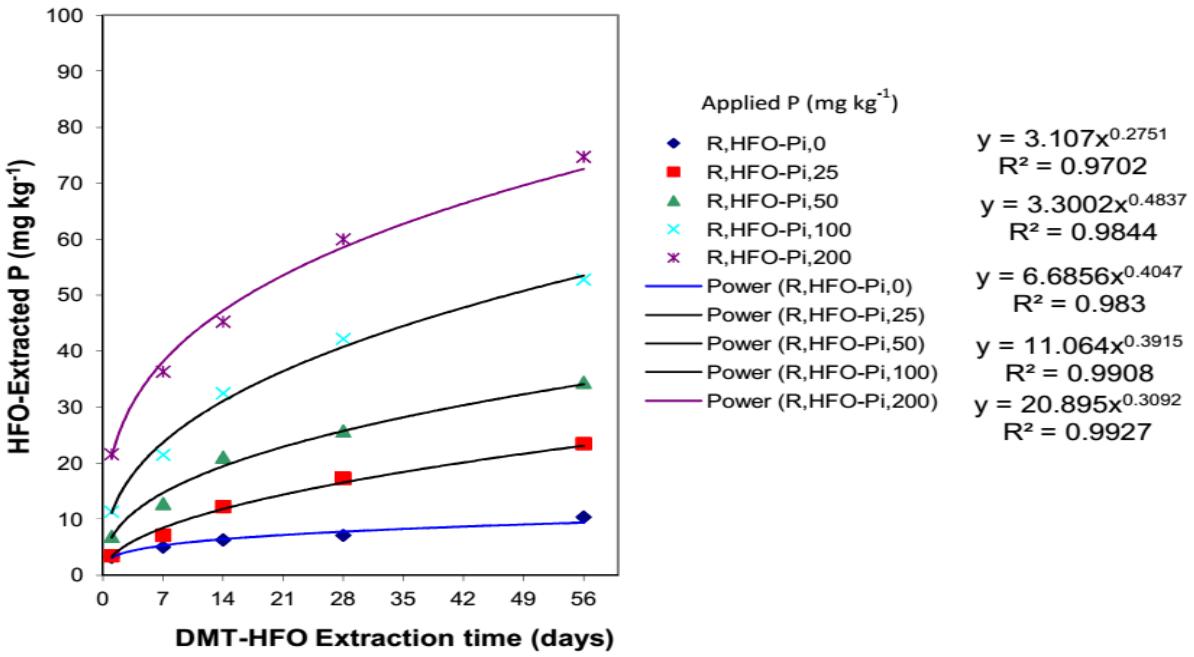

Figure 4. The effects of the applied P on successive DMT-HFO extractable P after 120 days of incubation (Ochwoh *et al*., 2016)

Cumulative P extraction curves reached plateaux where no more P could be recovered, while others continued to release P slowly (Figure 4). This property could be relevant for the crops in the field with respect to the residual effect of added fertilizer P. Thus, knowledge of the type of cumulative P extraction curve of the soil, i.e. whether it reaches a plateau or continues to release P could be important in the management of fertilizer applications. In a related experiment, (Indiati, 1998; Ochwoh *et al*., 2005) observed that soil extractable (labile) P alone, may not provide adequate information on P status of the soil especially in terms of the long-term capacity of the soil to supply P for plant growth and concluded that the successive soil P extraction procedure carried out using Fe oxide impregnated paper strips (or in this case DMT-HFO) provided a convenient laboratory method for characterizing P desorption from soils by simulating plant P uptake.

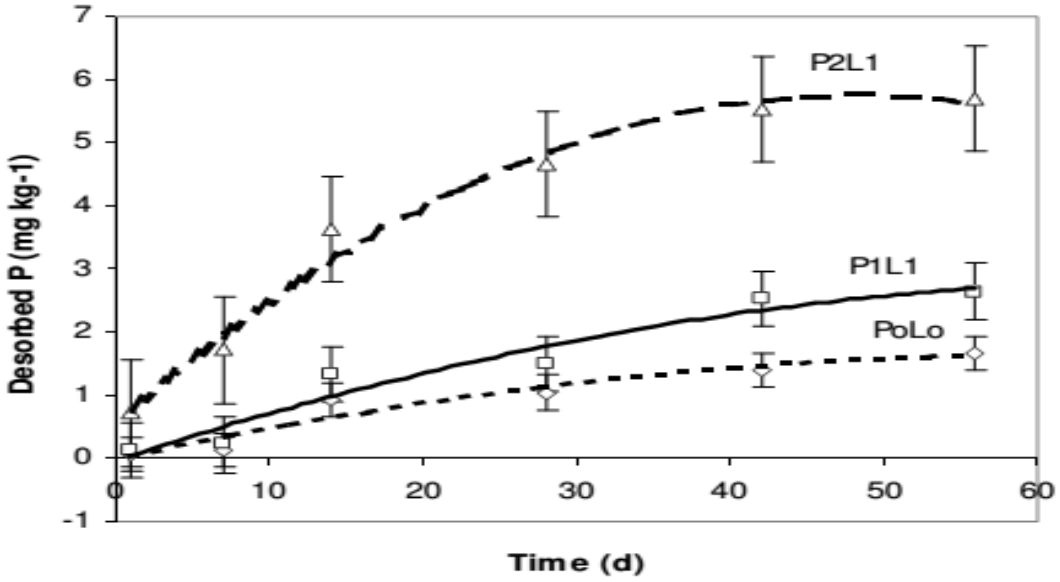

Figure 5. Cumulative P desorbed over time, extracted using DMT-HFO for the different treatments (Taddesse *et al*., 2008a)

The cumulative P desorbed was higher in the P_2L_1 treatment and lower in the control (P_0L_0) at all levels of extraction time (1-56 days) (Figure 5). Cumulative P released with time followed, in general, the same pattern for all treatments, with an initial rapid release of P, roughly with in the first two weeks (14 days), followed by a slower release that was still continuing after 56 days of extraction.

2.7.2. Theory of Kinetic Studies

Desorption kinetics of soil as determined by DMT-HFO can be schematically represented as

$$SP \xrightarrow{K_R} P_{sol} \xrightarrow{K_T} P_{HFO} \quad (1)$$

Where S_P is the solid phase P, P_{sol} is P in solution, P_{HFO} is P adsorbed by HFO, k_T is the rate constant of P transport through the membrane at 0.09 ± 0.01 h^{-1} (Freese *et al*., 1995) and k_R is the rate constant of P release (De Jager and Claassens, 2005). The presence of two pools is assumed: the pool with the fast release kinetics is pool A (SP_A) and the pool with the slow release kinetics is pool B (SP_B). With this assumption, the mass balance equation for the total exchangeable solid phase soil P (SP_{total}) at time t = 0 is:

$$SP_{total\,(0)} = SP_{A0} + SP_{B0} \quad (2)$$

Where SP_{A0} is initial amount of P in pool A and SP_{B0} is initial amount of P in pool B. The mass balance equation at time t will therefore be:

$$SP_{total\,(t)} = SP_{A(t)} + SP_{B(t)} \quad (3)$$

Assuming the decrease in SPA and SPB follow first order kinetics, the integrated rate laws for the decrease of SPA and SPB will be:

$$SP_{A(t)} = SP_{A0}e^{-kAt} \text{ and } SP_{B(t)} = SP_{B0}e^{-kBt} \quad (4)$$

Where k_A and k_B are conditional first order rate constants (day^{-1}) for P desorption from pools A and B respectively.

The total solid phase soil P ($S_{Ptotal\,(t)}$) remaining at time t will be given by:

$$SP_{total\,(t)} = SP_{A0}\, e^{-kAt} + SP_{B0}\, e^{-kB\,t} \quad (5)$$

The total amount of P released at time t is expressed as:

$$P_{R(t)} = SP_{A0} - SP_{A\,(t)} + SP_{B0} - SP_{B\,(t)}$$

$$= SP_{A0} - SP_{A0}\, e^{-kAt} + SP_{B0} - SP_{B0}\, e^{-kBt}, \text{ by rearranging this equation:}$$

$$= SP_{A0}\,(1 - e^{-kAt}) + SP_{B0}\,(1 - e^{-kBt}) \quad (6)$$

It was assumed that the rate constant of P release from the soil was equal to the rate constant of P adsorption (k_A) by the DMT-HFO. The rate constant of P adsorption (k_A) by the DMT-HFO was obtained from a plot of the natural logarithm (ln) of the P adsorbed by the DMT-HFO against time with the slope as k_A. Sink methods have been used widely in P desorption studies and ideally, the DMT-HFO acts as an infinite sink for P desorbed from soil and maintains a negligible P concentration in solution, facilitating continuous P desorption (Freese *et al*., 1995).

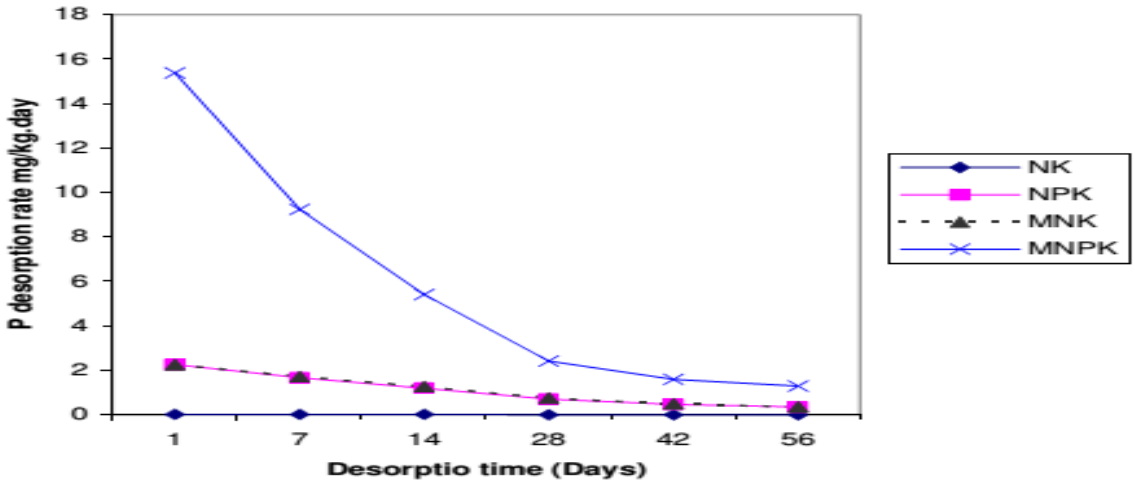

Figure 6. Desorption rates for the different P treatments over 56 days (Taddesse *et al*., 2008b)

The rate at which P desorbed from MNPK dropped faster up until 28 days and started to change slowly with progressive desorption time (Figure 6). The same trend was also observed for NPK and MNK treated soils although the rate of desorption declined faster up until 14 days and

varied slowly afterwards. Moreover, the degree of variation was much less pronounced as compared to MNPK. The reason for such variation could be attributed to the difference in the amount of desorbable P, which is much greater for MNPK than either NPK or MNK treated plots (Taddesse *et al*., 2008a,b). The control, however, showed almost negligible variation with time. These results are consonant with the reports made by De Jager and Claassens (2005). The reason for this could be ascribed to the very low P contents of the treatments that received no P and faster release kinetics are usually associated with desorption of adsorbed P directly in contact with the soil solution (Lookman *et al*., 1995).

2.8. Physicochemical Properties of Soil

There are many physicochemical properties which influence phosphorus desorption from the soil and example are pH, electrical conductivity, soil organic carbon, soil organic matter, cation exchange capacity, soil texture and bulk density, exchangeable acidity, exchangeable aluminum, exchangeable hydrogen, total nitrogen, available and total phosphorus, Fe and Mn Bounded to phosphate can affect P desorption in the soil. The amount of readily available phosphorus (P) in most acid soil is very low compared with the total amount of P because soluble inorganic P is fixed by Al, Fe and Mn due to the high content of Fe/Al-oxides, low pH and advanced stage of weathering of the soil that control the plant available P, and the high content of Al and Fe oxides and hydroxides are the main factors for the strong P fixation in acidic soil (Asmare *et al.*, 2015). In the soil fertility, P fixation is the process in which easily soluble fertilizer phosphates are transformed into such insoluble forms that their uptake by plants is hindered. This reaction contributes to less availability of P for crops. Information on the chemical forms of P is fundamental to the understanding of soil P dynamics and its interaction in acidic soil. This is necessary for the management of P in agriculture.

Abreha (2013) reports the availability of P is influenced by soil organic matter, pH, and exchangeable and soluble Al, Fe, and Ca. Soil acidity mainly at soil pH < 5.5 affects the growth of crops due to high concentration of aluminum (Al) and manganese (Mn), and deficiency of P, nitrogen (N), sulfur (S) and other nutrients. It is becoming a serious threat to crop production mainly in the areas of the western, southern and central highlands of Ethiopia (Wassie and Shiferaw, 2009). This low availability of P under most soil of Ethiopia is due to the impacts of P fixation by acidic cations, abundant loss of P by crop harvest and erosion and the inherent P deficiency of the soil by little or no P sourced fertilizers application (Asmare *et al.*, 2015).

3. MATERIALS AND METHODS

3.1. Description of Study Area and Experimental Site

3.1.1. Experimental Site

Synthesis of $Fe_3O_4/Al_2O_3/MnO_2$ ternary mixed oxide nanocomposite, FAAS analysis and desorption experiments using Uv-Vis spectrophotometry for determination of P were conducted at the Haramaya University, Chemistry Research Laboratory. The FTIR characterization of adsorbent was determined at the Chemistry Department of Addis Ababa University, whereas the XRD, BET, SEM and EDX analyses of as-synthesized nanocomposite were conducted at the Instituto de Catálisis Y. Petroleoquímica, CSIC, C/Marie Curie 2, Madrid, Spain.

3.1.2. Description of Study Area and Soil Sampling

Acidic soil samples were collected from West Wollega Zone, Oromia Region, Ethiopia located at about 477 - 575 km west of Addis Ababa with a geographical location of 09° 51' 28'' - 09° 25' 33'' N latitude and 35°36' 28'' - 35° 02' 13'' E longitude with an elevation between 1845 and 1930 meters. The location map of the sampling sites is presented in Figure 7.

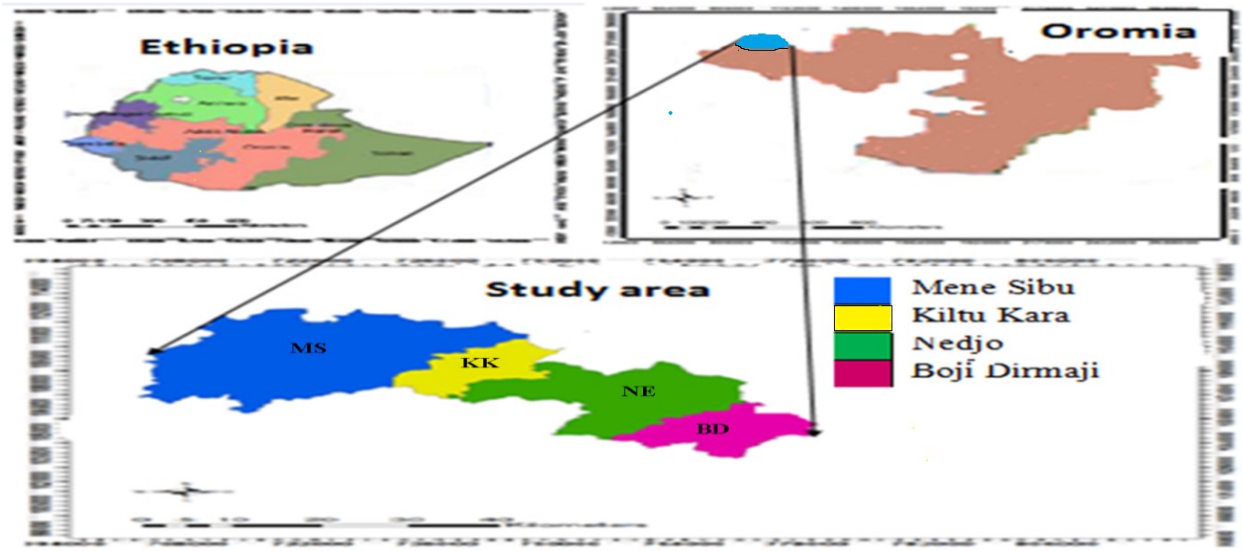

Figure 7. Map of the study area and soil sampling sites

The altitude, the mean annual rainfall, the minimum and maximum temperature of these areas range from 1300 to 1800 masl, 1000 to 2400 $mmyr^{-1}$ and 12.5 to 29 °C, respectively (Achalu *et al*., 2012b). The soil samples were collected from four districts, Boji Dirmaji (BD), Kiltu Kara (KK), Mene Sibu (MS) and Nedjo (NE) which are acidic in nature (Abdenna,

2013). Soil samples were collected during January 2017. The soil was randomly collected from farmers' crop fields. According to FAO (1990) soil classification system, the soil class of the study zone was Nitisol and reddish in colour. This soil contains about 12.5% of Ethiopian soil. Nitisols are inherently fertile, but large areas in Ethiopia have now been depleted due to continuous cultivation, leaching and erosion.

The major crops grown in the study zone include cereals (Maize, Teff, Millet, Sorghum, Coffee and Barley), pulses (Faba bean and Field peas) and oil crops (Niger seed, Rapeseed and Sesame). Surface soil samples (0-20 cm depth) were randomly collected from each sampling site in each district in January 2017 by using stainless steel augur (Poggio *et al*., 2008). The randomly collected soil samples were thoroughly mixed to form one composite sample for each site and a total of three composite soil samples were collected and packed in plastic bags and labelled with labelling tags and transported to Haramaya University for laboratory analysis. Then the soil samples were air dried at room temperature (25 ^{o}C ± 2 ^{o}C) for 7 days, ground and passed through a 2 mm sieve. For desorption study, soil samples collected from the same sites were mixed in plastic pot and different concentrations of P (0, 50,100 and 150) mg/kg were added to the 5 kg soil and incubated in greenhouse.

The soil physico-chemical parameters (pH_{H2O}, pH_{KCl}, electrical conductivity, organic carbon, organic matter, total nitrogen, exchangeable acidity, exchangeable Al, exchangeable hydrogen, available phosphorus, total phosphorus, cation exchange capacity, soil texture and bulk density, extractable Fe_d, Mn_d, Fe_{ox} and Mn_{ox}) and long term desorption studies were analyzed.

3.2. Apparatus and Instruments

3.2.1. Apparatus

The apparatus used in the present studies include; Erlenmeyer flasks, different sizes of beakers, burettes, funnels, graduated cylinders, volumetric flasks, capped test tubes, droppers, watch glass, pipettes, spatula, measuring cylinder, Kerry ultrasonic, fraction collector, suction filtration flask, stirrer, scissors, sears, polyethylene bottles, brush, conical flask, cuvvete, washing bottles, mortar and pestil, cork, bush, filter paper, acid digestion tube, fume hood, test tube ruck, N_2 gas cylinder, magnetic stirrer with hot plate, eye goggles, gloves, crucible, dish, water bath, rubber tube, test tube ruck, iron stand, whatman filter paper and sieve (2 mm) were used.

3.2.2. Instruments

The instruments used in this study were; pH meter (MP 220 JENWAY, Japan) used for determination of pH, X-ray diffractometer (XRD) (BRUKER D8 Advanced XRD, Japan) was used for the determination of size and phase of the as-synthesized powder sample, Fourier transform infrared spectrophotometer (spectrum 65 FTIR Perkin Elmer) was used for functional group identification of the as-synthesized adsorbent, Uv-Visible spectrophotometry (Uv professional, Galanakamp, UK) was used to determine the concentrations of P in the soil samples, BET (JW-04, Beijing), SEM (HITACHI S-4160, UK), EDX (VEGA\\-TESCAN, base director, German), Deionizer (B114,Oxford, UK), Drying oven (Contherm 260 M), and Orbital shaker (S01 Stuart, UK), Flame atomic absorption spectrophotometer ((Model 210/211 VGP, UK) and Micro Kjeldahl distillation unit and Kjaldahl digestion stand (for total nitrogen determination), Analytical balance (Denver Instrument XE 50A), Conductometry (model CO155), Centrifuge (Centurion scientific, UK), Refrigerator and Hydrometer which used for texture determination were used.

3.3. Chemicals and Reagents

Aluminum nitrate nanohydrate ($Al(NO_3)_3.9H_2O$) (95%-98% Merck Germany), Ferrous chloride tetra hydrate ($FeCl_2.4H_2O$), Ferric chloride hexahydrate ($FeCl_3.6H_2O$) (LOBAL chemie,India) and Manganese (IV) oxide (MnO_2)(BDH chemicals Ltd, England) were used for synthesis of the sorbent. The standard solutions of phosphorus was prepared from Potassium dihydrogen phosphate (KH_2PO_4) (99-101% High-tech health care, India), Sodium bicarbonate ($NaHCO_3$) (99.5-101% FINKEM) Potassium chloride (KCl, 99.0% loba, India), Ammonium fluoride (NH_4F, 99%, Switzerland), Hydrogen peroxide (H_2O_2, 30% Central drug house LTD, New Delhi, India), Potassium dichromate ($K_2Cr_2O_7$,99.9% BDH chemicals LTD Poole England), Sulfuric acid (H_2SO_4, 98%, laboratory reagent, loba, India), Potassium sulphate (K_2SO_4, 99.0% loba , India), Boric acid (H_3BO_3, 99.8% BDH chemicals Ltd, England), Buffer pH (4,7 and 9) (Blulux Ltd England).

Nitric acid (HNO_3) (69% LR, Breck land Scientific Supplies, U. K), Copper sulfate ($CuSO_4$, 99% Loba Merk , India), Selenium powder (Se, 99.7%, Germany), Ferrous sulfate heptahydrate ($FeSO_4.7H_2O$) (97% BDH chemicals Ltd England) to know amount of organic carbon, Potassium antimony tartarate ($KSbC_4H_4O_7$ (98.5% BDH chemicals Ltd, England) to know

total, available and P desorbed by adsorbent, Calcium chloride ($CaCl_2$) (High-tech Healthcare, India), Ethanol (C_2H_5OH) (97% Fine chemical general trading, Ethiopia).

Ammonium molybdate tetra hydrate, ($Mo_7O_{24}.6(NH_4).4(H_2O)$)(81- 83 % Riedel DeHaen AG), Ascorbic acid, ($C_6H_8O_6$) (99% Blux laboratory reagents) were used for colorimetric determination of phosphate, Sodium carbonate (Na_2CO_3, Blulux Lab, India), Sodium hexameta phosphate ($Na(PO_3)_6$ (Fine CHEM industries, India), was used for soil texture determination, Ammonium oxalate ($(NH_4)_2C_2O_4$. H_2O, 98% BDH chemicals Ltd Poole, England), Oxalic acid solution ($H_2C_2O_4.2H_2O$) (99%, Switzerland), Sodium hydrosulfite (dithionite) ($Na_2S_2O_4$) (Fisher scientific company, USA), Sodium citrate ($Na_3C_6H_5O_7 \cdot 2H_2O$) (BLULUX laboratories (P) Ltd, India), for determination of soil bounded Fe and Mn. Hydrochloric acid (HCl, 36-37%, BDH chemicals Ltd, England) and Sodium hydroxide (NaOH, 97.5% BDH chemicals Ltd, England) for pH adjustment, Sodium chloride (NaCl, 99.5% Chemical limited, Mumbai) and nano synthesis, Bromo crosel green (BDH chemicals Ltd Poole, England) and methyl red (BDH chemicals Ltd, England) were the chemicals and reagents used. All chemicals and reagents were analytical grade and they were used without further purification.

3.4. Experimental Procedures

3.4.1. Sample Preparation

A stock solution (1000 mg/L) of P was prepared from KH_2PO_4 by dissolving appropriate amount (4.39 g) in 1 L of deionized water. The intermediate (10 mg/L for P) was prepared by suitable dilution of the stock solution. The working standard solution were prepared by serial dilution from above concentration and used for P analysis.

3.4.2. Synthesis of $Fe_3O_4/Al_2O_3/MnO_2$ Ternary Mixed Oxide Nanocomposite

The Fe-Al-Mn ($Fe_3O_4/Al_2O_3/MnO_2$) ternary mixed oxide nanocomposite was prepared by co-precipetation method (Liyuan *et al*., 2013). For magnetite (Fe_3O_4) nano particles synthesis , stoichiometric factors of Fe^{+2} and Fe^{+3} are very important for composites products. Fe^{+2}/Fe^{+3} mole ratio < 0.1 is too small to achieve a stable solution. Fe^{+2}/ Fe^{+3} mole ratio < 0.3 from two different phase FeO(OH) surface functional group and low Fe content ≈ 0.07 and the second phase, increased Fe^{+2} content ≈ 0.33. The mole ratio of Fe^{+2}/ Fe^{+3} (0.5) was used to prepare homogeneous magnetic nanoparticle with uniform size (Anamaria *et al*., 2012). As-synthesis protocol, three different composition of $Fe_3O_4/Al_2O_3/ MnO_2$ with Fe: Al: Mn percent ratios (%)

(90, 5, 5), (80, 15, 5) and (70, 15, 15) or molar ratios of 18:1:1, 16:3:1 and 14:3:3, respectively, were prepared for this study. During synthesizing process, three beakers (1 L) were used.

Synthesis of Fe_3O_4

Synthesis of Fe_3O_4 (magnetic) nanoparticles was done by co-precipitation of ferric and ferrous salts under the presence of N_2 gas. In the first step stoichiometrically calculated (8.63 and 3.17 g) of $FeCl_3 .6H_2O$ and $FeCl_2 .4H_2O$, respectively were accurately measured and dissolved into 100 mL of 0.3 M HCl (Laurent *et al*., 2008). Then, the solution was added drop wise from separatory funnel into the solution of 120 mL of 3 M NaOH over a period of 2 h, under vigorous stirring at 80 ^oC in N_2 atmosphere. During this process, the pH of mixture was kept at 12.0 using 0.1, 0.01 and 0.001 M NaOH or HCl solutions. The suspension was left undisturbed for 4 h and the settled phase was separated from the liquor and washed with deionized water several times until addition of $AgNO_3$ solution to the filtrate show no formation of white precipitate and a suspension of Fe_3O_4 (ferrofliud) were obtained (Jiang *et al*., 2009; Fekadu, 2015).

$$Fe^{2+} + 2Fe^{3+} + 8OH^- \rightarrow Fe_3O_4 + 4H_2O$$

During magnetite synthesis, magnetic properties of magnetite depend on the ratio of iron ions concentrations and this ratio is called coefficient K ($k = \frac{C(Fe\ II)}{C(Fe\ III)}$) where C (Fe II) and C (Fe III) are concentrations of correspondingly bivalent and trivalent iron ions in magnetite. As the NaOH amount and pH increases, the nanoparticle size decreases, albeit a small amount. At higher pH, super saturation during co-precipitation is higher, promoting nucleation over growth, thus giving smaller particle sizes. By using the co-precipitation method over this wide range of pH values at room temperature, it is easy to prepare magnetite nanoparticles with an approximate size (Sophie *et al*., 2008; Mascolo *et al*., 2013).

The magnetite-alumina-manganese oxide nanocomposite of each sample was prepared by adding 100 mL of $Al(NO_3).9H_2O$ and MnO_2 (which obtained by dissolving stoichiometric amounts (2.25 and 0.09 g) of each, respectively in 100 mL of deionized water separately) into the obtained Fe_3O_4 suspension and ultrasonicated for 10 min prior to use. The pH of mixture was adjusted to 8.0 using 0.1, 0.01 and 0.001 M NaOH or HCl. Then the mixture was magnetically stirred under N_2 atmosphere for 1.5 h at 70 ^oC. Finally, the resulting black magnetic fluid was made to settle out until a clear supernatant solution was observed. The clear supernatant solution was decanted by holding permanent magnet under the beaker containing the product. The product was washed with deionized water several times to remove impurities

such as Cl^-, NO_3^- and excess OH^- ions and finally dried at 60 ^oC for 24 h to obtain the desired products (Fekadu, 2015).

3.5. Characterization of As-synthesized Adsorbent

3.5.1. X-Ray Powder Diffraction

The size of the primary crystallite (Ds) of the solid-phase ($Fe_3O_4/Al_2O_3/MnO_2$) was calculated from the XRD patterns for the major peak according to the Dubye Scherrer equation (Laurent *et al*., 2008):

$$Ds = \frac{k\lambda}{\beta \cos\theta} \quad (7)$$

Where, Ds is mean crystallite size (nm), k is the shape factor with a typical value of about = 0.9, λ is wavelength of the incident radiation (λ =1.5405 Å), β pure diffraction broadening (radians) and θ the Bragg angle (degrees, half-scattering angle). Usually β is taken as the full width at half maximum of the major diffraction band (FWHM).

3.5.2. Determination of Surface Area

Surface area of the synthesized adsorbent was determined using both single point and multipoint Brunauer Emmett-Teller (BET) nitrogen adsorption and desorption isotherms. A surface area was determined as a function of temperature for the lowest and the highest initial surface area sample (Kasahun, 2015).

3.5.3. SEM and EDX Analysis

The surface morphology of Fe-Al-Mn mixed oxide nanocomposites was examined by using scanning electron microscopy (SEM) and the presence of Fe, Al and Mn elements in the mixed nanocomposites were analyzed by the energy dispersive x-ray (EDX).

3.5.4. Infrared Spectroscopic Studies

The infrared spectrum of the as-synthesized powder (Fe-Al-Mn) ternary mixed oxide nanocomposite was determined by using a FTIR spectrometer (Spectrum 65 FTIR (Perkin Elmer)) at room temperature (Li *et al*., 2007) from the vibrational infrared spectra extending in the range of 4000 to 400 cm^{-1}. Appropriate amount of nanocomposite was ground and mixed

with KBr (Wubshet, 2016). Then percent transmittance of nanocomposite was read in the above range and recorded.

3.5.5. Elemental Determinations

The percentage of iron, aluminum and manganese in the selected as-synthesized powders were determined by flame atomic absorption spectrophotometer (FAAS). Here 0.5 g of the as-synthesized powder was digested for 25 minute at 350 ^{o}C with concentrated nitric acid (7 mL), concentrated hydrochloric acid (4 mL) and hydrogen peroxide (2 mL) using acid digestion tube till clear solution appeared. The sample was transfered to 100 mL volumetric flasks and brought to volume using deionized water. 1 mL of this solution was diluted further to 50 mL for FAAS analysis (Harvey and Rhue, 2008; Tofik *et al*., 2016). A series of standard solutions were prepared from their stock solutions and used to plot the calibration curve.

$$\% \text{ M} = \text{concentration (ppm)} \times \frac{\text{volume of diluted}}{\text{mass of sample taken} \quad \text{x1000}} \text{x100} \qquad (8)$$

Where M represents metals in the as-synthesized nanocomposite

3.6. Physicochemical Properties of Soil Samples

The collected soil samples were air dried and ground to pass through a 2 mm sieve and homogenized. Selected soil physico-chemical parameters (pH_{H2O}, pH_{KCl}, electrical conductivity, soil organic carbon, soil organic matter, cation exchange capacity, soil texture and bulk density, exchangeable acidity, exchangeable aluminum, exchangeable hydrogen, total nitrogen, available and total phosphorus, Fe and Mn bounded to P using dithionite and oxalate extractant) were investigated.

3.6.1. Soil pH

Soil pH is generally referred to as a “master variable” because it regulates almost all biological and chemical reactions in soil (Brady and Weil, 2002). It is a measure of the acidity or alkalinity of the sample. The pH in water and KCl of the samples were determined by dispersing 20 g of dried soil in 50 mL of water and 50 mL of 1 M KCl separately. After 2 h of end-over-end shaking at 20 rpm, the pH of soil suspension was determined (Freese *et al*., 1995; Taddesse *et al*., 2008a).

3.6.2. Electrical Conductivity

Electrical conductivity (EC) is a numerical expression of the ability of an aqueous solution to carry an electrical current. Soil to water suspension with 1:5 ratios was prepared by mixing 10 g air-dried soil (<2 mm) with 50 mL of deionised water in a beaker. The conductivity meter was calibrated according to the manufacturer's instructions using the KCl reference solution to obtain the cell constant. The cell was rinsed with deionised water between samples (Achalu *et al*., 2014) and conductivity values were recorded from the conductivitymeter.

3.6.3. Soil Texture and Bulk Density

The soil texture was determined by hydrometer method after destroying organic matter and dispersing the soil (Bouyoucos, 1962). A 50 g of soil sample was measured and added to 200 mL of beaker. Then 100 mL of calgon or dispersing solution was added. The solution was stirred for 5 minutes, transferred to 1000 mL graduate cylinder and rinsed by distilled water and mixed. First with 40 second measured and later with interval of 2 h soil samples were measured and the percent of each soil texture were calculated. Finally soil texture class was determined by USDA (2014) equilateral triangles or international equilateral triangles model. Bulk density was determined gravimetrically after oven drying soil sample for 24 h at 105 ^{o}C (Day, 1965). It was expressed as gram of soil per unit volume.

3.6.4. Soil Organic Carbon

Soil organic carbon was determined by oxidation with 1 N $K_2Cr_2O_7$ (Walkley and Black, 1934; Gemechu *et al*., 2015). A weighed amount (1 g) of the dried, grounded soil samples were treated with 10 mL of 1 N potassium dichromate solution ($K_2Cr_2O_7$) followed by addition of 20 mL of concentrated sulfuric acid. The mixture was gently swirled and left at room temperature in a fume hood for 25 minute.

$$2Cr_2O_7^{2-} + 3C + 16H^+ \rightarrow 4Cr^{3+} + 8H_2O + 3CO_2\uparrow$$

The excess dichromate was back titrated potentiometrically with the standard 0.2 N ferrous sulfate solution in which dipheny used as indicator. Blank titration of the acidic dichromate with ferrous ammonium sulfate solution was performed at the beginning of the batch analysis using the same procedure with no soil addition.

$$\text{Organic carbon (\%)} = \frac{(\text{B}-\text{S})\ \text{x}\ \text{N of}\ Fe^{+2}\ \text{X}\ 12}{\text{gram of soil}\ \text{x}\ 4000}\ \text{x}\ 100 \quad (9)$$

Where B is the volume of ferrous solution used in the blank titration, S is the volume of ferrous solution used in the sample titration; 12/4000 is milliequivalent weight of carbon in grams. No correction factor was applied to the OC content calculation.

3.6.5. Soil Organic Matter

The organic matter of soil includes the remains of plants, animals and microorganisms in all stages of decomposition. Soil organic matter was determined by oxidizing the soil organic carbon under standard condition with potassium dichromate in sulphuric acid solution (Walkely and Black, 1934; Achalu *et al*., 2013) and it was obtained by multiplying percent soil organic carbon by a factor of 1.724 following the assumptions that organic matter is composed of 58% carbon.

3.6.6. Exchangeable Acidity

Exchangeable acidity was determined by saturating (10 g) of the soil samples with 100 mL of 1 M standard potassium chloride solution. Then 25 mL of aliquot was taken and titrated with sodium hydroxide (0.02 M NaOH). On above step few drop of 0.02 M HCl and 10 mL of NH_4F added until solution become colorless. From the same extract, exchangeable Al in the soil sample was determined titrating with a standard solution of hydrochloric acid (0.02 M HCl). Finally, exchangeable H^+ was obtained by subtracting exchangeable Al from exchangeable acidity (Gemechu *et al*., 2015).

3.6.7. Total Nitrogen

Soil total nitrogen was determined by the Kjeldahl method using micro Kjeldahl distillation unit and Kjaldahl digestion stand (Jackson, 1958; Taddesse *et al*., 2008a; Ochwoh *et al*., 2016). Weighted amount 1 g, of each soil samples were measured and added to Kjeldahl distillation and at a time one blank was prepared for each soil sample to be analyzed. On the above steps, one spoon of K_2SO_4, $CuSO_4$ and selenium powder and 7 mL of concentrated H_2SO_4 acid were added to each soil samples and digested in fume hood for 2 h. Then the samples attached to the distiller containing sodium hydroxide and the product collected in conical flask. A 20 mL of 2% H_3BO_3, bromocresol green and methyl red indicator were added to the solution. Finally the obtained product was titrated with 0.1 N H_2SO_4 until the green color changes to pink and the total nitrogen determined according to equation 10.

$$\%N = \frac{(a-b)}{s} \text{ x N x } 0.014 \text{ x } 100 \text{ x mcf} \quad (10)$$

a = mL of H_2SO_4 required for titration of sample

b = mL of H_2SO_4 required for titration of blank

N = Normality of H_2SO_4

0.014 = Meq. weight of nitrogen in g

mcf = moisture correction factor

s = weight of dry soil sample

3.6.8. Cation Exchange Capacity

Cation exchange capacity (CEC) is a measure of the quantity of readily exchangeable cations neutralizing negative charge in the soil or it is defined as the capacity of soil to adsorb and exchange cations (Brady and Weil, 2002). A 5 g of soil sample was measured and added to the beaker and washed with 100 mL of ammonium acetate (1 M NH_4OAc) four times (pH 7) as described in Thomas (1982) which extract cations (Fe^{3+}, Al^{3+}, Ca^{2+}, Mg^{2+}, Na^{+}, K^{+}). Then soil samples were washed with 75 mL of ethanol to remove excess NH_4OAc. Then after, the samples were leached with 25 mL 10% NaCl solution four times in 100 mL volumetric flask and filled up to the mark with NaCl. Then it was titrated with 0.1 N NaOH and CEC of soil sample calculated.

3.6.9. Available and Total Phosphorus

The available phosphorus in the soil sample was determined using Bray and Kurtz (1945) extraction by (Bray II) method (0.03 M NH_4F + 0.1 M HCl) and quantified using spectrophotometry (at wave length of 882 nm) colorimetrically. Details of analytical methods are described in Kuo (1996) and the hand book of standard soil testing methods for advisory purposes (The Non-Affiliated Soil Analysis Work Committee, 1990). The Bray II extraction is considered to extract Al bound phosphates as the F- is exchanged and forms new complexes with Al, simultaneously prohibiting a fixation by soil colloids while the dilute HCl dissolves the Ca-phosphates. Weighted amount (2 g) of soil sample was added to flask and 20 mL of bray II extracting solution was added (section 3.8). The soil sample was shaken for 10 minute and filtered by whatman filter paper of No 42. Then 2 mL of filtrate was mixed with 2 mL of mixed reagent and P analyzed colorimetrically at 882 nm (section 3.8).

Total soil P (TP) was determined on sub samples of 0.5 g soil with the addition of 5 mL concentrated H_2SO_4 and heating to 360 ^oC on a digestion block with subsequent stepwise (0.5 mL) additions of H_2O_2 until the solution become clear (Thomas *et al*., 1967; Taddesse *et al*., 2008a) and the absorbance was measured by spectrophotometry at wave length of 882 nm by preparing standard solution.

3.6.10. Phosphate Bounded Fe and Mn

The phosphate bounded Fe and Mn in the soil samples were determined by dithionite–citrate and acid ammonium oxalate methods (Mehra and Jackson, 1960). The dithionite–citrate removes organically complexed Fe and Mn, amorphous inorganic Fe and Mn compounds and noncrystalline aluminosilicates. Acid ammonium oxalate removes organically complexed and amorphous inorganic forms of Fe and to a lesser extent, Mn and noncrystalline aluminosilicates from soil (McKeague, 1967). Ammonium oxalate extractable Fe and Mn were determined by shaking 0.5 g of soil with 20 mL of ammonium oxalate extracting solution in the dark in 250 mL of polyethylene bottle for 4 h and then filtered using whatman No. 42 filter paper (Jackson *et al*., 1986; Olayinka *et al*., 2015). Ammonium oxalate extractable Fe and Mn were determined by FAAS.

Dithionite-Citrate Fe and Mn were determined using the (Soil Survey Staff, 2006) soil conservation method. A 0.5 g of soil sample was grounded and pass through 2 mm sieve was weighed and added into a 15 mL plastic centrifuge tube. A 5 mL of the sodium citrate ($Na_3C_6H_5O_7 \cdot 2H_2O$) (0.68 M) solution and 0.2 g of dithionite (sodium hydrosulphite, $Na_2S_2O_4$) were added to soil samples. After that the mixture was mixed well with a stirring rod and the tubes were placed into a water bath at 80 ^oC and stirred every 2-3 minutes throughout a 15 minute extraction period. After the tubes were removed from the bath, 1 mL of saturated NaCl solution was added and mixed. Then centrifuge tubes were covered tightly and centrifuged for 5 minutes at 1500-1600 rpm. The centrifuge was poured off into a 100 mL volumetric flask. The supernatant was filtered and Fe and Mn in the soil samples were determined by FAAS. Finally, the concentration of each metals were determined from calibration curves by preparing standard solution of each metals from corresponding salts.

3.7. Incubation Study

In the present study, greenhouse was used for incubation experiments. Four treatments of P as KH_2PO_4 with concentrations of 0 (P0), 50 (P1), 100 (P2) and 150 (P3) mg/kg were added to soil samples of 5 kg separately and incubated at 25 ^oC for 112 days. Then the incubated soil was used to study long term desorption of P and kinetic studies using DMT-HFAMO (De Jager and Claassens, 2005; Ochwoh *et al*., 2016).

3.8. Long-Term Desorption Study

A desorption study was carried out using dialysis membrane tubes (Visking, size 320/32 inches, approximate pore size 2.5-5.0 nm; membrane thickness 3 μm, MWCO 12000 kDa) filled with ternary Fe-Al-Mn mixed oxide nanocomposite (Freese *et al*., 1995; Taddesse *et al*., 2008a,b; Gemechu *et al*., 2015). Then 0.15 m of DMT strip was filled with 20 mL of 0.1 g of HFAMO nanocomposite (sorbent). The sorbent suspension was stirred vigorously during the filling. The DMT-HFAMO was placed in 250 mL polyethylene containers with 1 g of soil sample, 80 mL of 2 mM $CaCl_2$ and 0.3 mM KCl solution. All the experiments were carried out in complete randomized design (CRD) having three replication. The polyethylene containers were continuously shaken (horizontally) for 28 days on an end-over-end shaker at 120 oscillations per minute (opm) at room temperature (25 ^oC).

On each of seven days intervals: 1, 7, 14, 21 and 28, the DMT-HFAMO was replaced with new DMT-HFAMO. In doing so, a glass rod was used to remove any attached soil from the dialysis membrane tubes. The suspension was dissolved by adding 1 mL of concentrated sulfuric acid and filtered by whatman No. 42. P in the solution was determined colorimetrically with the molybdate blue method using ascorbic acid as a reductant in which appropriate amount of each prepared separately (Murphy and Riley, 1962; Taddesse *et al*., 2008a,b; Gemechu *et al*., 2015).

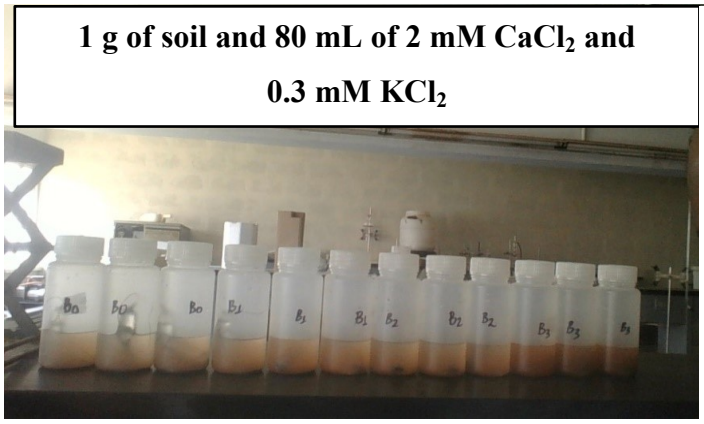

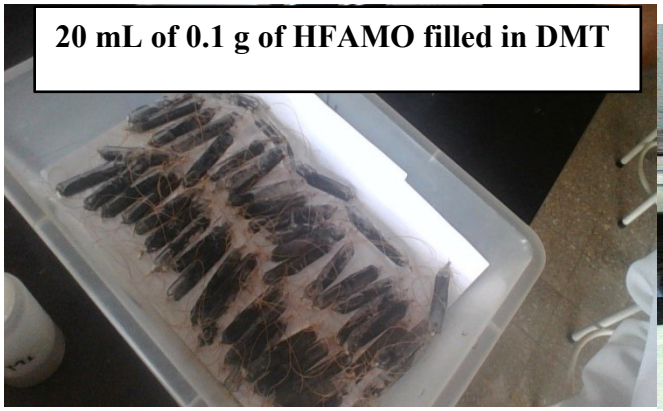

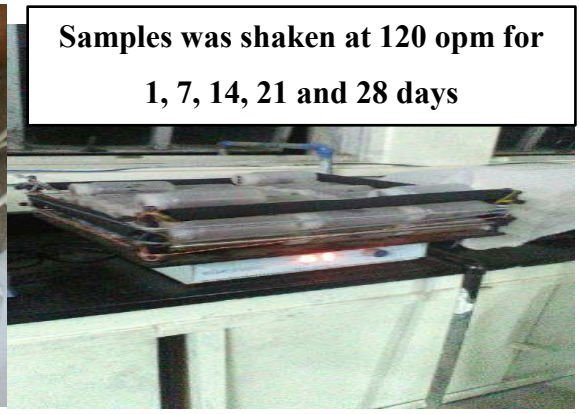

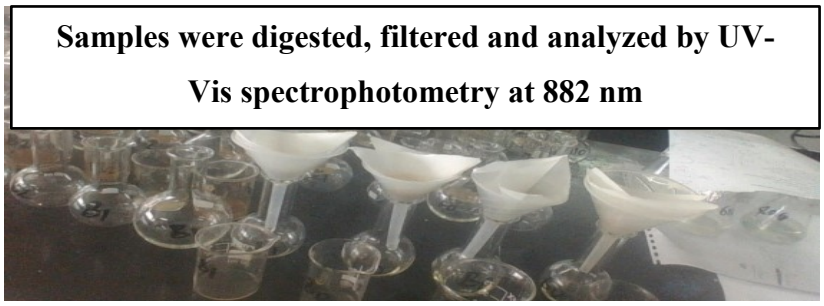

Each reagents were mixed and prepared by taking 50 mL of ammonium molybdate solution, 5 mL of potassium antimonyltartrate solution and 0.553 g of ascorbic acid were mixed in 100 ml volumetric flasks and filled up to the mark with deionized water. Then, 2 mL sample filtrate and 2 mL mixed reagent were mixed in 25 mL a conical flask and left for 30-40 minutes till blue color developed. The intensity of the blue color correlates to the concentration of phosphate. A series of standard and blank was prepared as same background Fe-Al-Mn and sulfuric acid and Uv-Visible spectrophotometry was used to analyze or determines concentration of P in the soil samples at wave length of 882 nm. All determinations were made in triplicate and results were given as means.

3.9. Data Analysis

The separations of significant differences between and among treatments were made by one-way analysis of variance (ANOVA) using SAS (Statistical Analysis System, 2004) and a correlation analysis was conducted to test the relationship between cumulative desorbed P (CD28P) and selected soil physicochemical parameters was done by SPSS. The calibration curves and FTIR graphs were done by Microsoft Excel 2010 and Origin 70, respectively. In addition, XRD data were analyzed with Match 2 softwaare to determine size and identifying the phase.

4. RESULTS AND DISCUSSION

4.1. Characterization of As-synthesized Adsorbent

4.1.1. XRD Patterns

X-ray diffraction (XRD) is one of the most important non-destructive tools to analyze all kinds of matter-ranging from fluids, to powders and crystals. The phases in each samples were identified using X-ray diffractometer (XRD) Figure 8. The average crystallite size was also determined from Scherer equation as shown in Table 1.

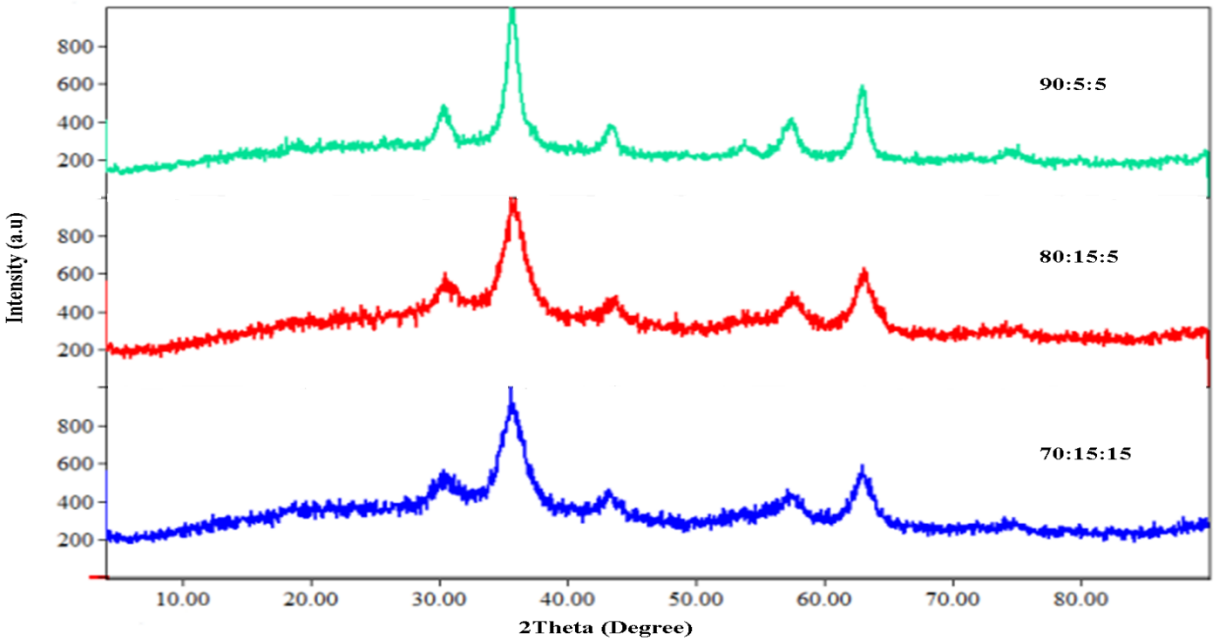

Figure 8. XRD pattern of as-synthesized ternary mixed oxide nanocomposite

The peaks observed by the three nanocomposites appeared to be similar except the additional peak exhibited by NC_1. The presence of peaks at 2θ values of (30.70, 35.80, 43.51, 54.04, 57.37, 62.90 and 74.76)^o [96-900-5815] for NC_1, (30.49, 35.84, 43.62, 57.48, 63.31 and 74.86)^o [96-900-5842] for NC_2 and (30.80, 35.70, 43.31, 57.06, 62.90 and 74.53)^o [96-900-2023] for NC_3 could be assigned to a face centered cubic spinel structure of pure magnetite (Fe_3O_4). This result agrees with the XRD pattern of pure magnetite (Fe_3O_4) reported by previously (Khayat and Khayat, 2012; Saranya *et al*., 2015). Here when it was analyzed by software the amount of magnetite at each peak was much higher than other. So that in each peak magnetite was observed and no specific peaks shows attributable to alumina (Al_2O_3) and manganese (MnO_2) implying that both might exist in amorphous forms at the temperature of synthesis and small

percentage of MnO_2 (<3%, as witnessed by the EDX) and similar result was reported by Buzuayehu *et al*.(2017). In fact, crystallized alumina such as α-Al_2O_3 and β-Al_2O_3 might present under thermal treatment at 800 ^oC and 1000 ^oC, respectively (Gulshan *et al*., 2009).

The average crystalline size of the as-synthesized nanocomposite was calculated using the Debye Scherrer formula. The most intense peak in the XRD pattern was used to calculate the average crystalline size (Ds) of as-synthesized nanocomposite. The nanocomposite with the smallest crystalline size (22.75 nm) was found to be NC_2 with Fe: Al: Mn ratio of 80: 15: 5 (Table 1).

Table 1. Particle sizes (Ds) of synthesized Fe-Al-Mn ternary mixed oxide nanocomposite with different composition

Sample Code	% Composition of Fe-Al-Mn	2θ (degree)	β (rad)	Cosθ	Ds (nm)
NC_1	90:5:5	35.80	0.0055	0.9516	26.51
NC_2	80:15:5	35.84	0.00641	0.9513	22.75
NC_3	70:15:15	35.70	0.00579	0.9519	23.93

Our findings indicate that the particle sizes of the as-synthesized Fe-Al-Mn ternary mixed oxides particle size increased with decrease in the percentage of the alumina in the samples and similar trends were reported by Tofik *et al.(*2016) and Mathewos (2016). However increasing of alumina oxide could delay the crystallization of iron oxides and shrink the size of the crystallites. The concomitant increase in manganese oxide could have counter effect which might have led to increase crystal size and similar results reported by Ayelew (2014) and this is due to the formation of core- shell structured nanoparticles or composite which is magnetite as core and manganese oxide as shell (Liu *et al*., 2015). Besides to this, the presence of large amount of manganese dioxide powder delays the uniformity of nanocomposite (Herranz *et al.,* 2006). Generally the calculated average crystalline size of as-synthesized ternary nanocomposite of Fe-Al-Mn confirm the involvement of good crystalline range between 10 and 50 nm (Akram *et al.,* 2016) (Table 1).

4.1.2. Surface Area

Specific surface areas of the nanocomposites were determined using both single point and multipoint Brunauer–Emmett–Teller (BET) analytical methods. The comparative specific surface areas of the nanocomposite take the following order of percentage compositions; NC_2 (80:15:5) > NC_3 (70:15:15) > NC_1 (90:5:5) (Table 2). Accordingly, the ternary oxide with the smallest size was found to exhibit the largest specific surface area and similar trend was observed by Gulshan *et al*. (2009) and Cava *et al*. (2007) but from this the amount of Mn can affect the surface area and our finding shows small amount of Mn must be used. This is due to the influence of content in the aluminum which may add additional binding site and manganese variation existed in the as-synthesized powders (Cava *et al*., 2007). The presence of manganese beyond a certain amount contributes less to enhance the surface area of the nanocomposite in contrast to alumina. From this, NC_2 with ratio of (80% Fe, 15% Al and 5% Mn), resulted relatively higher specific surface area.

Table 2. BET results of Fe-Al-Mn as-synthesized nanocomposites composition

Sample code	Surface area (m^2/g)
NC_1 (90:5:5)	114.38±0.69
NC_2 (80:15:5)	203.69±1.34
NC_3 (70:15:15)	193.95±1.29

Nanomaterials with high surface activity, high specific surface area and high surface energy, show promising potential in the preparation of high performance desorption and thus are widely used as adsorbents (Wang *et al*., 2004; Cao *et al*., 2012).

4.1.3. Elemental Determinations

Elemental content of the selected adsorbent in NC_2 (80:15:5) was analyzed with FAAS by using air-acetylene gas as oxidant for Fe, Al and Mn. The results pertaining to the percentages of iron and manganese oxides are obtained at wave lengths of 248.3 and 279.5 nm, respectively. The analysis was performed using a standard solution of each analyte. The unknown concentration of each metal was determined from its calibration plot from a series of concentrations of the standard solution versus the corresponding absorbance readings (Appendix Figure 6 and 7).

Table 3. Actual yield and theoretical composition of the as-synthesized adsorbent

Elements	Theoretical composition (%)	Actual composition (%)
Fe	80	78.82
Al	15	ND*
Mn	5	4.20

*ND = Not determined

The FAAS results indicated that the percentage compositions of Fe and Mn in the as-synthesized selected nanocomposite (NC_2) was determined and the values not far from the theoretical composition of the metals in NC_2 for Fe and Mn, but the expected value of the oxides are 80% for iron and 5% for manganese. The difference in the percentage compositions (between actual and theoretical values) may be due to insufficient dissolution, vaporization and lack of atomization (Ayelew, 2014; Fekadu, 2016). Aluminum was not determined due to lack of nitrous oxide gas (oxidant).

4.1.4. SEM-EDX Study

From the SEM image of the Fe-Al-Mn ternary oxide of various ratios, all the samples exhibit irregular particles of various sizes with no distinct morphology. Energy dispersive X-ray analysis of micrographs showed the presence of all the three metals (Al, Fe and Mn) constituents (Figure 9) and the weight of each metals in the nanocomposites were confirmed in different ranges. A relatively wider range of composition was registered for each element revealing the heterogeneity of the composites (Buzuayehu *et al*., 2017). The weight range and average percentage weight composition of aluminum, iron and manganese in the nanocomposite were given in Table 4.

Table 4. EDX results of aluminum, iron and manganese elements in the nanocomposite

Elements	Weight range (%)	Weight average (%)
Aluminum	1.4 -11.3	5.1$\pm$ 3.39
Iron	84.8 - 98.5	95.1$\pm$ 4.05
Manganese	0.8 -2.6	1.6$\pm$ 0.56

The observed slight variation of the Fe-Al-Mn metals percent weight ratio distribution might be due to the dispersion technique employed in the co-precipitation method (Nedkov *et al*., 2006).

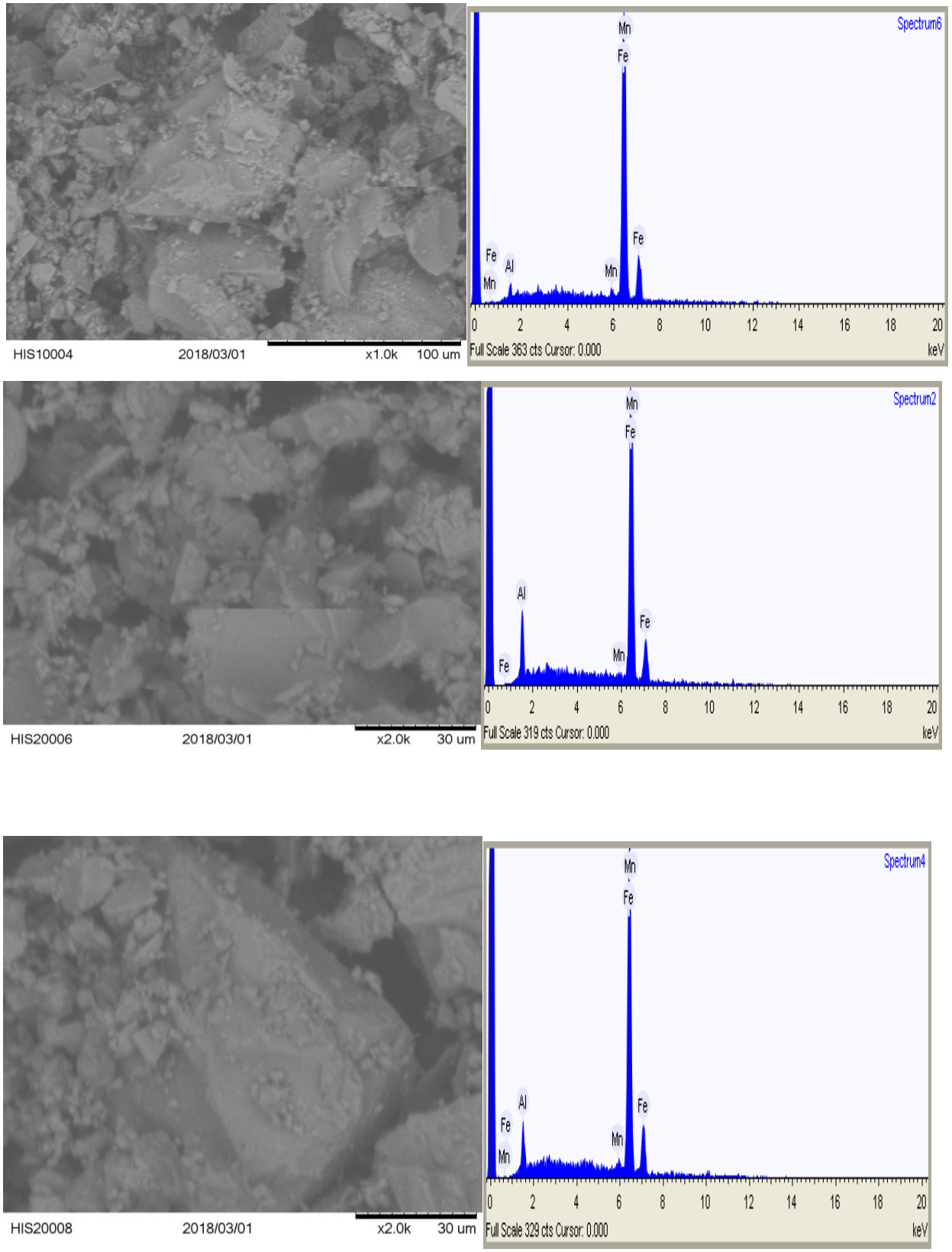

Figure 9. SEM-EDX of Fe-Al-Mn ternary mixed oxide nanocomposite

4.1.5. Infrared Spectroscopic Studies

There are usually as occurring metal hydroxyl groups on the surface of many metal oxides which are the most abundant and active adsorption sites for adsorbate and can be detected by IR spectroscopy. A strong and broad band in the 3600-3100 cm^{-1} region (O-H stretching vibration) was assigned for the presence of hydroxyl groups of coordinated water molecules (Long *et al*., 2011).

Spectrum of the selected (Fe-Al-Mn) mixed oxide nanocomposite was carried out in KBr medium and the results obtained as such are depicted in Figure 10 with the main absorption peaks located at 3414, 1628, 1384, 587 and 443.6 cm^{-1}. Accordingly, the absorption peak at 3414 cm^{-1} represents O-H stretching vibration of the adsorbed water molecules (Sujana and Anand, 2010; Tofik *et al*., 2016). Absorption peak at 1628 correspond to the bending vibrations of the H-O-H group and may actually be attributed to the presence of physiosorbed water on the surface of oxides (Thakkar and Chudasama, 2009; Jianbo *et al*., 2013; Kasahun, 2015). Absorption peak at 1384 cm^{-1} correspond to the Al-O stretching (Fekadu, 2016; Nejat *et al*., 2018). The bands at 587 cm^{-1} and 443.6 cm^{-1} can be assigned to the symmetrical stretching vibrations of the mixed metal oxides M-O and M-M-O (Zhang *et al*., 2009) or Fe-O (Fe_3O_4) bond presence in the nanocomposite and an example of some interactions among Fe(III), Al(III) and Mn(IV) though oxygen or hydroxide bridge (Tesfa *et al*., 2014).

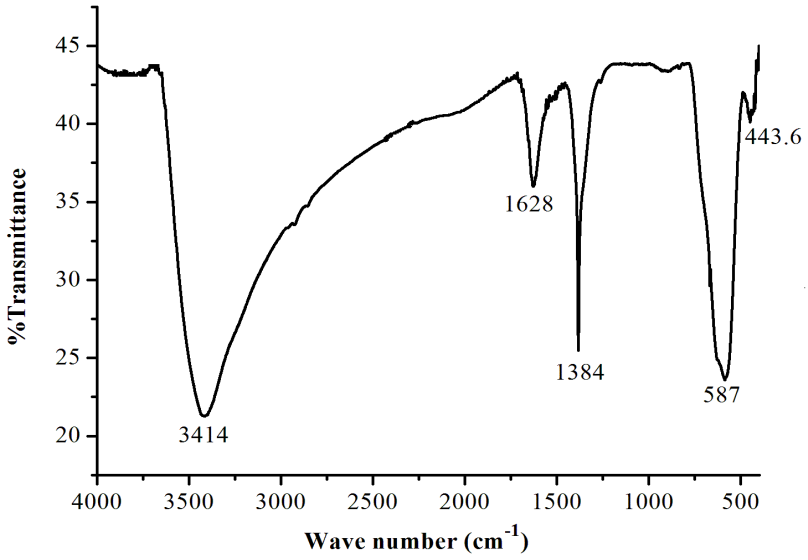

Figure 10. FTIR spectrum of the selected nano sized Fe-Al-Mn mixed oxide adsorbent

4.2. Physicochemical Properties of the Soil Samples

4.2.1. Soil Texture and Bulk Density

The relative percentage of soil separates (sand, silt and clay) of a given soil is referred to as soil texture. Soil samples from the studying districts comprised percent of Sand (58, 66, 66 and 71), Silt (15, 7, 12 and 8) and Clay (27, 27, 21 and 22) for Boji Dirmaji, Kiltu Kara, Mene Sibu and Nedjo sampling locations, respectively. The common textural classes, as recognized by USDA (2014) are given in equilateral triangles or international equilateral triangles model. Accordingly, the studied districts soil texture can be classified as sandy clay loam. Crops could grow well in such soils areas and it has a potentially well-balanced capacity to retain water, form a stable structure and provide adequate aeration (Mulugeta, 2015).

The Bulk density value was significantly different for each soil samples ($\alpha = 0.05$), However, numerically the highest mean (1.33 g/cm^3) value of bulk density was recorded at the Kiltu Kara and the lowest mean (1.14 g/cm^3) value under the Boji Dirmaji soil. Generally all soil samples had low bulk density except Kiltu Kara which have moderate bulk density (Table 5 and Appendix Table 3). Bulk density value of about 1.33 g/cm^3 was generally considered optimum for plant growth (Ashenafi and Bobe, 2016).

4.2.2. Soil pH

The soil pH represents a measure of the acidity, which plays an important role in determining the solubility of important elements and processes from soil. Soil pH is among the important environmental factors, which can influence plant growth. In this study, both pH (H_2O) and pH (KCl) of the soil were analyzed at ($\alpha = 0.05$) and even though the pH variation is not so large, there was significance difference between each soil samples (Table 5, Appendix Table 1). Accordingly, soil collected from Boji Dirmaji with pH (4.35) can be categorized as very strongly acidic and soil collected from Nedjo with pH (5.06) could be categorized as strongly acidic (Tekalign, 1991; Abdenna, 2013) (Table 5 and Appendix Table 1). According to Abreha *et al*. (2012) decreasing of the soil pH (increasing acidity) in western and southern Ethiopia was due to intensive rainfalls that can leaches soluble nutrients such as calcium and magnesium and with subsequent replacement by Al^{3+} and H^+ ions. A pH value of less than 5.5 is considered as a problematic for most microbial activities, and this directly influences availability of nutrients to plant (Solomon, 2008).

The pH (KCl) test is the more accurate of the two pH tests, as it reflects what the plant experiences in the soil. The values of pH (KCl) have similar trend with pH (H_2O): BD < KK< MS< NE but lower than pH (H_2O) by about one (1) unit (Table 5). A useful, but not consistently accurate, conversion is to subtract 1unit from the pH (H_2O) to obtain a pH (KCl) value because it may be less or more than the range depend on the soil type (Gavriloaiei, 2012; Gemechu *et al*., 2015). The main advantage of the measurement of soil pH in salt solution is the tendency to eliminate interference from suspension effects and from variable salt contents, such as fertilizer residues (George *et al*., 2013). Most plants and soil organisms prefer pH range between 6.0 and 7.5 (Hazelton and Murphy, 2007).

4.2.3. Electrical Conductivity

Electrical conductivity (EC) is a measure of soil salinity. The ability of soil solutions to conduct electricity (i.e. conductance) depends on the concentration of the ions present and their electrical charge. Significance difference ($\alpha = 0.05$) among soil samples were observed for this parameter. All of the soil samples have an electrical conductivity values ranging from 0.019 - 0.080 dS/m and lies at lower limit of saline soil (Achalu, 2014; EthioSIS, 2014). Hence the soil samples are non-saline soils due to low ions in soil solution.

4.2.4. Soil Organic Carbon

Organic carbon was higher in Nedjo and lower in Mene Sibu. According to Tekalign (1991) ratings of organic carbon content as very low < 0.50, low 0.5 - 1.5, medium 1.5 - 3.0, and high > 3.00. Based on this category, all the studied soils fall in the low range despite the various amount extracted from the soils. Tekalign and Haque (1987) and Dawit *et al.* (2002) reported OC as the main source of available P, but the availability of P in most soil of Ethiopia decline by the impacts of fixation, abundant crop harvest and erosion and soil OC analyzed however, showed significant difference ($\alpha = 0.05$) among the studied soils.

4.2.5. Soil Organic Matter

The SOM of Mene Sibu soil showed very low OM while the other have low (Murphy, 1968) (Table 5 and Appendix Table 3) in which MS < KK< BD < NE. Organic matter has an important influence on soil physical and chemical characteristics, soil fertility status, plant nutrition and biological activity in the soil (Brady and Weil, 2002). Even though a significant

difference was observed among the soil (α = 0.05), the organic matter of the soil is deficient for plant growth and this may also come from loss of OC.

4.2.6. Total Nitrogen

Total nitrogen contents of the soil was analyzed and there was significance difference (α = 0.05) among the soil. Among studied soil samples, total nitrogen was very low at Nedjo (0.027%) and medium in other soils (Bruce and Rayment, 1982; Havlin *et al*., 2013) (Appendix Table 3).

4.2.7. Cation Exchange Capacity

CEC of study area were rated as moderate for both Boji Dirmaji and Kiltu Kara (24.36 and 19.33 meq/100g), respectively and higher for other soil (Mene Sibu and Nedjo) (FAO, 2006; London, 2014) (Table 5 and Appendix Table 3). CEC value was significantly different for each soil (α = 0.05) and this was happened due to different physicochemical properties.

Table 5. Selected physicochemical properties of the acidic soil samples studied (n = 3)

Parameters		Soil Samples				
		BD	KK	MS	NE	LSD (5%)
pH (1:2.5)	H_2O	4.35±0.024^{d}	4.62±0.003^{c}	4.80±0.003^{b}	5.06±0.011^{a}	0.03
	KCl	3.54±0.010^{d}	3.61±0.006^{c}	3.70±0.001^{b}	3.79±0.006^{a}	0.01
EC (dS/m)		0.019±0.101^{d}	0.08±0.050^{a}	0.022±0.401^{c}	0.033±0.134^{b}	0.001
Ex A.		4.16±0.006^{a}	3.48±0.028^{b}	2.73±0.002^{c}	1.69±0.009^{d}	0.03
Ex Al.	meq/100g	3.37±0.030^{a}	2.61±0.005^{b}	2.62±0.005^{b}	1.18±0.002^{c}	0.03
Ex H^{+}.		0.79±0.029^{b}	0.87±0.002^{a}	0.11±0.031^{d}	0.51±0.008^{c}	0.04
%OC		0.95±0.006^{b}	0.69±0.014^{c}	0.51±0.009^{d}	1.05±0.011^{a}	0.02
%OM		1.64±0.011^{b}	1.18±0.025^{c}	0.88±0.015^{d}	1.80±0.019^{a}	0.03
%TN		0.18±0.003^{c}	0.22±0.003^{a}	0.21±0.004^{b}	0.03±0.001^{d}	0.01
CEC	meq/100g	24.37±0.651^{c}	19.33±0.640^{d}	32.40±0.800^{a}	26.43±1.040^{b}	1.51
P_{av}		3.53±0.017^{d}	10.11±0.047^{a}	5.62±0.056^{c}	9.95±0.062^{b}	0.09
P_T	g/kg	0.33±0.151^{d}	0.39±0.468^{c}	0.41±0.695^{b}	0.55±0.549^{a}	0.94
Fe_{ox}		0.27±0.530^{a}	0.27±0.010^{a}	0.12±0.150^{c}	0.15±1.000^{b}	1.07
Mn_{ox}	g/kg	0.069±0.020^{c}	0.06±0.001^{d}	0.07±0.060^{b}	0.10±0.050^{a}	0.84
Fe_d		0.83±0.050^{b}	1.02±0.040^{a}	0.30±0.020^{d}	0.80±0.050^{c}	0.08
Mn_d		0.10±0.080^{b}	0.08±0.040^{c}	0.43±0.080^{a}	0.03±0.050^{d}	0.12
Bd	g/cm^3	1.14±0.003^{d}	1.33±0.001^{a}	1.16±0.003^{c}	1.26±0.006^{b}	0.01
Soil	% sand	58	66	66	71	
Texture	% silt	15	7	12	8	
	% clay	27	27	22	21	
	class	Sandy clay loam	Sandy clay loam	Sandy clay loam	Sandy clay loam	

Mean values in the rows with different letters a, b, c and d are significantly different ($\alpha = 0.05$). *BD= Boji Dirmaji Soil, KK= Kiltu Kara Soil, MS =Mene Sibu Soil, NE = Nedjo Soil, P_{av} = Availability of P, Bd = Bulky density, CEC = Cation exchange capacity, EC = Electrical conductivity, Ex.A =Exchangeable acidity, Ex.Al=Exchangeable alumni, Ex.H^{+}= Exchangeable hydrogen, OC = Organic carbon, OM = Organic matter, TN = Total nitrogen, P_T =Total phosphorus, Fe_d = Iron extracted by dithionite, Mn_d = Manganese extracted by dithionite, Fe_{ox} = Iron extracted by oxalate, Mn_{ox} = Manganese extracted by oxalate, LSD =Least significance difference (5%), n = Number of replication.*

4.2.8. Exchangeable Acidity

Exchangeable acidity is an important parameter to describe the acidity of soil, which is the combined total exchangeable aluminum and reactive hydrogen ions; according to this study, it shows very acidic soil in which all treatments have > 2 meq/100g except Nedjo (1.691 meq/100 g). The high soil exchangeable acidity in the Bodji Dirmaji might be associated with the occurrence of lower soil pH (Gemechu *et al*., 2015).

Extractable aluminium closely follows the pH of the soil and becomes a problem when the pH (water) is less than 5.5 (in soils which contain significant aluminium). When extractable aluminium > 2, sensitive plants will be affected. The concentration of the H^+ in soil to cause acidity is pronounced at pH values below 4 while excess concentration of Al^{3+} is observed at pH below 5.5 (Table 5). When exchangeable acidity analyzed ($\alpha = 0.05$) and it was significantly different except Ex.Al of KK and MS which was not significantly different (Table 5).

4.2.9. Available and Total Phosphorus

The available P of the soil of the study area was in general was found to be low (Jones, 2003) (Table 5; Appendix Table 3). The low available P observed in the soil of the study area was in agreement with the results reported by Murphy (1968) and Eylachew (1987) that the availability of P under most soils of Ethiopia decline by the impacts of fixation, abundant crop harvest and erosion. Variations in available P content in soils are also related with the intensity of soil weathering or soil disturbance, the degree of P fixation by Fe, Al and Ca (Sanchez *et al*., 2003; Achalu *et al*., 2012a,b). Low available P status may also be related mainly to the presence of low pH and high exchangeable acidity (Paulos, 1996; Abreha *et al*., 2012) and there was significance difference ($\alpha = 0.05$) between each soil samples.

The distribution of total P content followed a similar pattern to available P distributions and ranged from 331.10 to 547.48 mg/kg. As per the ratings of Landon (1984), medium total P content was observed in all acidic soil of the studied districts, however numerically higher in the Nedjo. The total P contents of Ethiopian soil as reported by many studies ranged from 200 to 800 mg/kg (Eylachew, 1987), 185 to 1981 mg/kg (Tekalign and Haque, 1991), 226 to 1570 mg/kg (Duffera and Robarge, 1996) and 553 to 976 mg/kg (Achalu *et al*., 2012a).

4.2.10. Phosphate Bounded Fe and Mn

The percentages of Fe and Mn extracted by dithionite citrate bicarbonate and acid ammonium oxalate methods are shown in Table 5. Generally, the amount of Fe_{ox}, Mn_{ox}, Fe_d and Mn_d extracted were found to be significant ($\alpha = 0.05$) among the studied soils. Even though the dithionite citrate bicarbonate extracted elements are higher, the ammonium oxalate extractable Fe and Mn are also high evidencing the involvement of poorly crystalline and amorphous forms of Fe and Al in the soil. Poorly crystalline and amorphous forms have an extensive surface area to sorb P (Sharpley, 1983). The percentages of Fe, extracted by the dithionite citrate bicarbonate method was more than the percentage of Fe, extracted by the acid ammonium oxalate method and this was agrees with Gemechu *et al*.(2015) and Olayinka *et al*.(2015).

4.3. Long-Term Desorption Study

Long-term P desorption was carried out using the DMT-HFAMO on four acidic soils namely Boji Dirmaji (BD), Kiltu Kara (KK), Mene Sibu (MS) and Nedjo (NE). All soil samples received P doses of 0, 50, 100 and 150 mg/kg and equilibrated for 112 days. The amount of P desorbed by DMT-HFAMO was significantly influenced ($\alpha = 0.05$) both by the P treatments and extraction time (Table 6 and 7). Among all treatments, the amount of DMT-HFAMO extractable P significantly increased with increasing extraction time (effect of extraction time was found to be significantly different for all soil samples considered) and amount of phosphate loaded. However, the amount of P recovered decreased with increase in phosphate load evidencing the transformation of applied to the less labile form as the result of incubation (Appendix Table 5).

The cumulative P desorbed was more or less comparable among the studied soil samples: Nedjo (1.43-30.35 mg/kg), Mene Sibu (1.32-30.10 mg/kg) Kiltu Kara (1.01-28.13) and Boji Dirmaji soil (1.16-26.86 mg/kg) at all levels of extraction time (1-28 days). Cumulative P desorbed was higher in the P_{150} treatments (150 mg/kg) and lower in the P_0 or control (0 mg/kg) at all levels of extraction time (28 days) for all soils and these results concurred with the reports made by De Jager and Claassens (2005), Taddesse *et al*. (2008a) and Ochwoh *et al*.(2016). The fact that the control had very little DMT-HFAMO extractable P might be the result of the low amount of P. The high presence of Fe and Al in the soil samples reduce desorption process by forming complex with phosphate ions in acidic soils and as a result of incubation (Ochwoh *et al*., 2016) (Table 5, 6 and 7).

Table 6. Effect of phosphorus levels and extraction time on phosphorus desorption (n = 3)

		P desorbed (mg/kg) per days					
Soil Samples	P Treatments (mg/kg)	1	7	14	21	28	Averege P (mg/kg)
	0	z1.16^{c}	y3.01^{d}	x5.43^{d}	w7.62^{d}	v9.36^{d}	5.316
BD	50	z3.65^{b}	y8.31^{c}	x13.16^{c}	w18.13^{c}	v22.77^{c}	13.29
	100	z3.71^{b}	y8.98^{b}	x14.32^{b}	w19.43^{b}	v24.50^{b}	14.19
	150	z4.70^{a}	y10.41^{a}	x16.09^{a}	w21.24^{a}	v26.86^{a}	15.86
LSD (5%)		0.14	0.45	0.86	0.95	1.10	
CV (%)		2.29	3.13	3.71	3.04	2.82	
	0	z1.01^{d}	y3.27^{c}	x5.75^{d}	w7.99^{d}	v9.57^{d}	5.52
KK	50	z4.30^{c}	y9.74^{b}	x14.99^{c}	w20.06^{c}	v24.36^{c}	14.69
	100	z4.57^{b}	y10.12^{b}	x15.84^{b}	w21.18^{b}	v25.84^{b}	15.51
	150	z4.90^{a}	y10.73^{a}	x17.05^{a}	w23.47^{a}	v28.13^{a}	16.86
LSD (5%)		0.22	0.41	0.63	0.86	1.19	
CV (%)		3.12	2.59	2.50	2.50	2.88	
	0	z1.32^{d}	y4.07^{d}	x6.23^{d}	w8.74^{d}	v10.80^{d}	6.23
MS	50	z4.15^{c}	y9.56^{c}	x14.52^{c}	w20.02^{c}	v25.36^{c}	14.72
	100	z4.62^{b}	y10.55^{b}	x16.08^{b}	w21.67^{b}	v27.45^{b}	16.07
	150	z5.19^{a}	y11.93^{a}	x18.35^{a}	w24.06^{a}	v30.10^{a}	17.93
LSD (5%)		0.32	0.59	0.81	0.59	0.78	
CV (%)		4.48	3.44	3.11	1.69	1.77	
	0	z1.43^{d}	y4.02^{d}	x6.39^{d}	w9.01^{d}	v11.29^{d}	6.43
NE	50	z4.12^{c}	y9.78^{c}	x14.89^{c}	w20.14^{c}	v24.55^{c}	14.70
	100	z4.71^{b}	y10.59^{b}	x16.99^{b}	w22.40^{b}	v27.65^{b}	16.47
	150	z5.23^{a}	y11.91^{a}	x18.52^{a}	w24.32^{a}	v30.35^{a}	18.07
LSD (5%)		0.33	0.40	0.75	1.13	1.08	
CV (%)		4.20	2.10	2.67	3.06	2.37	

BD = Boji Dirmaji Soil, KK = Kiltu Kara Soil, MS = Mene Sibu Soil, NE = Nedjo Soil, CV = Coefficient of variation (%), LSD = Least significance difference (5%), n = Number of replications. Mean values in rows with different letters z, y, x, w and v are significantly different ($\alpha = 0.05$*), while mean values in the columns with different letters a, b, c and d are significantly different (*$\alpha = 0.05$*).*

Desorption of P increased with increasing the amount of sorbed P or the level of P added (Table 6 and 7). In general the cumulative P desorbed in the 28 days of extraction followed the order NE>MS>KK>BD on numerical basis although no statistically significant difference is observed in most respects. This signifies that the physicochemical properties of the soil samples are comparable. The fact that the control had very little DMT-HFAMO extractable P might be the result of the low amount of available P (Taddesse *et al*., 2008a,b). The amount of P extracted from the control during the 28 days of extraction was much higher than Bray II P for soil samples collected from BD and MS where as comparable amount with Bray-II P (Table 5) for soil samples from NE and KK (Table 6 and 7).

The percentages of the applied P recovered were calculated as: % P recovered = (Px–P0)/P1*100; where Px was P in the x^{th} fraction of the P treatments, and P0 was P in the 0^{th} fraction of the initial no P added (P0) treatments, while P1 was the applied P level of the x^{th} fraction (Ochwoh *et al*., 2005) (Appendix Table 4). From above the added amount was in opposite (which lower treatments have higher percent of recovery while treatments with high concentration have low percent of recovery for the same soil samples in each days (Appendix Table 4). For example for P3 (150 mg/kg) to get high %P RV, desorption must be too high, but this very hard for acid soils because acid soil had high degree of fixation P with Fe, Al (Achalu *et al*., 2012a) even though desorption was higher as compared to other treatments. According to the ANOVA and LSD values, there was highly significant responses ($\alpha = 0.05$) in the successive DMT-HFAMO extracted P, from all the different treatments (Table 6 and Appendix Table 4). The data fitted to regression equations and the R^2 values indicates very good correlations between treatments and P extractions (Figure 11 and 12).

Table 7. Effect of soil properties on the P desorption of different soil samples with the same treatments (n = 3)

Soil Samples	P Treatments (mg/kg)	P desorbed (mg/kg) per days				
		1	7	14	21	28
BD	0	z1.16^{c}	y3.01^{c}	x5.43^{c}	w7.62^{d}	v9.36^{c}
KK	0	z1.01^{d}	y3.27^{b}	x5.755^{b}	w7.99^{c}	v9.66^{c}
MS	0	z1.32^{b}	y4.07^{a}	x6.23^{a}	w8.74^{b}	v10.80^{b}
NE	0	z1.43^{a}	y4.02^{a}	x6.39^{a}	w9.01^{a}	v11.29^{a}
BD	50	z3.65^{b}	y8.31^{b}	x13.16^{b}	w18.13^{b}	v22.77^{b}
KK	50	z4.30^{a}	y9.74^{a}	x14.99^{a}	w20.06^{a}	v24.36^{a}
MS	50	z4.15^{a}	y9.56^{a}	x14.52^{a}	w20.02^{a}	v25.36^{a}
NE	50	z4.12^{a}	y9.78^{a}	x14.89^{a}	w20.14^{a}	v24.55^{a}
BD	100	z3.71^{b}	y8.98^{b}	x14.32^{c}	w19.43^{b}	v24.50^{b}
KK	100	z4.57^{a}	y10.12^{a}	x15.84^{b}	w21.18^{a}	v25.84^{b}
MS	100	z4.62^{a}	y10.55^{a}	x16.08^{ab}	w21.67^{a}	v27.45^{a}
NE	100	z4.71^{a}	y10.59^{a}	x16.99^{a}	w22.40^{a}	v27.65^{a}
BD	150	z4.70^{b}	y10.41^{b}	x16.09^{c}	w21.25^{c}	v26.86^{c}
KK	150	z4.90^{ab}	y10.73^{b}	x17.05^{b}	w23.47^{b}	v28.13^{b}
MS	150	z5.19^{a}	y11.93^{a}	x18.35^{a}	w24.06^{ab}	v30.10^{a}
NE	150	z5.23^{a}	y11.91^{a}	x18.52^{a}	w24.32^{a}	v30.35^{a}

BD= Boji Dirmaji Soil, KK= Kiltu Kara Soil, MS =Mene Sibu Soil, n = Number of replications. Mean values in rows with different letters z, y, x, w and v are significantly different ($\alpha = 0.05$*) ,while mean values in columns with different letters a, b, c and d are significantly different (*$\alpha = 0.05$*).*

The cumulative desorption of P extracted by DMT-HFAMO within 28 days was very low as compared to the total P, but it was larger as compared to the availability of P (Table 5). This implies that soil samples have almost comparable physicochemical properties which can influence desorption of P. Small amount significance of difference in the soil samples with the same treatments at ($\alpha = 0.05$) (Table 7) might be due to difference in the nature of soil (Gemechu *et al*., 2015; Ochwoh *et al*., 2016; Reyhanitabar *et al*., 2018) even not much change numerically. No desorption stable phase or desorption plateau was reached during the entire period of extraction time and this indicates desorption was continues for a longer period than 28

days or 672 h (Figure 11 and 12) (De Jager and Claassens, 2005; Ochwoh *et al*., 2005; Taddesse *et al*, 2008a). Generally, the degree desorption of P for given treatments had order of P0 < P1 < P2 < P3 for all soil samples within 28 days of desorption time and it was agreement with Ochwoh *et al*. (2016) (Figure 11 and 12) in which high amount of P was desorbed from higher P treatment.

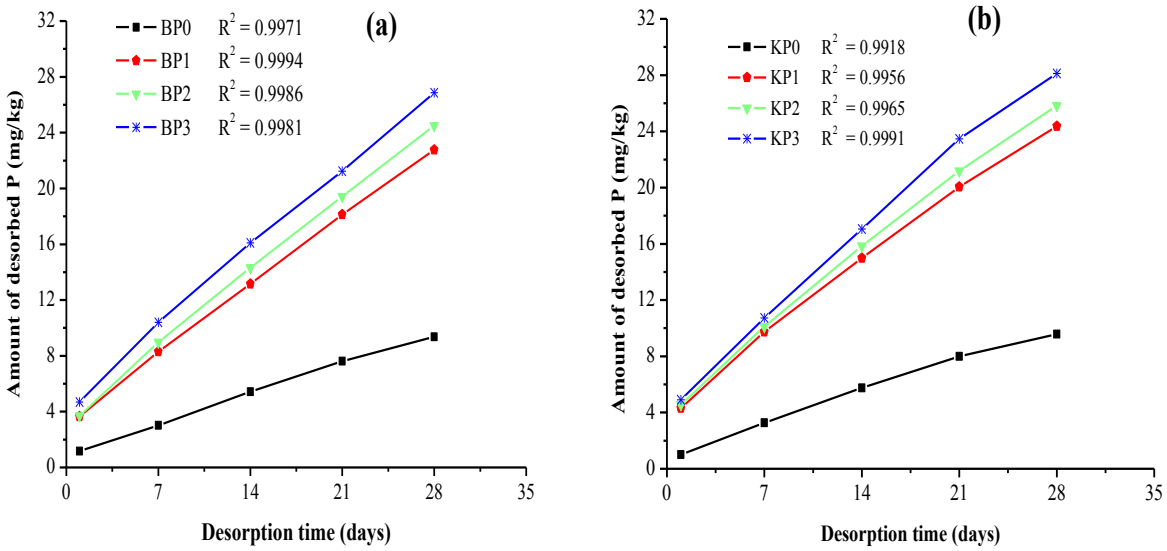

Figure 11. The effects of applied P on successive DMT-HFAMO extractable P over 28 days (a) Boji Dirmaji Soil (b) Kiltu Kara Soil

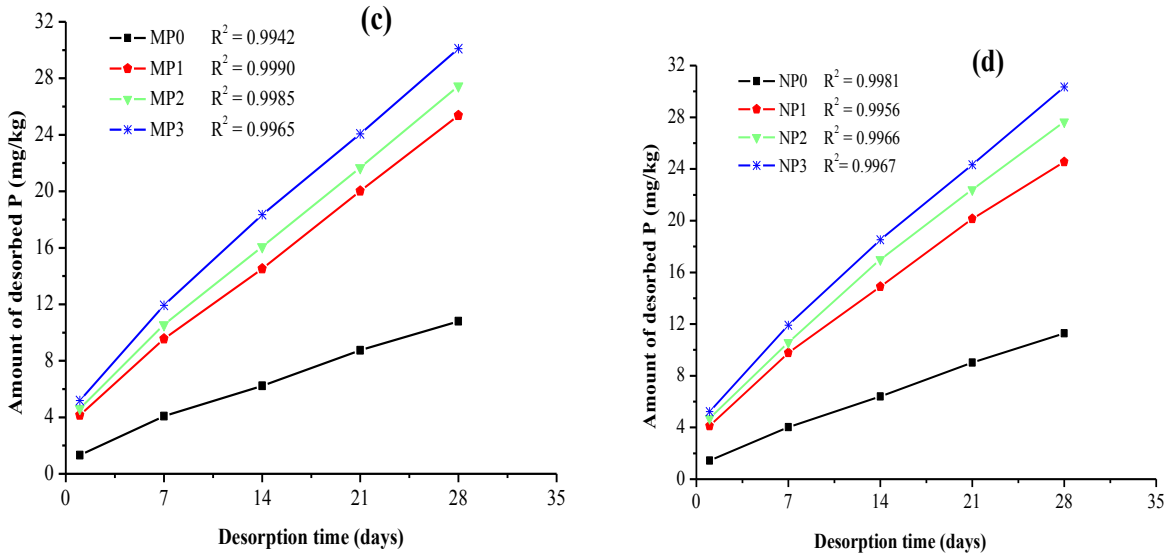

Figure 12. The effects of applied P on successive DMT-HFAMO extractable P over 28 days (c) Mene Sibu Soil (d) Nedjo Soil

4.4. Phosphorous Desorption Kinetics

Desorption kinetics of P in the soil sample was determined using the DMT-HFAMO as the sorbent and it can be schematically represented in equation (1)

$$SP \xrightarrow{K_R} P_{sol} \xrightarrow{K_T} P_{HFAMO}$$

Where SP is the solid phase P, P_{sol} is P in solution, P_{HFAMO} is P adsorbed by HFAMO, k_T is the rate constant of P transport through the membrane, and k_R is the rate constant of P release. The presence of two pools is assumed: the pool with the fast release kinetics is pool A (SP_A) and the pool with the slow release kinetics is pool B (SP_B). With this assumption, the mass balance equation for the total exchangeable solid phase soil P (SP_{total}) at time t = 0 equation (2):

$$SP_{total\,(0)} = SP_{A0} + SP_{B0}$$

Where SP_{A0} is initial amount of P in pool A and SP_{B0} is initial amount of P in pool B. The mass balance equation at time t equation (3):

$$SP_{total\,(t)} = SP_{A(t)} + SP_{B(t)}$$

Assuming the decrease in SPA and SPB follow first order kinetics, the integrated rate laws for the decrease of SPA and SPB will be as equation (4):

$$SP_{A(t)} = SP_{A0}e^{-kAt} \text{ and } SP_{B(t)} = SP_{B0}e^{-kBt}$$

Where k_A and k_B are conditional first order rate constants (day^{-1}) for P desorption from pools A and B, respectively.

The total solid phase soil P ($SP_{total\,(t)}$) remaining at time t will be given by equation (5):

$$SP_{total\,(t)} = SP_{A0}\, e^{-kAt} + SP_{B0}\, e^{-kBt}$$

The total amount of P released at time t is expressed as equation (6):

$$P_{R(t)} = SP_{A0} - SP_{A\,(t)} + SP_{B0} - SP_{B\,(t)}$$

$$= SP_{A0} - SP_{A0}\, e^{-kAt} + SP_{B0} - SP_{B0}\, e^{-kBt}, \text{ by rearranging this equation:}$$

$$= SP_{A0}\,(1 - e^{-kAt}) + SP_{B0}\,(1 - e^{-kBt})$$

It was assumed that the rate constant of P release from the soil was equal to the rate constant of P adsorption (k_A) by the DMT-HFAMO. The rate constant of P adsorption (k_A) by the DMT-HFAMO was obtained from a plot of the natural logarithm (ln) of the P desorbed by the DMT-HFAMO against time with the slope as k_A. Phosphorus desorption kinetic of soil sample was found to follow first order model (first order kinetics) which schematically shown in equation (1): $SP_A\,(t) = SP_{A0}\,e^{-kd}$ where k_d was the rate of the desorption P (0.021- 0.028 h^{-1}) and it was

comparable with Freese *et al*.(1995) and De Jager and Claassens (2005) but greater than Taddesse *et al.* (2008b) and Gemechu *et al*. (2015). The P desorption rates from the soil samples that received different phosphorus treatments had no significant variation after 7 days extraction time (Figure 13 and 14). This implies that the desorption proceed in similar manner, since the capacity of the membrane to pass the phosphate ion is similar except that of different P treatment, in which it may lead to difference in the amount of desorbed P. Desorption rates of the respective SPA decreased rapidly in the first 14 days and were almost the same after day 21 and approaches zero after day 35 (De Jager and Claassens, 2005) and this indicating that a fair amount of applied P could be extracted over the first 14 days with DMT-HFAMO and our result concurred with the findings of Ochwoh *et al*. (2016) and Reyhanitabar *et al*.(2018).

For the longer DMT-HFAMO extraction period (28^{th} day), the desorption rate was less than 1.2 mg/kg.day for all soil samples and it was decrease for the different P applications or P released decreased slowly with the increasing number of the extraction as well as time (Figure 13 and 14). The highest phosphorus release was noted on the first extraction of day one with P3(150 mg/kg) treatments for all soil samples. The results are in agreement with findings of Jalali and Zinli (2011), who reported that kinetics of P release from soil can be described as initial rapid rate followed by a slower rate. The same pattern of P release was also observed by Horta and Torrent (2007) and Nafiu (2009).

The kinetic study of soil had advantages that, approach potentially pose over existing methods is that the time frame of P release of potentially short and long-term plant available P of a soil can be estimated, and the distribution of applied P fertilizer between labile and less labile forms can be determined. The SP_A/SP_B distribution ratio can also be used to classify soils under cultivation according to plant P availability or potential P mobility (De Jager and Claassens, 2005) but in our case we have only one pool to study kinetic study of P desorption.

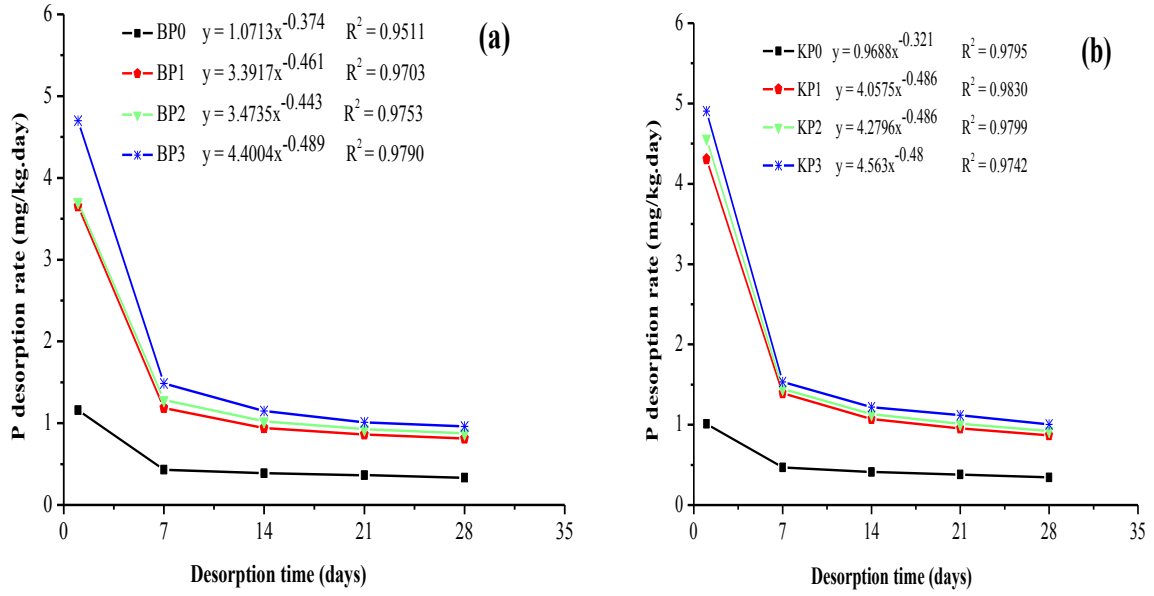

Figure 13. Desorption rates for the different P treatments over 28 days (a) Boji Dirmaji Soil (b) Kiltu Kara Soil

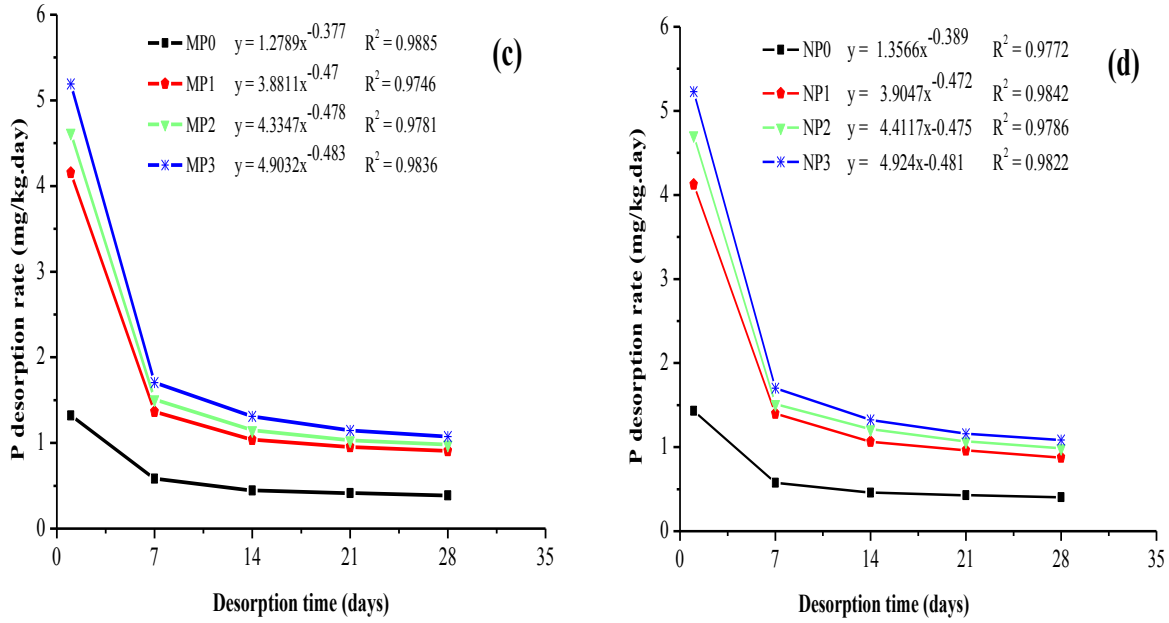

Figure 14. Desorption rates for the different P treatments over 28 days (c) Mene Sibu Soil (d) Nedjo Soil

4.5. Correlation of Soil Parameters with Cumulative Desorbed P

The correlation analysis is a bivariant method which was applied to describe the relation between two different parameters. The relationship between contents of physicochemical properties in the soil with cumulative phosphorus desorption (CD28P) were analyzed by Pearson's correlation coefficient for each soil with different treatments (Table 8). The high correlation coefficient (near +1 or −1) means a good relation between two variables and correlation around zero means no relationship between them at a significant level of 0.05 and 0.01 (Table 8 and Appendix Table 6, 7, 8 and 9).

Correlation can be also strongly correlated, if r > 0.7, whereas r values between 0.5 and 0.7 show moderate correlation between two different parameters (Sharma and Raju, 2013). When cumulative desorbed P correlated with contents of selected soil properties, low P-release was observed compared to total phosphorus, but higher as compared to available P (Table 5). It may be attributed due to high content of Fe and Mn which fix P and low pH (Gemechu *et al*., 2015). For example the negative significant relationship between soil pH (r = - 0.98) and similar manner for Mn_d (r = -1.00**) can reduce P desorption. This may be due to conversion of soluble phosphorus to insoluble calcium and magnesium phosphate thus reducing its availability with the rise in soil pH (Patil *et al*., 2015; Bhat *et al*., 2017). Bulk density of analyzed soil samples were inversely correlated (r = - 0.88) with cumulative desorbed P (CD28BP1) and it was consonant with Ashenafi and Bobe (2016).

Similarly, positive and highly significant correlation (r = 0.93), (r = 0.96) between cumulative desorbed P (CD28P) with P_T and P_{av}, respectively for CD28BP0 and CD28NP0. In addition, negative significant correlation between CD28P and Mn_d (r = - 1.00*), Fe_{ox} (r = - 0.99) and Mn_{ox} (r = - 0.94) for KK soil indicating the strong association between these soil parameters and desorbed P (Table 8 and Appendix Table 7). This implies that as the P_{av}, pH and P_T increase in the soils, the amount of desorbed soil P increase. Moreover, as the extractable composition of Fe and Mn increases in the soils, the amount of desorbed soil P decreases. In general the physicochemical properties of the soils were highly correlated with cumulative desorbed P (CD28P) (Table 8). However, the degree to which two securities are negatively or positively correlated might vary over time and are almost never exactly correlated, all the time. This condition may happen sometimes because one physicochemical property may affect other and it may make to don't have consistent.

Table 8. Correlation between soil properties and cumulative desorbed P with different treatments

Soil samples	Corre:	pH_{H2O}	pH_{KCl}	EC	OC	OM	TN	CEC	B_d	P_{av}	EX.A	EX.Al	$EX.H^+$	Fe_{Ox}	Mn_{Ox}	Fe_d	Mn_d	P_T
BD	CD28BP0	-0.52	0.04	0.84	0.40	0.41	0.62	0.91	0.37	-0.15	-0.54	0.58	-0.72	-0.45	-0.89	-0.99	-0.96	0.93
	CD28BP1	-0.15	-0.67	-0.31	-0.89	-0.90	0.02	-0.97	-0.88	-0.52	0.95	0.08	0.11	-0.23	0.98	0.85	0.92	-0.48
	CD28BP2	-0.90	-0.99	0.61	-0.88	-0.87	0.83	-0.34	-0.90	-0.99*	0.79	0.86	-0.76	-0.93	0.38	0.06	0.20	0.50
	CD28BP3	0.42	-0.15	-0.78	-0.50	-0.51	-0.53	-0.95	-0.47	0.04	0.62	-0.48	0.64	0.35	0.93	0.99*	0.98	-0.88
KK	CD28KP0	-0.45	-0.77	-0.77	-0.61	-0.60	-0.23	-0.98	0.17	-0.99	-0.93	-0.64	-0.93	-0.34	-0.94	0.07	-0.77	-0.22
	CD28KP1	-0.91	-1.00**	-1.00**	-0.97	-0.97	-0.79	-0.64	-0.49	-0.87	-0.95	-0.01	-0.95	-0.86	-0.51	0.68	-1.00**	0.45
	CD28KP2	0.79	0.97	0.97	0.90	0.89	0.64	0.80	0.28	0.96	1.00	0.24	1.00	0.72	0.69	-0.50	0.97	-0.23
	CD28KP3	-0.98	-0.82	-0.82	-0.92	-0.93	-1.00*	-0.07	-0.91	-0.42	-0.59	0.57	-0.59	-0.99	0.09	0.98	-0.82	0.89
MS	CD28MP0	-0.99	0.87	-0.39	-0.89	-0.87	-0.97	-0.51	-1.00	-0.29	0.99	-0.51	0.96	0.64	-0.07	0.98	-0.61	-0.68
	CD28MP1	0.96	-0.94	0.53	0.80	0.79	0.91	0.64	0.99*	0.13	-1.00*	0.64	-0.99	-0.51	-0.09	-0.93	0.73	0.56
	CD28MP2	-0.24	0.77	-1.00*	0.11	0.13	-0.12	-0.99	-0.46	0.79	0.49	-0.99	0.60	-0.48	0.90	0.17	-0.96	0.43
	CD28MP3	-0.38	-0.25	0.80	-0.67	-0.69	-0.49	0.70	-0.15	-0.99*	0.11	0.70	-0.01	0.90	-0.98	0.44	0.62	-0.88
NE	CD28NP0	0.23	0.97	-0.29	-0.65	-0.66	0.96	-1.00**	-0.29	0.91	-0.23	-0.84	-0.04	-0.96	0.68	0.01	0.53	0.67
	CD28NP1	-0.74	0.67	-0.98	-0.98	-0.98	0.21	-0.47	-0.98	0.80	0.74	0.07	0.85	-0.21	0.97	-0.87	0.99*	0.34
	CD28NP2	-0.99	0.14	-0.93	-0.69	-0.68	-0.38	0.11	-0.93	0.32	0.99	0.62	0.99*	0.38	0.66	-1.00	0.79	-0.81
	CD28NP3	-0.69	0.73	-0.96	-0.99	-0.99	0.29	-0.54	-0.96	0.85	0.69	-0.01	0.81	-0.29	0.99	-0.83	1.00*	0.27

BD = Boji Dirmaji Soil, KK = Kiltu Kara Soil, MS = Mene Sibu Soil, NE = Nedjo Soil

** Correlation is significant at the 0.05 level (2-tailed)* and *** = Correlation is significant at the 0.01 level (2-tailed), Corre:= Correlation and CD28P = Cumulative desorbed P for each treatments (P0 (0 mg/kg), P1(50 mg/kg), P2 (100 mg/kg) and P3 (150 mg/kg))*

5. SUMMARY, CONCLUSIONS AND RECOMMENDATIONS

5.1. Summary and Conclusions

Fe-Al-Mn ternary nanocomposite adsorbent was synthesized by co-precipitation method. The as-synthesized adsorbent was characterized by FTIR, XRD, SEM, EDX, BET and FAAS. The as-synthesized ternary nanocomposite had 22.75 nm crystalline size and 203.69± 1.34 m^2/g surface area and it had high capacity to desorb P. So that HFAMO ternary nanocomposite was found to be exhibit high sorption capacity compared to single system which makes the desorption process faster. Laboratory experiments were carried out to investigate desorption of P from acid soil using the synthesized adsorbent. Phosphorus (P) desorption patterns play a vital role in devising appropriate soil P management practices for its use efficiency in order to ensure better crop yields and environmental health. The P releasing soil test is fundamentally different from other soil tests in that it does not chemically extract P from soils; rather it removes P by sorption from solution into DMT-HFAMO filled with ternary oxide nanocomposite. This facilitates desorption of available P from soil colloids. The P releasing soil test has been reported to be effectively measure plant available P and P susceptible to loss in runoff that is biologically available to algae and other water plants. It should also be noted that routine soil extractable (labile) P alone by Bray 1 or 2, does not provide adequate information on the status of the soil especially in terms of the longterm capacity of the soil to supply P for plant growth.

The P desorption studies were conducted with the residual P in the soil using DMT-HFAMO (dialysis membrane tube filled with hydrous iron-aluminum-manganese mixed oxides nano composite) extractant. The phosphorus sorption capacity of soils depends on soil physicochemical properties (e.g. pH , clay, available P, organic matter, Available P, total nitrogen, organic matter, total P, soil texture, bulk density, oxalate and dithionite extractable Fe, Mn and other). In acid to neutral soils fixation of P mainly takes place with reactive forms of Fe and Al (as hydroxides, Al, and Fe bound to the organic matter). The Fe-Al-Mn mixed oxide nanocomposite was synthesized and studies of desorption properties were carried out to mimic the plant to absorb the P from four soil samples (BD, KK, MS and NE) with different treatments P0, P1, P2 and P3 having order of P desorption P0 < P1 < P2 < P3 for all soil samples. This precluded from establishment of equilibrium in the 28 period and desorbed P increases with increasing added P. The cumulative P released with time followed the same

pattern for all treatments of soil, with rapid release of P with 28 days (672 h). The cumulative P desorbed was more or less comparable among the studied soil samples but numerically higher in Nedjo soil and lower at the Boji Dirmaji soil. Only fast releasing of P was attained during the experimental periods and no desorption stable phase or desorption plateau was reached during the entire period of extraction time and this indicates desorption can continue for a longer period than 28 days.

P desorption kinetics of soil samples were characterized by using DMT-HFAMO as specific phosphorus sink and the first-order model described the kinetic data with rate constant of (0.021-0.028 h^{-1}), give valuable insight on the long-term desorption kinetics of P. At the end (28^{th} day) however desorption rate was very. The desorption kinetics of the soil were described relatively well expressed with a first order model with high R^2 or regression values and it indicates a very good correlations between treatments and P extracted. P desorption kinetics characterization of a soil, might be a more economical and environmentally responsible approach to P fertilizer recommendations. This property could be relevant for the crops in the field with respect to the residual effect of added fertilizer P and therefore, could be important in the economic management of fertilizer applications rates.

5.2. Recommendations

This work tried to use ternary system at nanoscale as a sorbent filled in DMT, mimicking the plant action to study P desorption from soil. The ternary nanocomposite (DMT-HFAMO) was found to exhibit high sorption capacity compared to single system which makes the desorption process faster. Therefore, this method is very important to implement low input P management strategy to alleviate the problem of soil acidity. Therefore, the following recommendations are made as a result of the outcome of this study.

- It is better if research conducted on other soils (basic and neutral) to compare efficiency of nanocomposite for P desorption.
- Carry out the research on the ability of the adsorbent selectivity with heavy metals from soil and aqueous.
- It is recommended to conduct a research on other fourth metal oxide doped to the already synthesized Fe-Al-Mn adsorbent to further enhance desorption efficiency by varying ratio.
- Desorption studies longer than 28 days also have to be conducted to verify extrapolated long-term P desorption and P desorption kinetics of soil.

6. REFERENCES

Abdenna Deressa. 2013. Evaluation of soil acidity in agricultural soils of smallholder farmers in south western Ethiopia. *Science, Technology and Arts Research Journal*, 2(2): 01-06.

Abdu, N. 2006. Soil-phosphorus extraction methodologies. *A Review African Journal of Agricultural Research*, 5: 159-161.

Abrams, M.M. and Jarrel, W.M. 1992. Bioavailability index of phosphorus using ion exchange resin impregnated membranes. *Soil Science Society of American Journal*, 56:1532-1537.

Abreha kidanemariam, Heluf Gebrekidan, Tekalign Mamo and Kibebew Kibret. 2012. Impact of altitude and land use type on some physical and chemical properties of acidic soils in tsegede highland, north Ethiopia. *Open Journal of Soil Science*, 2(3): 223-233.

Abreha kidanemariam. 2013. Soil acidity characterization and effects of liming and chemical fertilization on dry matter yield and nutrient uptake of wheat (*Triticum Aestivum* L.) on soils of Tsegede District, Northern Ethiopia. PhD Dissertation, Haramaya University, Ethiopia.

Achalu Chimdi, Heluf Gebrekidan, Kibebew Kibret and Abi Tadesse. 2012a. Status of selected physicochemical properties of soils under different land use systems of Western Oromia, Ethiopia. *Journal of Biodiversity and Environmental Sciences*, 2(3): 57-71.

Achalu Chimdi, Heluf Gebrekidan, Kibebew Kibret and Abi Tadesse. 2012b. Response of barley to liming of acid soils collected from different land use systems of Western Oromia, Ethiopia. *Journal of Biodiversity and Environmental Sciences*, 2(5): 37-49.

Achalu Chimdi, Heluf Gebrekidan, Abi Tadesse and Kibebew Kibret. 2013. Phosphorus desorption patterns of soils from different land use systems of East Wollega, Ethiopia. *Middle-East Journal of Scientific Research*, 17 (2): 245-251.

Achalu Chimdi. 2014. Assessment of the severity of acid saturations on soils collected from cultivated lands of east wollega zone, Ethiopia. *Science, Technology and Arts Research Journal*, 3(4): 42-48.

Agrawal, A. and Sahu, K.K. 2006. Kinetic and isotherm studies of cadmium adsorption on manganese nodule residue. *Journal of Hazardous Materials,* 137: 915-924.

Akram, M., Kanwal, Z., Rauf, A., Sabri, N., Riaz, S. and Naseem, S. 2016. Size and shape dependent antibacterial studies of silver nanoparticles synthesized by wet chemica routes. *Nanomaterials,* 6: 74-79.

Alamos, L.N.M. 2006. Estimated energy savings and financial impacts of nanomaterials by design on selected applications in the chemical industry. *Review Environmental Science and Technology,* 45: 12-23.

Alvarez, R., Evans, L. A., Milham, P. J and Wilson, M. A. 2004. Effects of humic material on the precipitation of calcium phosphate. *Geoderma,* 118: 245-260.

Anamarai, D., Mariana, P., Bogdan, C., Anamaria Duedureanu Anheluta, Mariana pinte alad Bogdan, C. and Simionencu. 2012. Tailored and functionalized magnetic particles for biomedical and industrial application. *Materials Science and Technology*, 3: 1-31.

Ashenafi Worku and Bobe Bedadi. 2016. Studies on soil physical properties of salt affected soil in amibara area, central rift valley of Ethiopia. *International Journal of Agricultural Sciences and Natural Resources*, 3(2): 8-17.

Asmare Melese, Heluf Gebrekidan, Markku Yli-Halla and Birru Yitaferu. 2015. Phosphorus status, inorganic phosphorus forms, and other physicochemical properties of acid soils of Farta District, Northwestern Highlands of Ethiopia. *Applied and Environmental Soil Science*, 2015:1-12.

Ayelew Manahilie. 2014. Chelating agent free solid phase extraction (CAF-SPE) of uranium, cadmium and lead by Fe-Al-Mn ternary mixed oxide nanocomposite. MSc. Thesis Haramaya University, Haramaya, Ethiopia.

Berner, E.K. and Berner, R.A. 1996. *Global Environment*: Water, air and geochemical cycles prentice hall, upper saddle river, NJ.

Bhat, ZA., Padder, SA., Ganaie, AQ., Dar, NA., Rehman, HU. and Wani, MY. 2017. Correlation of available nutrients with physicochemical properties and nutrient content of grape orchards of Kashmir. *Journal of Pharmacognosy and Photochemistry*, 6(2): 181-185.

Bhattacharjee, C.R., Purkayastha, D.D., Bhattacharjee, S. and Nath, A. 2011. Homogeneous chemical precipitation route to ZnO nanospherical. *Journal of Physical Science and Technology*, 7(2): 122-127.

Bolto, B.A. 1990. Magnetic particle technology for wastewater treatment. *Waste Management*, 10: 11-21.

Bouyoucos, G.J.1962. Hydrometer method improved for making particle size analysis of soil. *Journal of Agronomy*, 54: 464-465.

Brady, N.C. and Weil, R. R. 1999.*The nature and properties of soils 12th edition*. Prentice hall , upper saddle river, NJ.

Brady, N.C. and Weil, R. R. 2002. *The Nature and properties of soils 13th (Ed)*. Person Educated Ltd, USA.960.

Bray R.H. and Kurtz, L.T. 1945. Determination of total, organic and available forms of phosphorus in soils. *Soil Science*, 59: 39-45.

Bruce, R. C. and Rayment, G. E.1982. Analytical methods and interpretations used by the agricultural chemistry branch for soil and land use surveys. Queensland Department of Primary Industries. Bulletin QB8 (2004), Indooroopilly, Queensland.

Buzuayehu Abebe, Abi Taddesse, Tesfahun Kebede, Endale Teju and Isabel Diaz. 2017. Fe-Al-Mn ternary oxide nanosorbent: Synthesis, characterization and phosphate sorption property. *Journal of Environmental Chemical Engineering*, 5: 1330-1340.

Cai, W., Yu, J. and Jaroniec, M. 2010.Template free synthesis of hierarchical spindle like γ-Al_2O_3 materials and their adsorption affinity towards organic and inorganic pollutants. *Journal of Hazardous Materials*, 20: 4587- 4594.

Cao, C. Y., Qu, J., Yan, W. S., Zhu, J. F., Wu, Z. Y. and Song, W. G. 2012. Low-cost synthesis of flowerlike α-Fe_2O_3 nanostructures for heavy metal ion removal. *Adsorption Property and Mechanism,* 28: 4573-4579.

Carp, O., Huisman, C.L. and Reller, A. 2004. Photo induced reactivity of titanium dioxide. *Progress in Solid State Chemistry,* 32: 33-177.

Cava, S., Tebcherani, S.M., Souza, I. A., Pianaro, S.A., Paskocimas, C.A., Longob, E. and Varela, J.A. 2007. Structural characterization of phase transition of Al_2O_3 nano powders obtained by polymeric precursor method. *Materials Chemistry and Physics*, 103: 394-399.

Chen, X.S. and Mao, S. 2007. Titanium dioxide nanomaterials: synthesis, properties, modifications and applications. *Chemical Review*, 107: 2891-2897.

Chen, Y.H. and Li, F.A. 2010. Kinetic study on removal of copper (II) using goethite and hematite nano-photocatalysts. *Journal of Colloid Interface Science,* 347: 277-281.

Cheng, F.Y., Zhao, J.Z. and Song, W. 2006. Facile controlled synthesis of Mn_2O_4 nanostructures of novel shapes and their application in batteries. *Inorganic Chemistry*, 45(5): 2038-2044.

Choo, K.H. and Kang, S.K. 2003. Removal of residual organic matter from secondary effluent by iron oxides adsorption. *Desalination*, 154(2): 139-146.

Crittenden, B. and Thomas, W.J. 1998. Adsorption technology and design, *Butterworth Heinemann, 1st edition*.

Cumbal, L. and SenGupta. A.K. 2005. Arsenic removal using polymer-supported hydrated iron (III) oxide nanoparticles: role of donnan membrane effect. *Environmental Science and Technology*, 39: 6508-6515.

Cushing, B.L., Kolesnichenko, V.L. and O'Connor, C.J. 2004. Recent advances in the liquid phase syntheses of inorganic nanoparticles. *Chemical Reviews*, 104: 3893-3946.

Dawit, S., Fritzsche, F., Tekalign, M., Lehmann, J. and Zech, W. 2002. Phosphorus forms and dynamics as influenced by land use changes in the sub-humid Ethiopian highlands. *Geoderma*, 105: 21-48.

Day, P. R. 1965. *Particle fractionation and particle size analysis*. In C. A. Black, editor. Methods of soil analysis. American Society of Agronomy, Madison, Wisconsin, USA 545-566.

DEFRA (Department for Environment, Food and Rural Affairs). 2008. Consultation on options for controls on phosphates in domestic laundry cleaning products in England, London, UK.

De Jager, P.C. and Claassens, A. S. 2005. Long-term phosphate desorption kinetics of an acid sandy clay soil from Mpumalanga, South Africa. *Communications in Soil Science and Plant Analysis*, 36(1-3): 309-319.

De Ruddera, J., Van de Wielea, T., Dhoogeb, W., Comhaireb, F. and Verstraetea, W. 2004. Advanced water treatment with manganese oxide for the removal of 17a ethynylest radiol (EE2). *Water Research*, 38: 184 -192.

Diallo, M.S., Christie, S., Swaminathan, P., Johnson J.H. and Goddard, W.A. 2005. Dendrimer enhanced ultra-filtration recovery of Cu(II) from aqueous solutions using $GxNH_2$PAMA-M dendrimers with ethylene diamine core. *Environtal Science and Technology Journal*, 39: 1366-1377.

Duffera, M. and Robarge, W.P. 1996. Characterization of organic and inorganic phosphorus in the highland pleateau soil of Ethiopia. *Communications in Soil Science and Plant Analysis*, 27: 2799-2814.

EthioSIS (Ethiopian Soil Information System). 2014. Soil Fertility and Fertilizer recommendation atlas of Tigray Region. Ministry of Agriculture (MoA) and Agricultural Transformation Agency (ATA).

Eylachew Zewdie. 1987. Study on the phosphorous status of different soil types of charcher highlands, south eastern Ethiopia. A PhD Dissertation, the University of Jestus Liebig, Germany.

Fahmida, G., Kameshima, Y., Nakajima, A. and Okada, K. 2009. Preparation of alumina–iron oxide compound by gel evaporation method and its simultaneous uptake properties for $Ni^{2+,}$ NH_4^+ and $H_2PO_4^-$. *Journal of Hazardous Materials*, 169: 697-702.

FAO (Food and Agriculture Organization). 1990. Soil map of the world: Revised legend FAO (Food and Agriculture Organization), Rome, Italy.

FAO (Food and Agriculture Organization). 2006. *Plant nutrition for food security*: A guide for integrated nutrient management. FAO, Fertilizer and Plant Nutrition Bulletin *16*. FAO, Rome, Italy.

Fekadu Kassahun. 2015. Synthesis and characterization of $Al_2O_3/Fe_3O_4/ZrO_2$ heterojunction ternary oxides nanocomposite for nitrate sorption from aqueous solution. MSc Thesis, Haramaya University, Haramaya, Ethiopia.

Fekadu Tsegaye. 2016. Synthesis, characterization and study on the sorption property of $Fe_3O_4/Al_2O_3/ZrO_2$ nanocomposites toward the removal of cadmium, lead and chromium ions from aqueous solution. MSc Thesis, Haramaya University, Haramaya, Ethiopia.

Fekri, M., Gorgin, N. and Sadegh, L. 2011. Phosphorus desorption kinetics in two calcareous soils amended with P fertilizer and organic matter. *Environmental Earth Science*, 64:721-729.

Filippelli, G.M. and Souch, C. 1999. Effects of climate and landscape development on the terrestrial phosphorus cycle. *Geology,* 27: 171-174.

Freese, D., Lookman, R., Merckx, R. and van Riemsdijk, W.H. 1995. New method for the Assessment of long term phosphate desorption from the soil. *Soil Science of American Journal*, 59: 1295-1300.

Gavriloaiei, T. 2012. The Influence of electrolyte solutions on soil pH measurements. *Revista de Chimic-Bucharest*, 63 (4): 396-401.

Gayathri, J. 2007. Easy, economical and simple method to produce nanoparticles of zinc ferrites and zinc aluminates by co precipitation method, co-precipitation a simple method to produce nanoparticle spinel materials. *Journal of Environmental Science Technology,* 38: 3562-3686.

Gemechu Shumi, Abi Tadesse and Tesfahun Kebede. 2015. Phosphorus desorption study using dialysis membrane tube filling Fe-Al-Mn ternary mixed nanocomposite from different farming practice of acidic soil. *Chemistry and Materials Research*, 7(8): 82-91.

George, E., Rolf, S. and John, R. 2013. Methods of soil, plant, and water analysis: *A manual for the West Asia and North Africa Region, 3rd Edin.* International center of Agricultural Research in the Dry area.

Gichangi, E.M., Mnkeni, P.N.S. and Muchaonyerwa, P. 2008. Phosphate sorption characteristics and external P requirements of selected South African soils. *Journal of Agriculture and Rural Development in the Tropics and Subtropics,* 109(2): 139-149.

Gilbert, N. 2009. Environment: the disappearing nutrient. *Nature*, 461: 716-718.

Girma, W., Srivastava, B.B.L. and Ephrem, G. 2014. Synthesis of hydrous aluminum (III)-iron (III)-manganese (IV) ternary mixed oxide for fluoride removal. *International Journal of Scientific and Engineering Research,* 3: 885-892.

Gulshan, F., Kameshima, Y., Nakajima, A. and Okada, K. 2009. Preparation of alumina–iron oxide compounds by gel evaporation method and its simultaneous uptake properties for Ni^{2+}, NH^{4+} and $H_2PO_4^-$. *Journal of Hazardous Materials,* 169: 697-702.

Haber, J., Block, H. and Delmon, B. 1995. Manual of methods and procedures for catalyst characterization. *Pure and Applied Chemistry,* 67(8/9): 1257-1306.

Harish K., Manisha, A. and Poonam, S. 2013. Synthesis and characterization of MnO_2 nanoparticles using co-precipitation technique. *International Journal of Chemistry and Chemical Engineering*, 3(3): 155-160.

Harvey, O.R. and Rhue, R.D. 2008. Kinetics and energetic of phosphate sorption in a multicomponent Al(III)-Fe(III) hydr (oxide) sorbent system. *Journal of Colloid Interface Science*, 322: 384-393.

Havlin, J. L., Tisdale, S.L., Nelson, W.L. and Beaton, J. D. 2013. *Soil fertility and fertilizers: an introduction to nutrient management, 8th Edition*. Prentice Hall, New Jersey, USA. 528.

Haygarth, P.M. and Sharpley, A. 2000. Terminology for phosphorus transfer. *Journal of Environmental Quality,* 29: 10-15.

Hazelton, P. and B. Murphy, 2007. *Interpreting soil test results: What do all the numbers mean? 2nd edition*. CSIRO Publishing.

He, L. and Toh, CS. 2006. Recent advances in analytical chemistry–a material approach. *Analytica Chimica Acta*, 556: 1-15.

Hernandez, J. and Meurer, E.J. 2000. Phosphorus availability in six Uruguayan soils affected by temporal variation of oxidizing-reducing conditions. *Revista Brasileira of Cienciado Solo*, 24: 19-26.

Herranz, T., Rojas, S., Ojeda, M., Pe´rez-Alonso, F. J., Terreros, P., Pirota, K. and Fierro, J. L. G. 2006. Synthesis, structural features, and reactivity of Fe-Mn mixed oxides prepared by microemulsion. *Chemistry of Materials,*18: 2364-2375.

Horta, M. C. and Torrent, J. 2007. The Olsen P method as an agronomic and environmental test for predicting phosphate release from acid soils. *Nutrient Cycling in Agroecosystems*, 77: 283-292.

Hu, D., Zhang, J., Graff, G.L., Liu, J., Pope, M. A. and Aksay, I. A. 2010. Ternary self-assembly of ordered metal oxide-graphene nanocomposites for electrochemical energy storage. *Journal of American Chemical Society*, 4(3): 1587-1595.

Indiati, R. 1998. Changes in soil phosphorus extractability with successive removal of soil phosphate by iron oxide impregnated filter paper strips. *Communication of Soil Science Plant Analysis,* 29: 107-120.

Indiati, R. 2000. Addition of phosphorus to soils with low to medium phosphorus retention capacities II. Effect on soil phosphorus extractability. *Communication of Soil Science Plant Analysis,* 31: 2591-2606.

Jackson, M. L.1958. Soil Chemical Analysis: Prentice-Hall, Englewood Cliffs, 498.

Jackson, M.L., Lim, C.H. and Zelazny, L.W. 1986. Oxides, Hydroxides and Aluminosilicates. In: Klute, A., Ed., *Methods of Soil Analysis, Part 1, Physical and Mineralogical Methods, 2nd Edition*, Agronomy Monogram 9, ASA and SSSA, Madison, 101-150.

Jalali, M. and Zinli, N. M. 2011. Kinetics of phosphorus release from calcareous soils under different land use in Iran. *Journal of Plant Nutrition and Soil Science,*174: 38-46.

Jianbo, L., Huijuan, L., Ruiping L., Zaho, X., Liping, S. and Jiuhui, Q. 2013. Adsorptive removal of phosphate by a nanostructured Fe-Al-Mn trimetal oxide sorbent. *Powder Technology*, 233: 146-154.

Jiang, J.S., Gan, Z.F., Yang, Y., Du, B., Qian, M. and Zhang, P. 2009. A novel magnetic fluid based on starch-coated magnetite nanoparticles functionalized with homing peptide. *Journal of Nanoparticle Research*, 11: 1321-1330.

Jones, J.B. 2003. Agronomic Handbook: Management of crops, soils, and their fertility. CRC Press LLC, Boca Raton, FL, USA. 482.

Kamper, M. and Claassens, A.S. 2005. Exploitation of soil by roots as influenced by phosphorus applications. *Communication Soil Science and Plant Analysis*, 36: 309-319.

Karageorgiou, K., Paschalis, M. and Anastassakis, G.N. 2007. Removal of phosphate species from solution by adsorption onto calcite used as natural adsorbent. *Journal of Hazardous Material A*, 139: 447-452.

Karn, B., Kuiken, T. and Otto, M. 2009. Nanotechnology and in situ remediation: a review of the benefits and potential risks. *Environmental Health Perspectives,* 117: 1823– 183.

Kasahun Chala . 2015. Chelating gent free solid phase extraction (CAF–SPE) of lead, cadmium and chromium by Fe-Al-Zr ternary mixed oxides nanocomposite. MSc Thesis, Haramaya University, Haramaya, Ethiopia.

Kentish, S.E. and Stevens, G.W. 2001. Innovation in separations technology for recycling and re-use of liquid waste streams. *Journal of Chemical Engineering*, 84: 149-159.

Keshmiri, M., Troczynski, T. and Mohseni, M. 2006. Properties of amorphous and crystalline titanium dioxide from first principles. *Journal of Hazardous Materials*, 128: 130-153.

Khayat, Z. and Khayat, S. 2012. Synthesis and magnetic properties investigations of Fe_3O_4 nanoparticles. *Proceedings of the 4th International Conference on Nanostructures (ICNS4) 12-14* March, 2012, Kish Island, I.R. Iran.

Klabunde, K. J. 2001. *Nanoscale materials in chemistry 2nd ed*. Wiley-Interscience, New Jersey.

Koopmans, G.F., Van der zeew, M.E., Chardon, W.J. and Dolfing. J. 2001. Selective extraction of labile phosphorus using dialysis membrane tubes filled with hydrous iron hydroxide. *Soil Science*, 166: 475-483.

Kuo, S. 1996. Phosphorus determination. In Methods of Soil Analysis. Part 3.Chemical Methods ; Sparks, D.L. (ed.) SSSA: Madison. Wisconsin, 869-919.

Landon, JR.1984. Booker tropical soil manual. *A handbook for soil survey and agricultural land evaluation in the tropics and subtropics*. Booker Agricultural International, London.

Laurent, S., Forge, D., Port, M., Roch, A., Robic, C., Elst, L.V. and Muller, R.N. 2008. Magnetic iron oxide nanoparticles: synthesis, stabilization, vectorization, physico-chemical characterizations, and biological applications. *Chemical Review*, 108: 2064-2076.

Li, F.B., Li, X.Z., Liu, C.S. and Liu, T.X. 2007. Effect of alumina on photo catalytic activity of iron oxides for bisphenol degradation. *Journal of Hazardous Materials*, 149: 199-207.

Li, J.D., Shi, Y.L., Cai, Y.Q., Mou, S.F. and Jiang, G.B. 2008. Adsorption of di-ethyl-phthalate from aqueous solutions with surfactant-coated nano/microsized alumina. *Journal of Chemical Engineering,* 140: 214-220.

Li, J.H., Hong, R.Y., Zheng, H., Li Z., Ding, Y.J. and Wei, D.G. 2009. Synthesis surface modification surface and characterization of nanoparticles. *Physical Chemistry Materials* ,113: 140-144.

Li,Y.H., Ding, J., Luan, Z.K., Di, Z.C., Zhu, Y.F., Xu, C. ,Wu, D.H. and Wei, B.Q. 2003. Competitive adsorption of Pb^{2+}, Cu^{2+} and Cd^{2+} ions from aqueous solutions by multi walled carbon nanotubes. *Journal of Hazardous Materials*, 41(14): 2787-2792.

Liong, S. 2005.A Multifunctional approach to development, fabrications and characterizations of Fe_3O_4 (magnetite) composite. Georgia Institut of Technology, North Ave, Atlanta , Georgia, 213-217.

Liu, X., Wu, N., Cui, C., Bi, N. and Sun, Y.2015. One pot synthesis of Fe_3O_4/MnO_2 core–shell structured nanocomposites and their application as microwave absorbers. *RSC Advances,* 5: 24016-24022.

Liyuan, C., Yuan, W., Zhhao, Na., Weichum, Y. and Xiangyu, Y. 2013. Sulfate doped Fe_3O_4/Al_2O_3 nanoparticles as a novel adsorbent for fluoride removal from drinking water. *Water Research*, 47: 4040-4049.

London, T.R. 2014. Booker tropical soil manual: a hand book for soil survey and Agricultural land evaluation in the tropic and subtropics. Routledge, Abingdon, UK. 532.

Long, F., Gong, J.L., Zeng, G.M. and Chen, L. 2011. Removal of phosphate from aqueous solution by magnetic Fe-Zr binary oxide. *Journal of Chemical Engineering*, 171: 448-455.

Lookman, R., Freese, D., Merckx, R., Vlassak, K. and van Riemsdijk, W.H. 1995. Long-term kinetics of phosphate release from soil. *Environmental Science and Technology*, 29(6): 1569-1575.

Maeng, M., Lee, H. and Dockko, S. 2013. Phosphate removal using novel combined Fe-Mn-Si oxide adsorbent. *Journal of Korean Society of Water and Wastewater*, 27(5): 631-639.

Maguire, R.O., Sims, J.T. and Foy, R.H. 2001. Long term kinetics for phosphorus sorption desorption by high phosphorus soils from Ireland and Delmarva Peninsula, USA. *Soil Science*, 166: 557-565.

Mäkiea, P., Persson, P. and Österlunda, L. 2013. Adsorption of trimethyl phosphate and triethyl phosphate on dry and water pre-covered hematite, maghemite, and goethite nanoparticles. *Colloid Interface Science,* 392: 349-358.

Manahan, S.E. 1994. *Environmental Chemistry 6th edition*. Lewis Publishers, Boca Raton,FL.

Mansoori, G.A., Rohani, T., Ahmadpour, A. and Eshagh, Z. 2008. Environmental application of nanotechnology. *Annual Review of Nano Research*, 2: 1-73.

Mascolo, M.C., Pei, Y.and Ring, T.A. 2013. Room temperature co-precipitation synthesis of Fe_3O_4 nanoparticles in a large pH window with different bases. *Materials,* 6:5549-5567.

Masel, R.I. 1996**.** Principles of adsorption and reaction on solid surfaces, John Wiley and sons.

Masue, Y., Loeppert, R.H. and Kramer, T.A. 2007. Arsenate and arsenite adsorption and desorption behavior on co-precipitated aluminum: iron hydroxides. *Environtal Science and Technology*, 41: 837-842.

Mathewos Mano. 2016. Chelating agent free solid phase extraction (CAF SPE) of fluoride and phosphate by Fe-Al-Zr ternary mixed oxide nanocomposite. MSc Thesis, Haramaya University, Haramaya, Ethiopia.

Mayo, J.T., Yavuza, C.,Yeanb, S., Congb, L., Shipleyb, H., Yua, W., Falknera, J., Kanb, A.,Tomsonb, M. and Colvina, M. 2008.The Effect of Nano Crystalline magnetite size on arsenic removal. *Journal of Science and Technology Materials*, 8: 71-75.

McDowell, R.W.and Stewart, I. 2006. The phosphorus composition of contrasting soils in P astora, native and forest management in Otago, New Zealand: Sequential extraction and 31P NMR. *Geoderma*, 130: 176-179.

McKeague, J.A. 1967. An evaluation of 0.1 M pyrophosphate and pyrophosphate–dithionite in comparison with oxalate as extractants of the accumulation products in Podzols and some other. *Canadian Journal of Soil Science*, 47: 95-99.

Mehra, O.P. and Jackson, M.L. 1960. Iron oxide removal from soils and clays by dithionitecitrate system buffered with sodium bicarbonate. *Clays Clay Mineral*, 7: 317-327.

Moazed, H., Hoseini, Y., Naseri, A. A. and Abbasi, F. 2012. Determining phosphorus adsorption isotherm in soil and its relation to soil characteristics. *Journal of Food, Agriculture and Environment*, 8 (2): 1153-1157.

Mulugeta Aytenew. 2015. Effect of slope gradient on selected soil physicochemical properties of dawja watershed in enebse sar midir district, Amhara national regional state. *American Journal of Scientific and Industrial Research*, 6(4): 74-81.

Murphy, H.F. 1968. *A report on fertility status and other data on some soils of Ethiopia*. Collage of Agriculture HSIU. Experimental Station Bulletin No. 44, Collage of Agriculture.

Murphy, J. and Riley, J.P. 1962. Modified single solution methods for the determination of available phosphate in natural water. *Analytica Chimica Acta*, 27: 31-36.

Nafiu, A. 2009. Effects of soil properties on the kinetics of desorption of phosphate from Alfisols by anion-exchange resins. *Journal of Plant Nutrition and Soil Science*, 172: 101-107.

Nair, A.S. and Pradeep, T. 2004. Reactivity of Au and Ag nanoparticles with halo carbons. *Applied Nanoscience*, 19: 59-63.

Nedkov, T., Merodiiska, L., Slavov, R.E., Vandenberghe, Y. and Kusano, J.T. 2006. Surface oxidation, size and shape of nano-sized magnetite obtained by coprecipitation. *Journal of Magnetism and Magnetic Materials*, 300: 358-367.

Nejat Redwan, Abi Taddesse and Ayalew Temesgen. 2018. Synthesis, Characterization and photocatalytic activity of $Mn_2O_3/Al_2O_3/Fe_2O_3$ nanocomposite for degradation of malachite green. *Bulletin Chemical Society of Ethiopia*, 32(1), 101-109.

Ochwoh, V.A., Claassens, A.S. and De Jager, P.C. 2005. Chemical changes of applied and native phosphorus during incubation and distribution into different soil phosphorus pools. *Communication Soil Science and Plant Analysis*, 36: 535-556.

Ochwoh, V. A., Nankya, E., De Jager, P. C. and Claassens, A. S. 2016. The impact of phosphorous applications and incubation periods on P-desorption characteristics with successive DMT-HFO-P extractions on P fixing soils. *International Journal of Plant and Soil Science*, 13(6): 1-14.

Olayinka, O.O., Yetunde, O. and Gbade, O.O. 2015. Assessment of dithionite and oxalate extractable iron and aluminium oxides on a landscape on basement complex soil in south-western Nigeria. *Open Journal of Soil Science*, 5: 266-27.

Park, J., An, K.J., Hwang, Y.S., Park, J.G., Noh, H.J., Kim, J.Y., Park, J.H., Hwang, N.M. and Hyeon, T. 2004. Ultra large scale syntheses of monodisperse nanocrystals. *Nature Materials*, 3: 891-895.

Patil, RB., Saler, RS. and Gaikwad, VB. 2015. Nutritional survey of different vineyards in Nashik district Maharashtra. *Journal of Basic Sciences*, 1: 6-12.

Paulos Dubale.1996. Availability of phosphorus in the coffee soils of southwest Ethiopia. pp.119-129. *In*: Tekalign Mamo and Mitiku Haile (Eds.). Soil: The Resource Base for Survival. *Proceeding of the 2nd Conference of the Ethiopian Society of Soil Science (ESSS)*, 23-24 September 1993, Addis Ababa, Ethiopia.

Paulter, M.C. and Sims, J.T. 2000. Relationships between soil test phosphorus, soluble phosphorus and phosphorus saturation in Delaware soils. *Soil Science Society of American Journal*, 2: 765-773.

Poggio, M., Hepperle, E. and Marsan, A.M. 2008. Metals pollutions and human bioaccessibility of topsoils in Grugliasco, Italy. *Environmental Pollution*, 157: 680-689.

Pradhan, S.D., Sathaye, S.D. and Patil, K.R. 2001. Low temperature synthesis of lead zirconate and titanate powder by hydroxide co-precipitation in non- aqueous medium. *Material Letters*, 48: 351-355.

Ransom, T.S. and Billak, B. J. 2015. Differences in soil characteristics between field and forest may influence the distribution of an invasive earthworm. The American Microscopical Society, DOI: 10.1111/ivb.12078.

Raven, K.P. and Hossner, L.R. 1994. Sorption and desorption quantity intensity parameters to plant available soil phosphorus. *Soil Science Society of American Journal,* 58: 405-410.

Reyhanitabar, A., Heidari, S., Oustan, S. and Gilkes, R. 2018. A modified DMT-HFO technique for investigating the kinetics of phosphorus desorption from calcareous soils and its relationship with maize growth. *Communications in Soil Science and Plant Analysis*,1-8.

Saha, B., Chakraborty, S. and Das, G. 2009. A mechanistic insight into enhanced and selective phosphate adsorption on a coated carboxylated surface. *Journal of Colloid Interface Science,* 331: 21-26.

Salabata, A., Baratib, A. and Banijamalib, N. 2012. Synthesis and characterization of the Pt/SiO_2 nanocomposite by the sol-gel method. *Journal of Nanostructure,* 1:1-6.

Samadi, A. 2006. Phosphorus sorption characteristics in relation to soil properties in some calcareous soils of Western Azerbaijan. *Province Journal Agricultural and Science Technology,* 8: 251-264.

Sanchez, P.A. and Uehara, G. 1980. Management considerations for acid soils with high phosphorus fixation capacity: In: Khasawneh. The role of phosphorus in agricul ture, American Society of Agronomy, Madison, I.

Sanchez, P.A., Palm, C.A. and Buol, S.W. 2003. Fertility capability soil classification: a tool to help assess soil quality in the tropics. *Geoderma*, 114: 157-185.

Saranya, T., Parasuraman, K., Anbarasu, M. and Balamurugan, K. 2015. XRD, FT-IR and SEM Study of magnetite (Fe_3O_4) nanoparticles prepared by hydrothermal method. *An International Research Journal of Nano Science and Technology*, 5: 149-154.

SAS (Statistical Analysis System). 2004. SAS/STAT user's guide. *Proprietary software version 9.1.* SAS Inst., Inc., Cary, NC.

Senthil, M. and Ramesh, C. 2012. Biogenic synthesis of Fe_3O_4 nanoparticles using tridax procumbens leaf extract and its antibacterial activity on pseudomonas aeruginosa. *Journal of Nanomaterials and Biostructures*, 7: 1655-1660.

Sharma, M.S.R. and Raju, N.S. 2013.Correlation of heavy metal contamination with soil properties of industrial areas Mysore, of Karnataka, India by Cluster Analysis. *International Research Journal of Environment Sciences,* 2: 22-27.

Sharpley, A. N. 1983. Effect of soil properties on the kinetics of phosphorus desorption. *Soil Science Society of America Journal*, 47(3): 462-467.

Sharpley, A.N. 1996. Availability of residual phosphorus in manure soils. *Soil Science Society of America Journal*, 60: 1459-1466.

Soil Survey Staff. 2006. *Keys to Soil Taxonomy. 9th Edition*, US Department of Agriculture, NRCS, Washington DC, 281.

Solomon Dewit. 2008. Presentation on the relationships existing in minerals soil between pH on the one hand and the activity of microorganisms and the availability of plant nutrients on the other. Bahir Dar University, Bahir Dar, Ethiopia.

Sophie, L., Delphine, F., Marc, P., Alain, R., Caroline, R., Luce, V. E. and Robert, N. M. 2008. Magnetic iron oxide nanoparticles: synthesis, stabilization, vectorization, physico-chemical characterization and biological applications. *Chemical Review*, 108: 2064-2110.

Sujana, M.G. and Anand, S. 2010. Iron and aluminum based mixed hydroxides: A novel Sorbents for fluoride removal from aqueous solution. Journal of *Applied Surface Science*, 256: 6956-6962.

Taddesse, A.M., Claassens, A.S. and De Jager, P.C. 2008a. Long-term phosphorus desorption using dialysis membrane tubes filled with iron hydroxide and its effect on phosphorus Pools. *Journal of Plant Nutrition,* 31(8): 1507-1522.

Taddesse, A.M., Claassens, A.S. and De Jager, P.C. 2008b. Long term kinetics of phosphate desorption from soil and its relationship with plant growth. *South African Journal of Plant and Soil*, 25(3): 131-134.

Tekalign, M. and Haque, I. 1987. Phosphorus status of some Ethiopian soils. I. Sorption characteristics. *Plant and Soil*, 102: 261-266.

Tekalign Tadesse. 1991. Soil, plant, water, fertilizer, animal manure and compost analysis manual. Working Document No. B13. *Soil Science and Plant Nutrition Section, International Livestock Center for Africa,* Addis Ababa, Ethiopia.

Tesfa Oluma, Abi Taddesse and Om Prakash Yadav. 2014. Synthesis, characterization and photocatalytic activity of $MnO_2/Al_2O_3/Fe_2O_3$ nanocomposite for phenol degradation. *Chemistry and Materials Research*, 6: 73-86.

Thakkar, R. and Chudasama, U. 2009. Synthesis and characterization of zirconium titanium phosphate and its application in separation of metal ions. *Journal of Hazardous Materials*, 172: 129-137.

Thomas, G.W. 1982. Exchangeable cations. In A.L. Page et al. (*2nd Edn*.) *methods of soil analysis,* Agronomical Monographs. 9. ASA and SSSA, Madison, WI. 159-164.

Thomas, R.L., Sheard, R.W. and Moyer, J.R. 1967. Comparison of conventional and automated procedures for nitrogen, phosphorus, and potassium analysis of plant material using a single digestion. *Agronomy Journals,* 59: 240-243.

Tofik Ahmed, Abi Taddesse, Tesfahun Kebede and Girma Goro. 2016. Fe-Al binary oxide nanosorbent: Synthesis, characterization and phosphate sorption property. *Journal of Environmental Chemical Engineering,* 4: 2458-2468.

Tretyakov, YD. and Goodilin, EA. 2009. Key trends in basic and application-oriented research on nanomaterials. *Russian Chemical Reviews*, 78: 801-820.

USDA (United States Department of agriculture). 2014. Online, soil texture calculator. USDA NRCS. (Accessed on October, 2014).

USEPA (United State Environmental Protection Agency). 2005. Nanotechnology white paper external review draft.

USEPAR (United State Environmental Protection Agency Report). 2007. Environmental protection agency export EPA 100/B-07/001, EPAWashington DC.

Van der zee, S.E.A.T.M., Fokkink, L.G.J. and Reimsdijk, W.H.A.Van.1987. A new technique for assessment of reversibly absorbed phosphate. *Soil Science Society of American Journal*, 51: 599-604.

Verma, A., Samanta, S.B., Bakhshi, A.K. and Agnihotry, S. A. 2005. Effect of stabilizer on structural, optical and electrochemical properties of sol-gel derived spin coated TiO_2 films. *Solar Energy Materials and Solar Cells,* 88: 47-64.

Wakene Negassa and Heluf Gebrekidan. 2003. Forms of phosphorus and status of available micronutrients under different land-use systems of Alfisols in Bako area of Ethiopia. *Journal of Ethiopian Natural Resources*, 5: 17-37.

Walkley, A. and Black. I.A. 1934. An examination of Degtjareff method for determining soil organic matter and a proposed modification of the chromic acid titration method. *Soil Science*, 37: 29-37.

Wang, F., Dai, H., Deng, J., Bai, G., Ji, K. and Liu, Y. 2012. Manganese oxides with rod, wire, tube and flower like morphologies: Highly effective catalysts for the removal of toluene. *Environmental Science and Technology*, 46: 4034-4041.

Wang, J. 2005. Nanomaterial based electrochemical biosensors. *Journal of Analyst*, 130: 421-26.

Wang, X., Liu, F., Tan, W., Li, W., Feng, X. and Sparks, D. L. 2013. Characteristics of phosphate adsorption desorption onto Ferrihydrite: Comparison with well crystalline Fe (Hydr) oxides. *Soil Science*, 178:1-11.

Wang, X., Zhuang, J., Peng, Q. and Li, Y. D. 2005. A general strategy for nanocrystal synthesis. *Journal of Nature*, 437: 121-124.

Wang, Y., Zhao, X.L. and Yan, J.L. 2004. An application of nano-technology in environmental protection. *Shanghai Environmental Science*, 23(4): 178-181.

Wassie Haile and Shiferaw Boke. 2009. Mitigation of Soil Acidity and Fertility Decline Challenges for Sustainable Livelihood Improvement: Research Findings from Southern Region of Ethiopia and its Policy Implications. Awassa Agricultural Research Institute, Ethiopia.

Wubshet Legese. 2016. Synthesis and characterization of $Al_2O_3/Fe_3O_4/ZrO_2$ ternary nanocomposite for fluoride and phosphate sorption from aqueous solution. MSc Thesis, Haramaya University, Haramaya, Ethiopia.

Xiaofang, Y., Dongsheng, W., Zhongxi, S. and Hongxiao, T. 2007. Adsorption of phosphate at the aluminum hydroxide water interface: Role of the surface acid base propertyes. *Colloids Surface A*, 297: 84-90.

Yang, J.J., Pickett, M.D., Li, X., Ohlberg, D.A.A., Stewart, D.R. and Williams, R.S. 2008. Memristive switching mechanism for metal/oxide/metal nano devices. *Nature Nanotechnology*, 3(7): 429-433.

Yang, T., Zhu, S.H., Zhang, D. and Xu, S.H. 2008. Synthesis and properties of magnetic Fe_3O_4 activated carbon nanocomposite particles for dye removal. *Materials Letters*, 62: 645-647.

Yu, D.G., Zhou, J., Chatterton, N.P., Li, Y.,Huang, J. and Wang, X. 2012. Poly acrylonitrile nano fibers coated with silver nanoparticles using a modified coaxial electro spining process. *International Journal of Nano Medicine*, 7: 5725-5732.

Yu, P., Zhang, X., Wang, D., Wang, L. and Ma,Y. 2009. Shape-controlled synthesis of 3D hierarchical MnO_2 nanostructures for electrochemical supercapacitors, crystal growth and design. *Journal of Material Science*, 9(1): 528-533.

Zhang, GS., Liu, HJ., Liu, RP. and Qu, JH. 2009. Removal of phosphate from water by a Fe-Mn binary oxide adsorbent. *Journal of Colloid Interface Science,* 335: 168-174.

Zhang, Y., Wu, X., Dou, X. and Yang, M. 2007. Fluoride removal performance of novel Fe-Al-Ce trimetal oxide adsorbents. *Chemosphere*, 69: 1758-1764.

Zhou, X., Xu, M., Wang, B., Cai, Z. and Colinet, G. 2018. Changes of soil phosphorus fractionation according to pH in red soils of China: An incubation experiment. *Communication in Soil Science and Plant Analysis*, 49: 791-802.

Zhu, ZQ., Zeng, HH., Zhu, YN., Yang, F., Zhu, HX., Qin, H., Chen, Y. and Xie, L. 2013. Kinetics and thermodynamic study of phosphate adsorption on the porous biomorph genetic composite of a Fe_2O_3/Fe_3O_4/C with eucalyptus wood microstructure. *Separation and Purification Technology*, 117: 124-130.

7. APPENDICES

7.1. Appendix Tables

Appendix Table 1. Classification of soil reaction based on pH (H_2O)

Rating	pH (H_2O)
Very strongly acid	≤4.5
Strongly acid	4.5-5.2
Moderately acid	5.3-5.9
Slightly acidic	6.0-6.6
Neutral	6.7-7.3
Moderately alkaline	7.4-8.0
Strongly alkaline	> 8.0

Source: Tekalign (1991)

Appendix Table 2. Rating of soil electrical conductivity

Rating EC	EC (dS/m)
Salt free (non-saline)	≤ 2
Very slightly saline	2-4
Slightly saline	4- 8
Moderately saline	8-16
Strongly saline	> 16

Source: EthioSIS (2014)

Appendix Table 3. Rating (interpretive) values of soil organic matter, total nitrogen, bulk density, cation exchange capacity and bray II P of soil sample

Ratings	%OM[a]	%TN[b]	Bd (g/cm^3)[c]	CEC (meq/100g)[d]	Bray II P (mg/kg)[e]
Very high	>5.0	>0.5	>1.9	>40	>35
High	3-5	0.25-0.50	1.6-1.9	25-40	26-35
Medium	2-3	0.15-0.25	1.3-1.6	12-25	18-25
Low	1-2	0.05-0.15	1.0-1.3	6-12	10-17
Very low	≤1.0	<0.05	≤1.0	<6	1-9

Source:[a] = Murphy (1968),[b] = Bruce and Rayment (1982),[c] = Hazelton and Murphy (2007), [d] = FAO (2006), [e] = Jones (2003)

Appendix Table 4. Effect of phosphorus levels and extraction time on phosphorus desorption with percent recovery (n = 3)

Soil Samples	P Treatments (mg/kg)	P desorbed (mg/kg) per days 1	7	14	21	28	Average P (mg/kg)
BD	0	z1.16^{c} C	y3.01^{d} C	x5.43^{d} C	w7.62^{d} C	v9.36^{d} C	5.316 -
	50	z3.65^{b}	y8.31^{c}	x13.16^{c}	w18.13^{c}	v22.77^{c}	13.29
	% P RV	4.98	10.6	15.46	21.02	26.82	15.78
	100	z3.71^{b}	y8.98^{b}	x14.32^{b}	w19.43^{b}	v24.50^{b}	14.19
	% P RV	2.55	5.97	8.89	11.81	15.14	8.87
	150	z4.70^{a}	y10.41^{a}	x16.09^{a}	w21.24^{a}	v26.86^{a}	15.86
	% P RV	2.36	4.93	7.11	9.08	11.67	7.03
LSD (5%)		0.14	0.45	0.86	0.95	1.10	
CV (%)		2.29	3.13	3.71	3.04	2.82	
KK	0	Z1.01^{d} C	y3.27^{c} C	x5.75^{d} C	w7.99^{d} C	v9.57^{d} C	5.52 -
	50	z4.30^{c}	y9.74^{b}	x14.99^{c}	w20.06^{c}	v24.36^{c}	14.69
	% P RV	6.58	12.94	18.48	24.14	29.58	17.06
	100	z4.57^{b}	y10.12^{b}	x15.84^{b}	w21.18^{b}	v25.84^{b}	15.51
	% P RV	3.56	13.70	20.18	13.19	16.27	13.38
	150	z4.90^{a}	y10.73^{a}	x17.05^{a}	w23.47^{a}	v28.13^{a}	16.86
	% P RV	2.59	4.97	7.53	10.32	12.37	7.56
LSD (5%)		0.22	0.41	0.63	0.86	1.19	
CV (%)		3.12	2.59	2.50	2.50	2.88	
MS	0	z1.32^{d} C	y4.07^{d} C	x6.23^{d} C	w8.74^{d} C	v10.80^{d} C	6.23 -
	50	z4.15^{c}	y9.56^{c}	x14.52^{c}	w20.02^{c}	v25.36^{c}	14.72
	% P RV	5.66	10.98	16.58	22.56	29.12	16.98
	100	z4.62^{b}	y10.55^{b}	x16.08^{b}	w21.67^{b}	v27.45^{b}	16.07
	% P RV	3.30	6.48	9.85	12.93	16.65	9.84
	150	z5.19^{a}	y11.93^{a}	x18.35^{a}	w24.06^{a}	v30.10^{a}	17.93
	% P RV	2.58	5.24	8.08	10.21	12.87	7.80
LSD (5%)		0.32	0.59	0.81	0.59	0.78	
CV (%)		4.48	3.44	3.11	1.69	1.77	

Table 4 (*Continued*)

NE	0	z1.43^{d} C	y4.02^{d} C	x6.39^{d} C	w9.01^{d} C	v11.29^{d} C	6.43 -
	50	z4.12^{c}	y9.78^{c}	x14.89^{c}	w20.14^{c}	v24.55^{c}	14.70
	% P RV	5.38	11.52	17.00	22.26	26.52	16.54
	100	z4.71^{b}	y10.59^{b}	x16.99^{b}	w22.40^{b}	v27.65^{b}	16.47
	% P RV	3.28	6.57	10.60	13.39	16.36	10.04
	150	z5.23^{a}	y11.91^{a}	x18.52^{a}	w24.32^{a}	v30.35^{a}	18.07
	% P RV	2.53	5.26	8.09	10.21	12.71	7.76
LSD (5%)		0.33	0.40	0.75	1.13	1.08	
CV (%)		4.20	2.10	2.67	3.06	2.37	

BD = Boji Dirmeji Soil, KK = Kiltu Kara Soil, MS = Mana Sibu Soil, NE = Nedjo Soil, CV = Coefficient of variation (%), C= Control (P0), LSD = Least significance difference (5%), % P RV = Percent of P recovered, n = Number of replications. Mean values in rows with different letters z, y, x, w and v are significantly different ($\alpha = 0.05$*), while mean values in the columns with different letters a, b, c and d are significantly different (*$\alpha = 0.05$*).*

Appendix Table 5. Effect of soil properties on the P desorption of different soil samples with the same treatments with LSD and CV (n = 3)

Soil Samples	P Treatments (mg/kg)	P desorbed (mg/kg) per days				
		1	7	14	21	28
BD	0	z1.16^{c}	y3.01^{c}	x5.43^{c}	w7.62^{d}	v9.36^{c}
KK	0	z1.01^{d}	y3.27^{b}	x5.755^{b}	w7.99^{c}	v9.66^{c}
MS	0	z1.32^{b}	y4.07^{a}	x6.23^{a}	w8.74^{b}	v10.80^{b}
NE	0	z1.43^{a}	y4.02^{a}	x6.39^{a}	w9.01^{a}	v11.29^{a}
LSD (5%)		0.09	0.15	0.23	0.21	0.28
CV (%)		3.84	2.21	2.03	3.88	1.42
BD	50	z3.65^{b}	y8.31^{b}	x13.16^{b}	w18.13^{b}	v22.77^{b}
KK	50	z4.30^{a}	y9.74^{a}	x14.99^{a}	w20.06^{a}	v24.36^{a}
MS	50	z4.15^{a}	y9.56^{a}	x14.52^{a}	w20.02^{a}	v25.36^{a}
NE	50	z4.12^{a}	y9.78^{a}	x14.89^{a}	w20.14^{a}	v24.55^{a}
LSD (5%)		0.23	0.51	0.54	0.96	1.03
CV (%)		3.02	2.89	2.00	2.60	2.26
BD	100	z3.71^{b}	y8.98^{b}	x14.32^{c}	w19.43^{b}	v24.50^{b}
KK	100	z4.57^{a}	y10.12^{a}	x15.84^{b}	w21.18^{a}	v25.84^{b}
MS	100	z4.62^{a}	y10.55^{a}	x16.08^{ab}	w21.67^{a}	v27.45^{a}
NE	100	z4.71^{a}	y10.59^{a}	x16.99^{a}	w22.40^{a}	v27.65^{a}
LSD (5%)		0.28	0.56	1.03	1.30	1.45
CV (%)		3.36	2.98	3.45	3.27	2.92
BD	150	z4.70^{b}	10.41^{b}	x16.09^{c}	w21.25^{c}	v26.86^{c}
KK	150	z4.90^{ab}	y10.73^{b}	x17.05^{b}	w23.47^{b}	v28.13^{b}
MS	150	z5.19^{a}	y11.93^{a}	x18.35^{a}	w24.06^{ab}	v30.10^{a}
NE	150	z5.23^{a}	y11.91^{a}	x18.52^{a}	w24.32^{a}	v30.35^{a}
LSD (5%)		0.36	0.50	0.94	0.72	1.06
CV (%)		3.77	2.39	2.87	1.64	1.95

BD= Boji Dirmaji Soil, KK= Kiltu Kara Soil, MS =Mene Sibu Soil, CV= Coefficient of variatio n (%), LSD = Least significance difference (5%), n = Number of replications. Mean values in rows with different letters z, y, x, w and v are significantly different (α = 0.05), while mean values in columns with different letters a, b, c and d are significantly different (α = 0.05).

Appendix Table 6. Correlation between soil properties and cumulative P desorbed with different treatments of Boji Dirmaji Soil

Corre:	pH_{H2O}	pH_{KCl}	EC	OC	OM	TN	CEC	Bd	P_{av}	EX.A
pH_{H2O}	1.00									
pH_{KCl}	0.83	1.00								
EC	-0.90	-0.50	1.00							
OC	0.58	0.93	-0.16	1.00						
OM	0.57	0.93	-0.14	1.00*	1.00					
TN	-0.99	-0.76	0.94	-0.47	-0.46	1.00				
CEC	-0.11	0.46	0.54	0.75	0.76	0.23	1.00			
Bd	0.61	0.94	-0.19	0.99*	0.99*	-0.50	0.73	1.00		
P_{av}	0.92	0.98	-0.65	0.85	0.84	-0.87	0.29	0.87	1.00	
EX.A	-0.44	-0.87	0.00	-0.99	-0.99	0.33	-0.84	-0.98	-0.76	1.00
Ex.Al	-0.99*	-0.79	0.92	-0.52	-0.51	0.99*	0.18	-0.55	-0.89	0.38
$EX.H^+$	0.97	0.66	-0.98	0.35	0.34	-0.99	-0.36	0.38	0.79	-0.20
Fe_{Ox}	1.00	0.88	-0.86	0.64	0.63	-0.98	-0.03	0.67	0.95	-0.52
Mn_{Ox}	0.06	-0.50	-0.50	-0.78	-0.79	-0.19	-0.99*	-0.76	-0.33	0.87
Fe_d	0.39	-0.19	-0.76	-0.53	-0.54	-0.50	-0.96	-0.50	0.00	0.65
Mn_d	0.25	-0.33	-0.65	-0.64	-0.66	-0.37	-0.99	-0.62	-0.14	0.76
P_T	-0.80	-0.33	0.98	0.03	0.05	0.87	0.69	0.00	-0.50	-0.19
CD28BP0	-0.52	0.04	0.84	0.40	0.41	0.62	0.91	0.37	-0.15	-0.54
CD28BP1	-0.15	-0.67	-0.31	-0.89	-0.90	0.02	-0.97	-0.88	-0.52	0.95
CD28BP2	-0.90	-0.99	0.61	-0.88	-0.87	0.83	-0.34	-0.90	-0.99*	0.79
CD28BP3	0.42	-0.15	-0.78	-0.50	-0.51	-0.53	-0.95	-0.47	0.04	0.62

Corre:	Ex.Al	$EX.H^+$	Fe_{Ox}	Mn_{Ox}	Fe_d	Mn_d	P_T	BP0	BP1	BP2	BP3
Ex.Al	1.00										
$EX.H^+$	-0.98	1.00									
Fe_{Ox}	-0.99	0.94	1.00								
Mn_{Ox}	-0.13	0.31	-0.02	1.00							
Fe_d	-0.45	0.61	0.31	0.94	1.00						
Mn_d	-0.32	0.49	0.17	0.98	0.99	1.00					
P_T	0.84	-0.92	-0.74	-0.65	-0.87	-0.79	1.00				
CD28BP0	0.58	-0.72	-0.45	-0.89	-0.99	-0.96	0.93	1.00			
CD28BP1	0.08	0.11	-0.23	0.98	0.85	0.92	-0.48	-0.77	1.00		
CD28BP2	0.86	-0.76	-0.93	0.38	0.06	0.20	0.50	0.09	0.57	1.00	
CD28BP3	-0.48	0.64	0.35	0.93	0.99*	0.98	-0.88	-0.99	0.83	0.02	1.00

** Correlation is significant at the 0.05 level (2-tailed)*

Appendix Table 7. Correlation between soil properties and cumulative P desorbed with different treatments of Kiltu Kara Soil

Corre:	pH_{H2O}	pH_{KCl}	EC	OC	OM	TN	CEC	Bd	P_{av}	EX.A
pH_{H2O}	1.00									
pH_{KCl}	0.92	1.00								
EC	0.92	1.00**	1.00							
OC	0.98	0.98	0.98	1.00						
OM	0.98	0.97	0.97	1.00**	1.00					
TN	0.97	0.80	0.80	0.91	0.92	1.00				
CEC	0.27	0.63	0.63	0.45	0.44	0.04	1.00			
Bd	0.80	0.50	0.50	0.67	0.68	0.92	-0.36	1.00		
P_{av}	0.59	0.86	0.86	0.74	0.73	0.39	0.94	-0.01	1.00	
EX.A	0.74	0.94	0.94	0.85	0.85	0.56	0.85	0.19	0.98	1.00
Ex.Al	-0.40	0.00	0.00	-0.21	-0.22	-0.60	0.78	-0.87	0.51	0.33
$EX.H^+$	0.74	0.94	0.94	0.85	0.85	0.56	0.85	0.19	0.98	1.00**
Fe_{Ox}	0.99	0.87	0.87	0.95	0.96	0.99	0.16	0.87	0.49	0.65
Mn_{Ox}	0.11	0.50	0.50	0.31	0.29	-0.11	0.99	-0.50	0.87	0.76
Fe_d	-0.92	-0.69	-0.69	-0.83	-0.84	-0.99	0.12	-0.97	-0.23	-0.42
Mn_d	0.92	1.00**	1.00**	0.98	0.97	0.80	0.63	0.50	0.86	0.94
P_T	-0.78	-0.46	-0.46	-0.64	-0.65	-0.90	0.40	-0.99*	0.05	-0.15
CD28KP0	-0.45	-0.77	-0.77	-0.61	-0.60	-0.23	-0.98	0.17	-0.99	-0.93
CD28KP1	-0.91	-1.00**	-1.00**	-0.97	-0.97	-0.79	-0.64	-0.49	-0.87	-0.95
CD28KP2	0.79	0.97	0.97	0.90	0.89	0.64	0.80	0.28	0.96	1.00
CD28KP3	-0.98	-0.82	-0.82	-0.92	-0.93	-1.00*	-0.07	-0.91	-0.42	-0.59

Corre:	Ex.Al	$EX.H^+$	Fe_{Ox}	Mn_{Ox}	Fe_d	Mn_d	P_T	KP0	KP1	KP2	KP3
Ex.Al	1.00										
$EX.H^+$	0.33	1.00									
Fe_{Ox}	-0.50	0.65	1.00								
Mn_{Ox}	0.87	0.76	0.00	1.00							
Fe_d	0.72	-0.42	-0.96	0.28	1.00						
Mn_d	0.00	0.94	0.87	0.50	-0.69	1.00					
P_T	0.89	-0.15	-0.84	0.54	0.96	-0.46	1.00				
CD28KP0	-0.64	-0.93	-0.34	-0.94	0.07	-0.77	-0.22	1.00			
CD28KP1	-0.01	-0.95	-0.86	-0.51	0.68	-1.00**	0.45	0.77	1.00		
CD28KP2	0.24	1.00	0.72	0.69	-0.50	0.97	-0.23	-0.90	-0.97	1.00	
CD28KP3	0.57	-0.59	-1.00	0.09	0.98	-0.82	0.89	0.26	0.81	-0.66	1.00

** Correlation is significant at the 0.05 level (2-tailed)*

*** Correlation is significant at the 0.01 level (2-tailed)*

Appendix Table 8. Correlation between soil properties and cumulative P desorbed with different treatments of Mene Sibu Soil

Corre:	pH_{H2O}	pH_{KCl}	EC	OC	OM	TN	CEC	Bd	P_{av}	EX.A
pH_{H2O}	1.00									
pH_{KCl}	-0.80	1.00								
EC	0.26	-0.79	1.00							
OC	0.94	-0.55	-0.09	1.00						
OM	0.93	-0.53	-0.11	1.00*	1.00					
TN	0.99	-0.72	0.14	0.97	0.97	1.00				
CEC	0.40	-0.87	0.99	0.06	0.03	0.28	1.00			
Bd	0.97	-0.92	0.48	0.83	0.82	0.94	0.60	1.00		
P_{av}	0.41	0.22	-0.77	0.70	0.72	0.52	-0.67	0.19	1.00	
EX.A	-0.96	0.93	-0.51	-0.81	-0.80	-0.92	-0.63	-0.99*	-0.15	1.00
Ex.Al	0.40	-0.87	0.99	0.06	0.03	0.28	1.00**	0.60	-0.67	-0.63
$EX.H^+$	-0.92	0.97	-0.61	-0.73	-0.72	-0.87	-0.72	-0.99	-0.03	0.99
Fe_{Ox}	-0.74	0.19	0.46	-0.93	-0.93	-0.82	0.33	-0.56	-0.92	0.53
Mn_{Ox}	0.20	0.43	-0.89	0.52	0.54	0.32	-0.82	-0.03	0.97	0.07
Fe_d	-0.99*	0.76	-0.19	-0.96	-0.96	-0.99*	-0.33	-0.95	-0.48	0.94
Mn_d	0.50	-0.92	0.97	0.17	0.15	0.39	0.99	0.68	-0.59	-0.71
P_T	0.77	-0.24	-0.42	0.94	0.95	0.84	-0.28	0.60	0.90	-0.57
CD28MP0	-0.99	0.87	-0.39	-0.89	-0.87	-0.97	-0.51	-1.00	-0.29	0.99
CD28MP1	0.96	-0.94	0.53	0.80	0.79	0.91	0.64	0.99*	0.13	-1.00*
CD28MP2	-0.24	0.77	-1.00*	0.11	0.13	-0.12	-0.99	-0.46	0.79	0.49
CD28MP3	-0.38	-0.25	0.80	-0.67	-0.69	-0.49	0.70	-0.15	-0.99*	0.11

Corre:	EX.Al	$EX.H^+$	Fe_{Ox}	Mn_{Ox}	Fe_d	Mn_d	P_T	MP0	MP1	MP2	MP3
Ex.Al	1.00										
$EX.H^+$	-0.72	1.00									
Fe_{Ox}	0.33	0.42	1.00								
Mn_{Ox}	-0.82	0.20	-0.81	1.00							
Fe_d	-0.33	0.89	0.79	-0.27	1.00						
Mn_d	0.99	-0.80	0.22	-0.75	-0.43	1.00					
P_T	-0.28	-0.46	-0.99*	0.78	-0.82	-0.17	1.00				
CD28MP0	-0.51	0.96	0.64	-0.07	0.98	-0.61	-0.68	1.00			
CD28MP1	0.64	-0.99	-0.51	-0.09	-0.93	0.73	0.56	-0.99	1.00		
CD28MP2	-0.99	0.60	-0.48	0.90	0.17	-0.96	0.43	0.36	-0.51	1.00	
CD28MP3	0.70	-0.01	0.90	-0.98	0.44	0.62	-0.88	0.25	-0.09	-0.81	1.00

** Correlation is significant at the 0.05 level (2-tailed)*

*** Correlation is significant at the 0.01 level (2-tailed)*

Appendix Table 9. Correlation between soil properties and cumulative P desorbed with different treatments of Nedjo Soil

Corre:	pH_{H2O}	pH_{KCl}	EC	OC	OM	TN	CEC	Bd	P_{av}	EX.A
pH_{H2O}	1.00									
pH_{KCl}	0.00	1.00								
EC	0.87	-0.50	1.00							
OC	0.59	-0.81	0.91	1.00						
OM	0.58	-0.82	0.91	1.00**	1.00					
TN	0.50	0.87	0.00	-0.41	-0.42	1.00				
CEC	-0.24	-0.97	0.28	0.64	0.65	-0.96	1.00			
Bd	0.87	-0.50	1.00**	0.91	0.91	0.00	0.28	1.00		
P_{av}	-0.19	0.98	-0.66	-0.91	-0.91	0.75	-0.91	-0.66	1.00	
EX.A	-1.00**	0.00	-0.87	-0.59	-0.58	-0.50	0.24	-0.87	0.19	1.00
Ex.Al	-0.72	-0.69	-0.28	0.14	0.15	-0.96	0.85	-0.28	-0.54	0.72
$EX.H^+$	-0.98	0.19	-0.94	-0.73	-0.72	-0.33	0.05	-0.94	0.37	0.98
Fe_{Ox}	-0.50	-0.87	0.00	0.41	0.42	-1.00**	0.96	0.00	-0.75	0.50
Mn_{Ox}	-0.55	0.83	-0.90	-0.99*	-1.00*	0.44	-0.67	-0.90	0.92	0.55
Fe_d	0.97	-0.23	0.96	0.75	0.75	0.29	-0.02	0.96	-0.41	-0.97
Mn_d	-0.70	0.71	-0.96	-0.99	-0.99	0.26	-0.52	-0.96	0.83	-0.88
P_T	0.88	0.47	0.23	0.14	0.13	0.85	-0.67	0.53	0.29	-0.56
CD28NP0	0.23	0.97	-0.29	-0.65	-0.66	0.96	-1.00**	-0.29	0.91	-0.23
CD28NP1	-0.74	0.67	-0.98	-0.98	-0.98	0.21	-0.47	-0.98	0.80	0.74
CD28NP2	-0.99	0.14	-0.93	-0.69	-0.68	-0.38	0.11	-0.93	0.32	0.99
CD28NP3	-0.69	0.73	-0.96	-0.99	-0.99	0.29	-0.54	-0.96	0.85	0.69

Corre:	Ex.Al	$EX.H^+$	Fe_{Ox}	Mn_{Ox}	Fe_d	Mn_d	P_T	NP0	NP1	NP2	NP3
Ex.Al	1.00										
$EX.H^+$	0.58	1.00									
Fe_{Ox}	0.96	0.33	1.00								
Mn_{Ox}	-0.18	0.70	-0.44	1.00							
Fe_d	-0.55	-0.99*	-0.29	-0.73	1.00						
Mn_d	0.01	0.83	-0.26	0.98	-0.85	1.00					
P_T	-0.96	-0.78	-0.85	-0.10	0.76	-0.29	1.00				
CD28NP0	-0.84	-0.04	-0.96	0.68	0.01	0.53	0.67	1.00			
CD28NP1	0.07	0.85	-0.21	0.97	-0.87	0.99*	0.34	0.48	1.00		
CD28NP2	0.62	0.99*	0.38	0.66	-1.00	0.79	-0.81	-0.10	0.83	1.00	
CD28NP3	-0.01	0.81	-0.29	0.99	-0.83	1.00*	0.27	0.55	1.00	0.78	1.00

** Correlation is significant at the 0.05 level (2-tailed)*

*** Correlation is significant at the 0.01 level (2-tailed)*

7.2. Appendix Figures

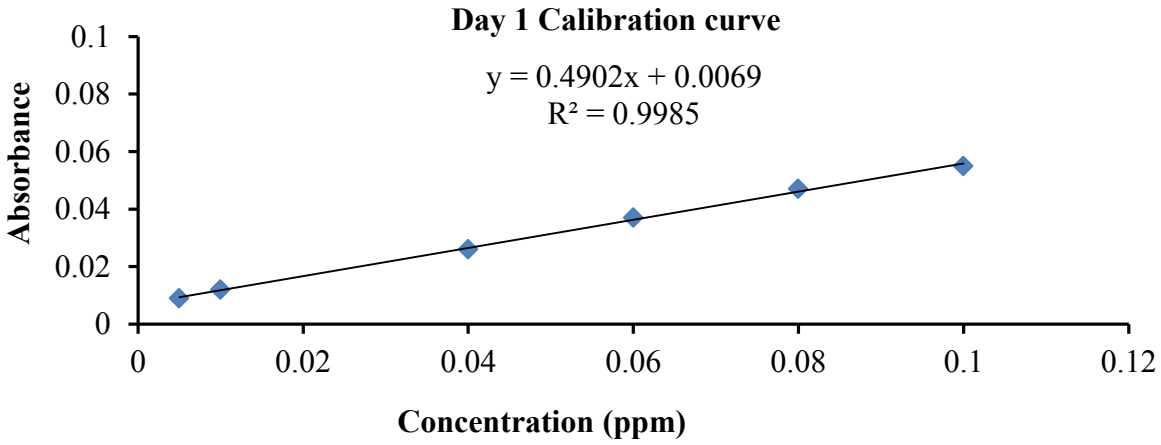

Appendix Figure 1. Calibration curve for day 1 P desorption

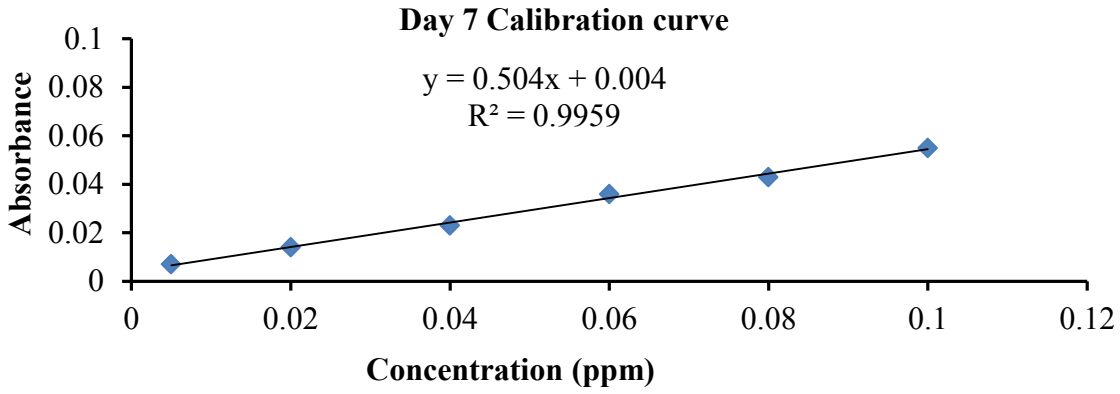

Appendix Figure 2. Calibration curve for day 7 P desorption

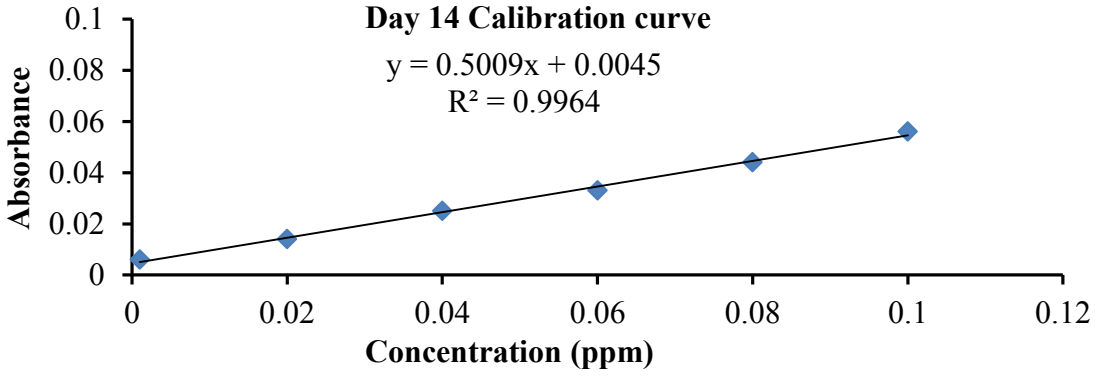

Appendix Figure 3. Calibration curve for day 14 P desorption

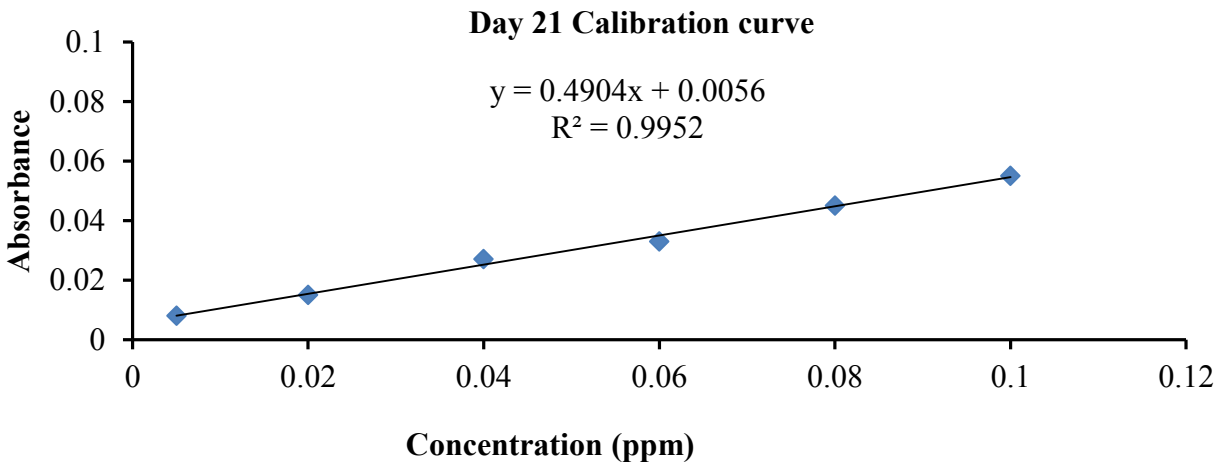

Appendix Figure 4. Calibration curve for day 21 P desorption

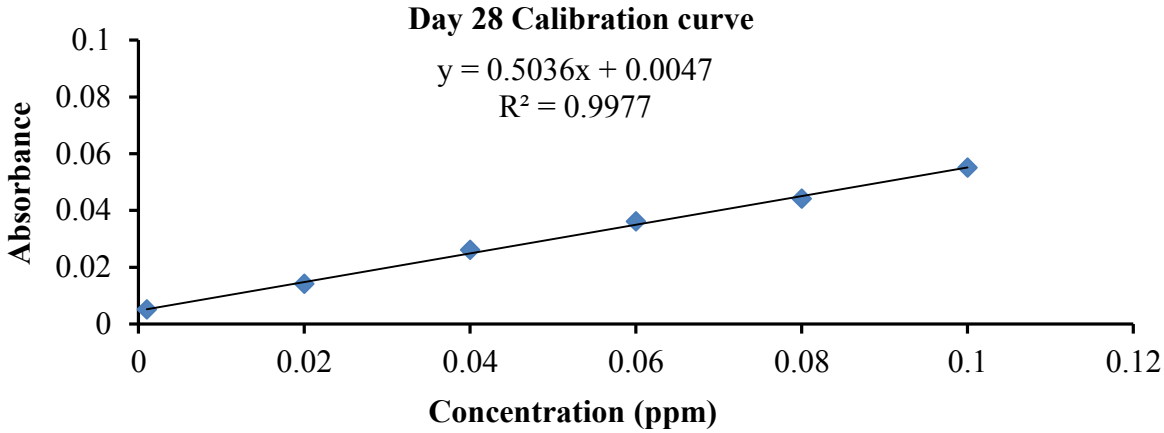

Appendix Figure 5. Calibration curve for day 28 P desorption

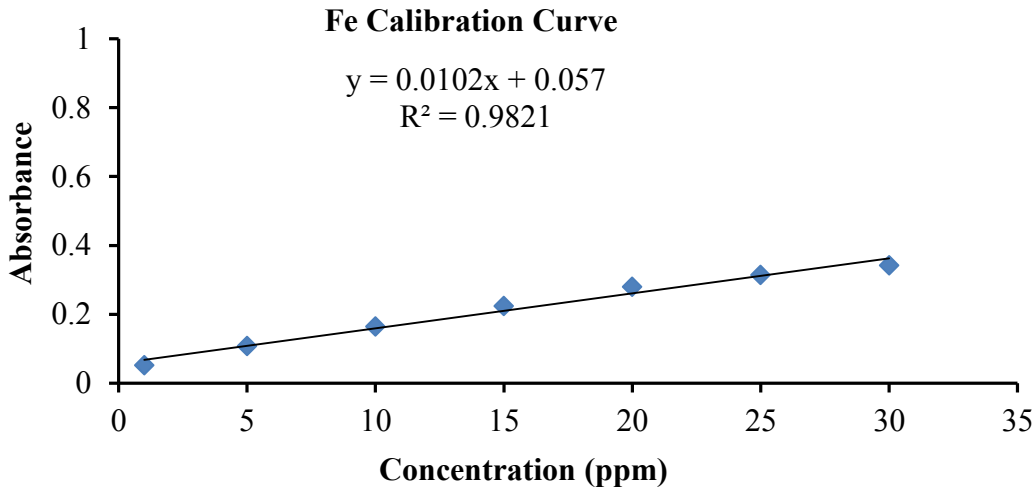

Appendix Figure 6. Calibration curve for Fe in as-synthesized adsorbent

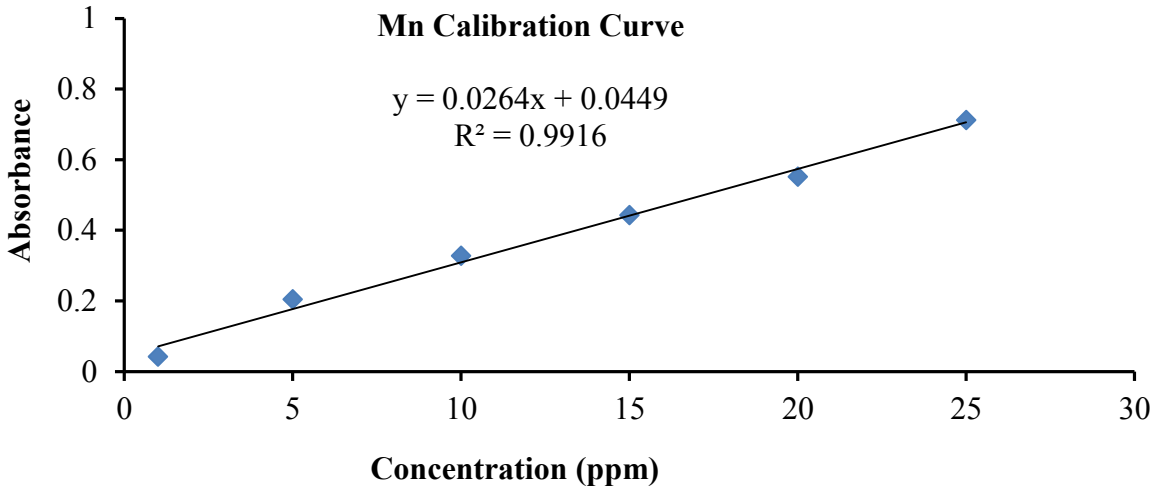

Appendix Figure 7. Calibration curve for Mn in as-synthesized adsorbent

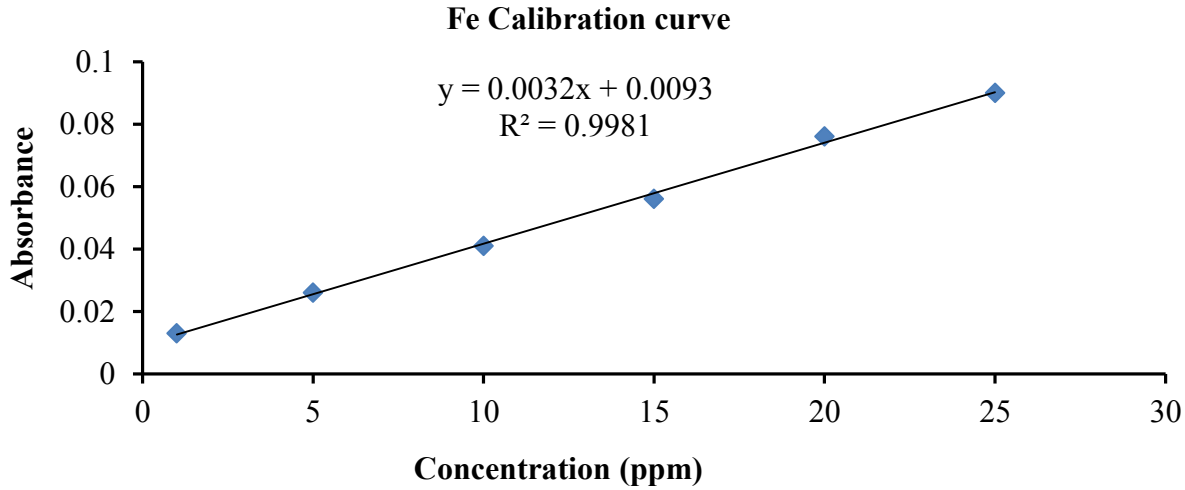

Appendix Figure 8. Calibration curve for Fe in soil for dithionate extractant

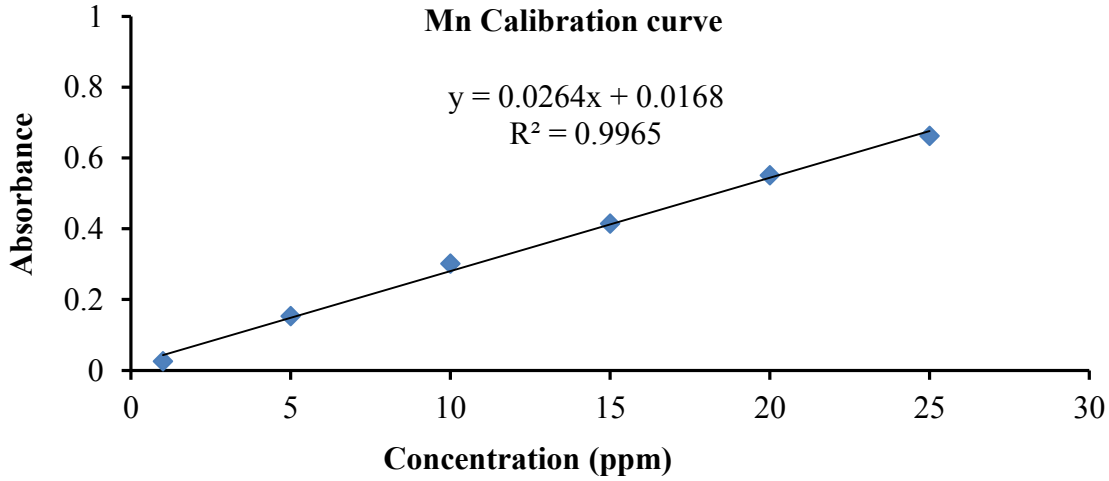

Appendix Figure 9. Calibration curve for Mn in soil for dithionate extractant

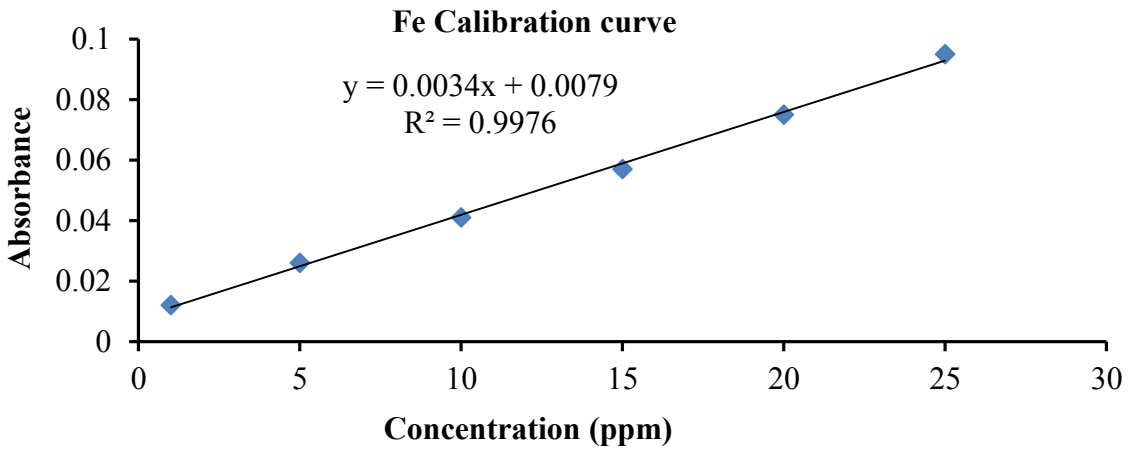

Appendix Figure 10. Calibration curve for Fe in soil for oxalate extractant

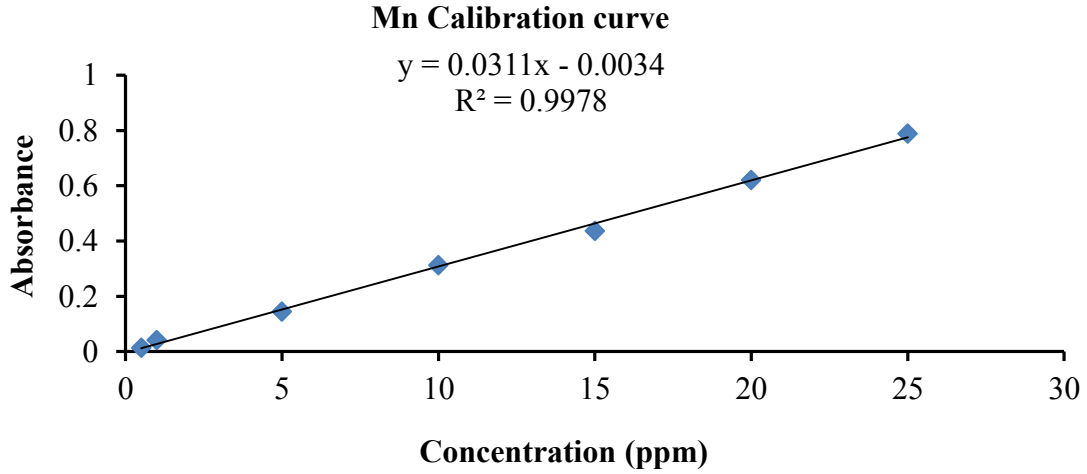

Appendix Figure 11. Calibration curve for Mn in soil for oxalate extractant

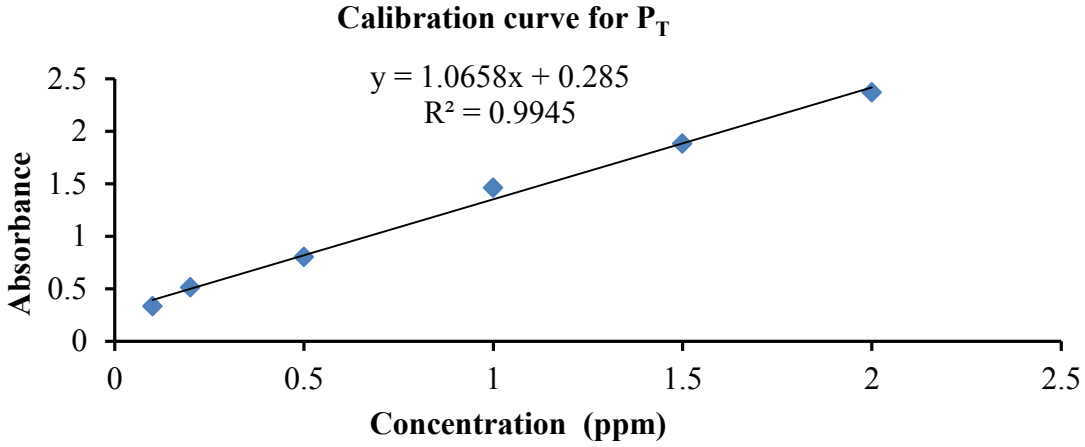

Appendix Figure 12. Calibration curve for total phosphorus

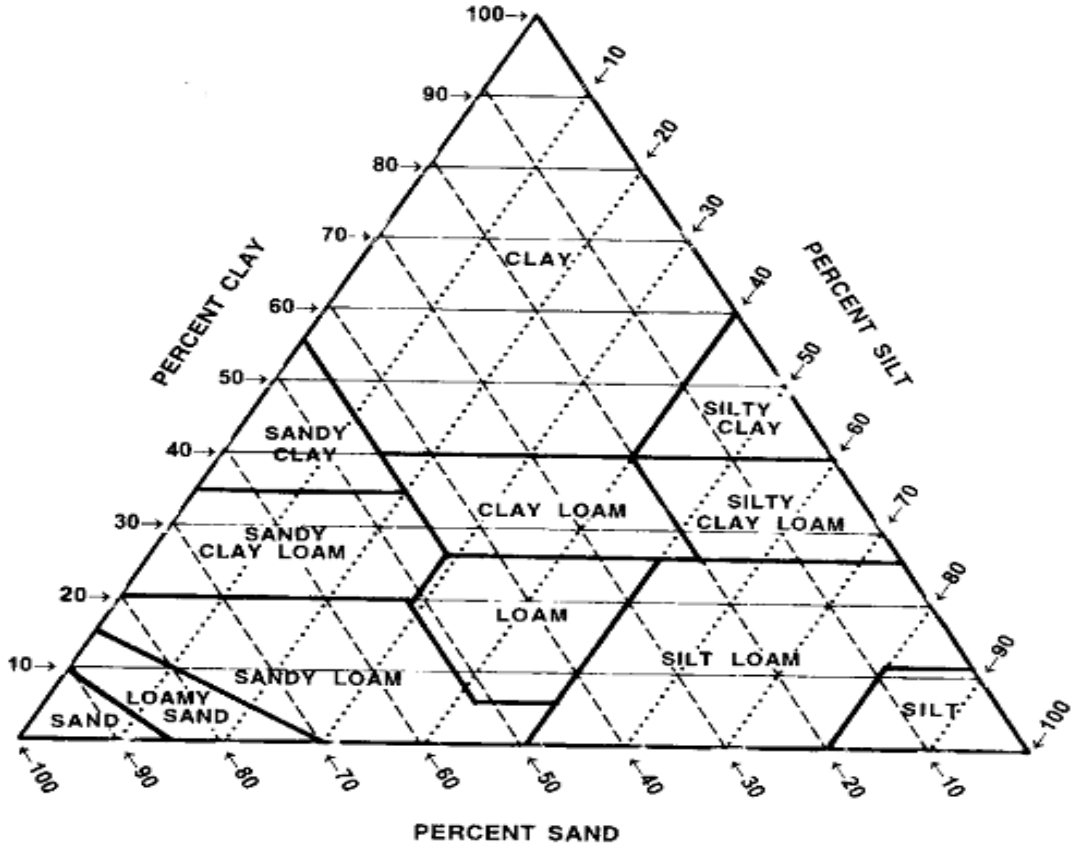

Appendix Figure 13. Soil texture triangle

Appendix Figure 14. Method of synthesis Fe-Al-Mn ternary mixed oxide nanocomposite

Appendix Figure 15. Step of analysis P desorbed by DMT-HFAMO